AD NUMBER

AD418467

LIMITATION CHANGES

TO:

Approved for public release; distribution is unlimited. Document partially illegible.

FROM:

**Distribution authorized to U.S. Gov't. agencies and their contractors;
Administrative/Operational Use; MAR 1963. Other requests shall be referred to Defense Advanced Research Projects Agency, ASBD-TIO, 675 North Randolph Street, Arlington, VA 22203-2114. Document partially illegible.**

AUTHORITY

esd ltr, 22 aug 1967

DISCLAIMER NOTICE

THIS DOCUMENT IS THE BEST QUALITY AVAILABLE.

COPY FURNISHED CONTAINED A SIGNIFICANT NUMBER OF PAGES WHICH DO NOT REPRODUCE LEGIBLY.

Final Report

IONIZATION AND DE-IONIZATION IN THE LOWER IONOSPHERE

Prepared for:

AIR FORCE CAMBRIDGE RESEARCH LABORATORIES
OFFICE OF AEROSPACE RESEARCH
LAURENCE G. HANSCOM FIELD
BEDFORD, MASSACHUSETTS

CONTRACT AF 19(604)-8355

STANFORD RESEARCH INSTITUTE

MENLO PARK, CALIFORNIA

STANFORD RESEARCH INSTITUTE
MENLO PARK, CALIFORNIA

March 31, 1963

Final Report

(6)

IONIZATION AND DE-IONIZATION IN THE LOWER IONOSPHERE

Prepared for:

AIR FORCE CAMBRIDGE RESEARCH LABORATORIES
OFFICE OF AEROSPACE RESEARCH
LAURENCE G. HANSCOM FIELD
BEDFORD, MASSACHUSETTS

CONTRACT AF 19(604)-8355

(10) *By: I. G. Poppoff R. C. Whitten*

SRI Project No. PAU-3624

This research is sponsored by the Advanced Research Projects Agency, Washington, D.C. ARPA Order No. 6-61, Amd. No. 47; Amount of Contract: $58,800; Date of Contract February 28, 1961; Contract No. AF 19(604)-8355; Expiration date: March 31, 1963; Project Scientist at AFCRL: Dr. George J. Gassmann, CRZIC; ARPA Code Number: 7200; OAR Project Number: 4988.

Approved:

Felix Smith

FELIX T. SMITH, DIRECTOR
CHEMICAL PHYSICS DIVISION

Copy No. 25

CONTENTS

BLANK PAGE

LIST OF ILLUSTRATIONS

TABLES

I INTRODUCTION

This is the final report of a series that was initiated under a former contract (AF 29(601)-1994, ARPA Order No. 6-58, Task 5) and has continued for a period of approximately 3-1/2 years. This report contains much of the earlier work, brought up to date, as well as new material generated during the final phase of the present contract.

The objective of this study has been to learn as much as possible about the relaxation of the lower ionosphere following a pulse of ionizing radiation.

Ideally, the approach would be to measure several ionospheric parameters directly, simultaneously, and continuously during the course of an ionospheric disturbance. The parameters of interest would be radiation flux, electron concentrations, ion species and concentrations, and gas and electron temperatures. For many reasons, which include limitations of the state of the art and financial support, the ideal experiments are not likely to be performed in the near future. Therefore, the approach adopted in this study has been to review published and unpublished measurements of the above parameters, especially those made during disturbed conditions. Pertinent geophysical measurements were considered, together with laboratory data and current theory, in an effort to delineate the phenomena involved and subsequently to estimate the rates of the various relaxation processes.

The report is divided into two principal parts--ionization processes and de-ionization processes. This separation, as the reader will see, is not clear-cut. Inasmuch as natural ionization processes must, at present, be studied by considering fragmentary observations of the ionizing flux together with the resulting radio signal absorption, an inescapable dependence on de-ionization processes, which is not yet clearly defined, always exists. Hence, in Section III A, a model of solar flare ionization is used to deduce an effective dissociative

recombination coefficient; the other necessary relaxation parameters were obtained from the literature. In III B, solar X-ray observations were used with parameters discussed in Section IV to gain an insight of quiescent solar effects. In III C, a model of auroral electron-bremsstrahlung events is constructed utilizing parameters derived in IV to check the adequacy of those parameters in describing ionospheric perturbations. In a similar vein, the associative recombination coefficient discussed in IV C was derived from observations of solar flares, and sunrise-sunset radio effects are used in IV A to evaluate possible candidate negative-ions. Also in Section IV C, the dissociative recombination coefficient derived from solar flare studies is shown to be consistent with laboratory and other ionospheric measurements.

Thus, although definitive atmospheric measurements have not been made, a reasonable consistency was found to occur between estimates, laboratory measurements, and pertinent geophysical observations and models. However, this apparent consistency should not lull the reader into complete complacency. The inherent errors in many of the necessary assumptions are such that it would not be at all surprising to find that a good measurement of one or more of the important parameters will show these models and assumptions to be far from adequate.

Significant data have been and are being acquired that have materially increased our understanding of ionospheric processes. Present knowledge is far from complete, of course. Although significant first steps have been taken, it is clear that the entire field of solar-terrestrial relationships is only beginning to develop. A continuing review of laboratory and geophysical observations is certainly required; definitive in situ measurements are urgently needed.

Earlier work on this study is described in the following reports and papers.

(1) Poppoff, I. G., R. C. Whitten, and R. L. Ludwig. The Determination of Ionospheric Recombination Coefficients Phase I: Feasibility of Utilizing Solar Flare-Sudden

Ionospheric Disturbance Relationships. Final Report Contract No. AF 29(601)-1994, ARPA Order No. 6-58, Task 5. GRD-TR-60-289. Stanford Research Institute, May 26, 1960.

(2) Poppoff, I. G. and R. C. Whitten, Determination of Ionospheric Recombination Coefficients, Semiannual Report No. 1 Contract AF 19(604)-8355. Stanford Research Institute, September 30, 1961.

(3) Whitten, R. C. and I. G. Poppoff, A Model of Solar Flare-Induced Ionization in the D-region. J. Geophys. Res. 66, 2779 (1961).

(4) Whitten, R. C. and I. G. Poppoff. Associative Detachment in the D-region. J. Geophys. Res. 67, 1183 (1962).

(5) Poppoff, I. G. and R. C. Whitten. D-region Ionization by Solar X-rays. J. Geophys. Res. 67, 2986 (1962).

(6) Poppoff, I. G. and R. C. Whitten. Determination of Ionospheric Recombination Coefficents. Semiannual Reports 2 and 3. Contract AF 19(604)-8355. Stanford Research Institute, September 30, 1962.

II SUMMARY AND CONCLUSIONS

A body of information pertaining to ionization and dc-ionization in the lower ionosphere was compiled from various sources. Part of the data was derived by the authors from studies of geophysical observations, part of it from published and unpublished laboratory measurements, and part from other ionospheric studies. Models of lower ionospheric processes were prepared which are consistent with presently available data from these sources.

The following conclusions may be drawn from this study:

A. Ionization Processes

1. Solar Flare-Induced Ionization

Solar flare effects can be considered to be X-ray ionization phenomena. Consideration of sudden cosmic noise absorption events leads to an effective dissociative recombination coefficient of about 2×10^{-7} cm^3 sec^{-1}.

2. Ionization by Background Solar X-rays

Normal D-region ionization sources have not been definitely established. Consideration of present knowledge of nitric oxide recombination coefficients and background solar X-ray fluxes indicates that the role of solar X-rays may be greater than previously supposed and that the role of solar hydrogen Lyman-α radiations may be less important.

3. Ionization by Auroral Electrons

Studies of auroral electron-bremsstrahlung events indicate that at least the temporal characteristics of associated radio noise absorption are consistent with the model suggested in this study. The model is not yet complete enough to judge its adequacy for computing the magnitude of the absorption.

B. De-ionization Processes

1. Negative Ions

a. Significant concentrations of O^- and H^- ions in the lower ionosphere are not consistent with observed "sunrise-sunset" effect. O^- may be important in the upper D-region.

b. O_2^-, OH^-, O_3^-, and/or NO_2^- may be the dominant negative ion species without contradicting present knowledge.

c. Radiative attachment to O_2 and three-body attachment to O are probably not important.

d. Associative detachment is probably the dominant nighttime mode of electron detachment from the species O_2^- and OH^-. Detachment from NO_2^- and O_3^- can occur via dissociative processes.

e. Previously proposed values of photodetachment rate for O_2^- and, perhaps, O^- are not reliable.

f. Diffusion to dust is an unimportant mode of negative ion removal.

2. Charge Transfer and Ion-Atom Interchange

a. The following rate constants were derived

(1) $O^+ + O_2 \rightarrow O + O_2^+$, $k \sim 2 \times 10^{-11}$ cm^3 sec^{-1}

(2) $N_2^+ + O \rightarrow N_2 + O^+$, $k \sim 2 \times 10^{-11}$ cm^3 sec^{-1}

(3) $N_2^+ + O_2 \rightarrow N_2 + O_2^+$, $k \sim 2 \times 10^{-10}$ cm^3 sec^{-1}

(4) $O^+ + N_2 \rightarrow NO^+ + N$, $k \sim 6 \times 10^{-13}$ cm^3 sec^{-1}

b. Rate constants for (1) and (3) above are in good agreement with recent laboratory measurements, whereas the rate constant for (4) is not. The discrepancy cannot be explained at this time.

c. The dominant ions in the D-region under disturbed conditions must be O_2^+ and/or NO^+. The model presented in this report cannot be extended below ~ 75 km because of the possible importance of such ions as N_3^+, N_4^+, and O_3^+.

3. Dissociative Recombination

a. Probable values of important dissociative recombination coefficients in the D^- and E^- regions are:

(1) $\alpha_D(N_2^+) = 5 \times 10^{-5}\ T^{-3/4}\ cm^3\ sec^{-1}$

(2) $\alpha_D(O_2^+) = 9 \times 10^{-5}\ T^{-1}\ cm^3\ sec^{-1}$

(3) $\alpha_D(NO^+) = 2.6 \times 10^{-4}\ T^{-3/2}\ cm^3\ Sec^{-1}$

b. Most important coefficients in the upper D-region and the E-region are $\alpha_D(O_2^+)$ and $\alpha_D(NO^+)$.

c. Identities of dominant positive ions in the lower D-region are not known.

4. Ion-Ion Recombination

a. Two-body reactions are important in the D-region.

b. Three-body reactions are not important above ~ 45 km but may be important in low-altitude effects of nuclear explosions.

5. Diffusion to Dust

This is not likely to be important in the normal unperturbed ionosphere or during perturbing events.

III IONIZATION PROCESSES

A. Solar Flare-Induced Ionization

1. Introduction

It has long been known that so-called sudden ionospheric disturbances (SID), such as short-wave fade-out, sudden cosmic noise absorption, sudden enhancement of atmospherics, etc., are manifestations of ionization in the D-region which in turn is associated with the occurrence of a solar flare. Only recently, however, has the nature of the ionizing portion of the solar flare radiation come to light. Measurements (Friedman, Chubb, Kupperian, and Lindsay 1958; Chubb, Friedman, and Kreplin, 1960a; Chubb, and others, 1960b; Kreplin, Chubb, and Friedman, 1962) by the Rocket Astronomy Group at the U.S. Naval Research Laboratory (NRL) have indicated that this radiation in the hard portion of the spectrum penetrates deeply into the D-region and during large disturbances apparently produces ionization at altitudes of less than 60 km.

The electron concentration is influenced not only by the intensity of the ionizing radiation but also by the recombination rate and by the electron detachment and attachment rates. It will be shown later, however, that the photodetachment rate is sufficiently large so that the effect of electron attachment to molecular oxygen is of negligible importance at altitudes above 75 km; this statement is true during the decay phase as well as during the build-up.

In section 2 we consider the NRL measurements of solar flare radiation and their implications with respect to the D-region, and on the basis of these data we construct a model of the electron production profile. In section 3 we estimate the dissociative recombination coefficient and construct a model of radio signal absorption based on the NRL data.

2. The Nature and Effects of Ionizing Radiation from Solar Flares

Since World War II several theories have appeared regarding the nature of the radiation responsible for sudden ionospheric disturbances. The first was that the increase in ionization is caused by an enhancement in Lyman-α emission during a flare. The difficulties inherent in this suggestion are now apparent: Lyman-α would have to increase in intensity by a factor of $\sim 10^6$ or more in order to produce the high frequency absorption observed during sudden ionospheric disturbances. The detection of X-rays in the rocket and satellite observations of solar flares (Sunflare I and II) by Friedman, Chubb, Kupperian, and Lindsay (1958); Chubb, Friedman, and Kreplin (1960a); Kreplin, Chubb, and Friedman, (1962), provides a basis for a much better explanation of the origin of sudden ionospheric disturbances. The X-ray flux is spread out in a spectrum which can cause sufficient ionization at all levels of the D-region to produce the observed electron concentrations. It has also been suggested (Mitra, 1960) that both X-rays and Lyman-α are important in producing SID's. However, recent satellite measurements of the Lyman-α intensity during a class 1^+ solar flare (Chubb and others, 1960b) indicate that no such enhancement in the Lyman-α intensity occurs. A larger flare may, of course, produce an observable Lyman-α enhancement, but it is doubtful if it could compete with X-radiation in its ionospheric effects at any level of the D-region. All the measurements of the NRL group (Friedman, Chubb, Kupperian, and Lindsay, 1958; Chubb, Friedman, and Kreplin, 1960a; Chubb and others, 1960b) indicate that the electromagnetic solar radiations producing the enhanced ionization in the D-region are X-rays of wavelength $\lambda < 8$ A; X-rays of wavelengths $\lambda > 8$ A will be absorbed almost entirely in the E-region. This is shown in Table III-1, which gives the intensity at several wavelengths required to produce given electron production rates at two levels of the D-region.

A partial X-ray flux spectrum was obtained from a Sunflare II rocket (Chubb, Friedman, and Kreplin, 1960a) launched during a class 2^+ flare on August 31, 1959. Unfortunately, only a lower limit of the intensity in the 2-8 A range was observed owing to saturation of some of

Table III-1

INTENSITY REQUIRED TO PRODUCE GIVEN ELECTRON PRODUCTION RATES AT TWO LEVELS IN THE D-REGION

Altitude, km	Electron Production Rate q, cm^{-3} sec^{-1}	Intensity, erg cm^2 sec^{-1}		
		$2 > \lambda > 8$ A	$\lambda > 8$ A	L_α
70 km	30	0.2	$\gg 1$	$\sim 10^6$
90 km	2500	0.2	~ 1	$\sim 10^5$

the sensors. Because of this gap in the spectral data it was necessary to estimate the missing portion by extrapolating from other data. Several other successful rocket flights in the Sunflare II program yielded essentially complete X-ray spectra in the range 2-60 A, but because they were made during a small flare and under quiet sun conditions, the cosmic noise absorption data were inadequate for the construction of a model of the disturbed D-region. However, since we had X-ray spectra for several lower levels of X-ray intensity, it was possible to extrapolate the shape of the X-ray spectrum to the level of X-ray intensity corresponding to the class 2^+ flare considered in this report. The spectrum so constructed, together with its estimated upper and lower limits (the broken curves) at time 22:54 UT, is shown in Figure III-1. In addition, counter measurements in the energy range 15 to 80 keV were also made at two different times during the flight. These data indicated a softening of the hard X-radiation as it decreased in intensity (Chubb, Friedman, and Kreplin, 1960a).

When X-rays are absorbed in the ionosphere, they produce (a) primary ionization by photoelectric "stripping" of electrons from neutral molecules, and (b) secondary ionization by the "stripped" electrons. A photon of wavelength 2 A will produce about 200 free electrons by this process. The electron production rate can be written

$$q = \int \sigma_{air}(\lambda) \frac{dQ(\lambda)}{d\lambda} n \frac{E(\lambda)}{E_e} d\lambda \qquad (1)$$

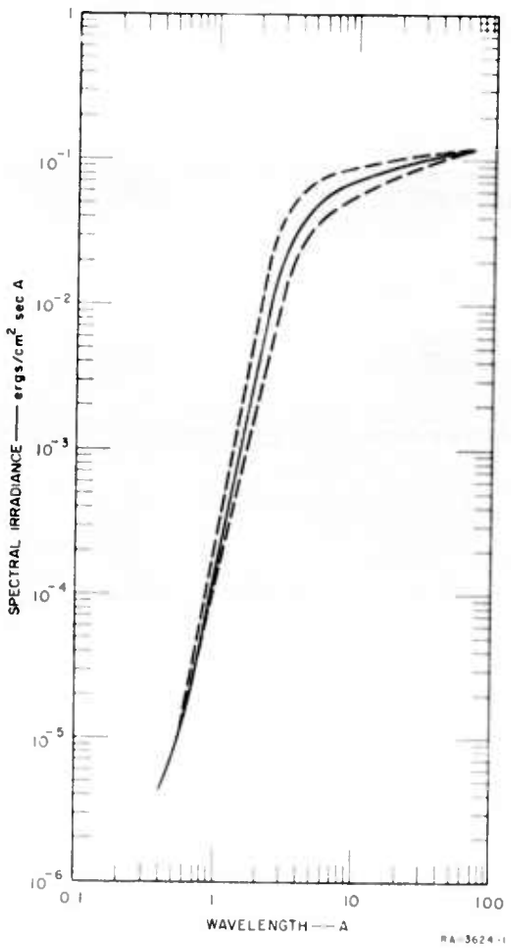

FIG. III-1 X-RAY SPECTRUM OF THE FLARE OBSERVED AT 22:50 UT ON 31 AUGUST 1959. THE SOLID CURVE REPRESENTS THE MOST PROBABLE SPECTRUM BASED ON EXTRAPOLATED DATA. THE BROKEN LINES REPRESENT THE ESTIMATED UPPER AND LOWER LIMITS OF INTENSITY.

where $\sigma_{air}(\lambda)$ is the absorption cross section of X-rays in air as a function of wavelength λ; $Q(\lambda)$ is the X-ray photon flux density; n is the neutral particle number density; $E(\lambda)$ is the energy of a photon of wavelength λ; and E_e is the mean energy required to remove an electron from a neutral molecule in air ($\sim$ 32 eV). Owing to absorption by the atmosphere, the X-ray photon flux density $Q(\lambda)$ is also a function of altitude. Figure III-2 shows the attenuation of L-α and X-radiation

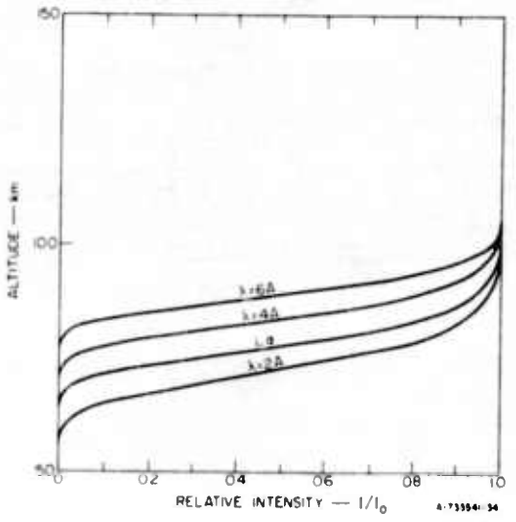

FIG. III-2 ATTENUATION OF SOLAR RADIATION IN THE UPPER ATMOSPHERE. THESE CURVES ARE BASED ON THE ARDC 1959 MODEL ATMOSPHERE (MINZNER, 1959)

of several wavelengths in the upper atmosphere. Figure III-3 shows the electron-production-rate profile computed from the data presented in Figure III-1.

We shall assume in our model that the electron production rate bears the same functional relationship to time at all altitudes; this is equivalent to assuming that the shape of the X-ray spectrum is time-independent or that Q can be separated into two factors, one of which

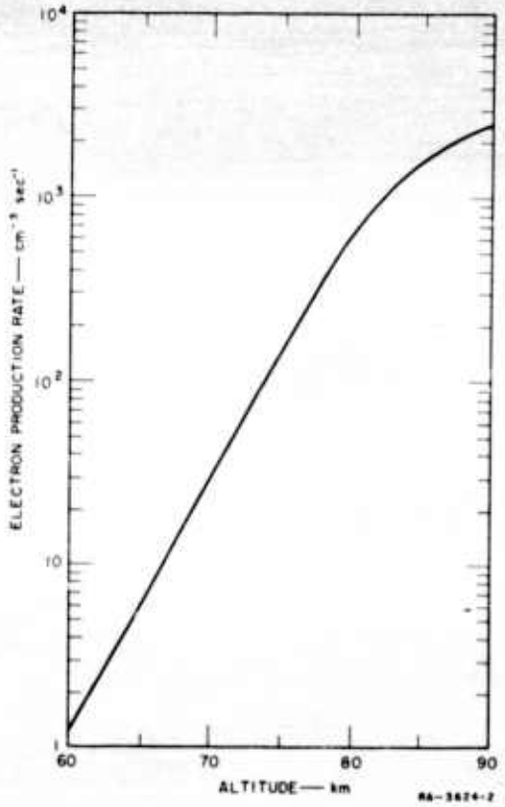

FIG. III-3 ELECTRON PRODUCTION RATES AT VARIOUS ALTITUDES AS COMPUTED FROM THE SOLID CURVE IN FIG. III-1

depends only on wavelength λ and altitude h, and the other only on time

$$Q(\lambda, h, t) = \int \Lambda(\lambda, h) T(t) \qquad (2)$$

We can establish the start of the X-ray emission at the time of the commencement of sudden cosmic noise absorption (see Figure III-4) and the maximum of the X-ray emission curve at roughly the time of minimum cosmic noise intensity. This is an oversimplification, since there is no reason to believe that the entire X-ray spectrum bears exactly the same functional relationship to time.

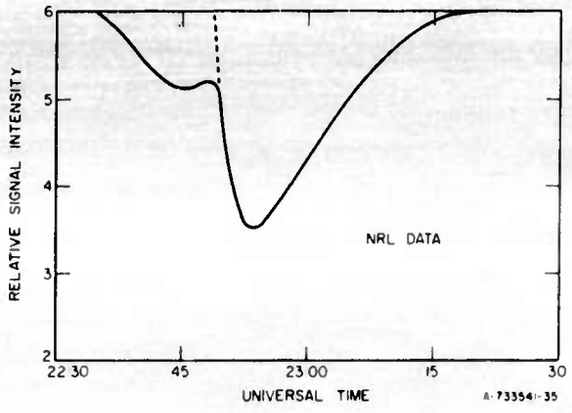

Data reproduced through courtesy of U.S. Naval Research Laboratory

FIG. III-4 INTENSITY AT LOS ANGELES OF 18-Mc COSMIC NOISE DURING THE OCCURRENCE OF A CLASS 2+ SOLAR FLARE ON 31 AUGUST 1959. THE RECORD INDICATES THE EXTRAPOLATION TO ITS ORIGIN OF THE LARGER OF THE SUDDEN COSMIC NOISE-ABSORPTIONS

3. Model of Ionization, Recombination, and Radio Signal Absorption

A sudden ionospheric disturbance may be divided into two phases: the build-up phase and the decay phase. The former is characterized by a rapid increase in electron density due to the increasing solar X-ray photon flux and thus the electron production rate; the latter, on the other hand, is characterized by a gradual decrease in electron density. The electron density maxima do not necessarily occur simultaneously at all altitudes, however, since there is at present no known reason for the intensity maxima of all parts of the the X-ray spectrum to occur simultaneously. In spite of this, we shall assume in our model that the electron densities do simultaneously reach their maxima at all altitudes in the D-region and that each maximum occurs at the same time as the minimum in the cosmic noise intensity curve (Figure III-4). The time rate of change of electron density is related to the production and removal processes by the well-known equation

$$\frac{dN_e}{dt} = \frac{q}{1+\lambda} - (\alpha_D + \lambda\alpha_i)N_e^2 - \frac{N_e}{1+\lambda}\frac{d\lambda}{dt} \qquad (3)$$

in which N_e is the electron density; q is the electron production rate; λ is the negative ion to electron-density ratio ($\lambda = N^-/N_e$); α_D is the dissociative recombination coefficient; and α_i is the mutual ionic neutralization coefficient. The meaning of the symbol λ (wavelength or negative-ion to electron concentration ratio) in the following will be clear from the context.

The differential equation obeyed by the negative ion to electron density ratio λ is (Bates and Massey, 1946)

$$\frac{1}{1+\lambda}\frac{d\lambda}{dt} = \beta m - \lambda\left[\rho + \gamma n + N_e(\alpha_i - \alpha_D) + \frac{q}{N_e(1+\lambda)}\right] \qquad (4)$$

where β is the electron attachment coefficient; ρ is the photodetachment rate; γ is the electron collisional detachment coefficient; n is the neutral particle density; and m is the molecular oxygen concentration (taken to be 1/5 n in our computations). In the model to be developed in this report the neutral particle concentrations given in the ARDC 1959 model atmosphere (Minzner, Champion, and Pond, 1959) are adopted.

The second term in brackets on the right-hand side of equation (4) is of importance only in the lower D-region. Recent estimates of the collisional detachment coefficient γ based on polar cap absorption (Bailey and Branscomb, 1960) are of the order $\gamma \approx 2 \times 10^{-17}$ cm^3/sec. However, other workers (Phelps and Pack, 1961) have found evidence that $\gamma \ll 10^{-17}$ cm^3/sec for O_2^-, and that N_2 is an ineffective detaching agent. Whitten and Poppoff (1962) have suggested that an associative detachment mechanism may be dominant. Be that as it may, our investigation showed that collisional detachment is not very important in the solar flare-disturbed D-region. The third and fourth terms in brackets are, according to our computations, approximately equal in magnitude but of opposite sign; hence they tend to cancel. The negative sign of the third term in brackets $[N_e(\alpha_i - \alpha_D)]$ is due to the fact that $\alpha_D \gg \alpha_i$ (Crain, 1961). Because of its very slight dependence on N_e

and q, λ is a slowly varying function of time[1] and can be approximated by

$$\lambda \approx \frac{\beta m}{\rho} \qquad (4a)$$

Because of the weak time-dependence of λ, the last term on the right-hand side of equation (3) can be neglected. The most recent investigations of electron-O_2 attachment (Chanin, Phelps, and Biondi 1959; Holt, 1959) indicate that in the D-region it is primarily a three-body process and that the coefficient K where

$$\beta = Km \qquad (5)$$

has the value $K = (2 \pm 1) \times 10^{-30}$ cm^6/sec for an electron temperature of 250°K. Equation (4a) can then be written

$$\lambda \approx \frac{Km^2}{\rho} \qquad (4b)$$

The photodetachment rate ρ was computed using recent measurements (Burch, Smith, and Branscomb 1958) of photodetachment cross section for O_2 and solar radiation flux measurements (Kuiper, 1953). These yield a value of $\rho = 0.35$ sec^{-1}. The value of the electron affinity of O_2 derived by Burch and others from the cross section data was 0.15 eV compared with the value of 0.46 eV obtained by Phelps and Pack (1961). Since the photodetachment cross sections are expected to be decreasing functions of the threshold energy of the process, our computed value of ρ may be too large. Hence λ was also computed for values of ρ of 0.10 sec^{-1} and 0.035 sec^{-1}; the λ profiles are shown in Figure III-5. The value $\rho = 0.1$ sec^{-1} is provisionally suggested as the most probable value (see section IVA).

[1]The insensitivity of λ to changes in q and N_e indicates that the approach to equilibrium of the attachment and detachment processes is quite rapid. This is merely the result of relatively large attachment and detachment coefficients.

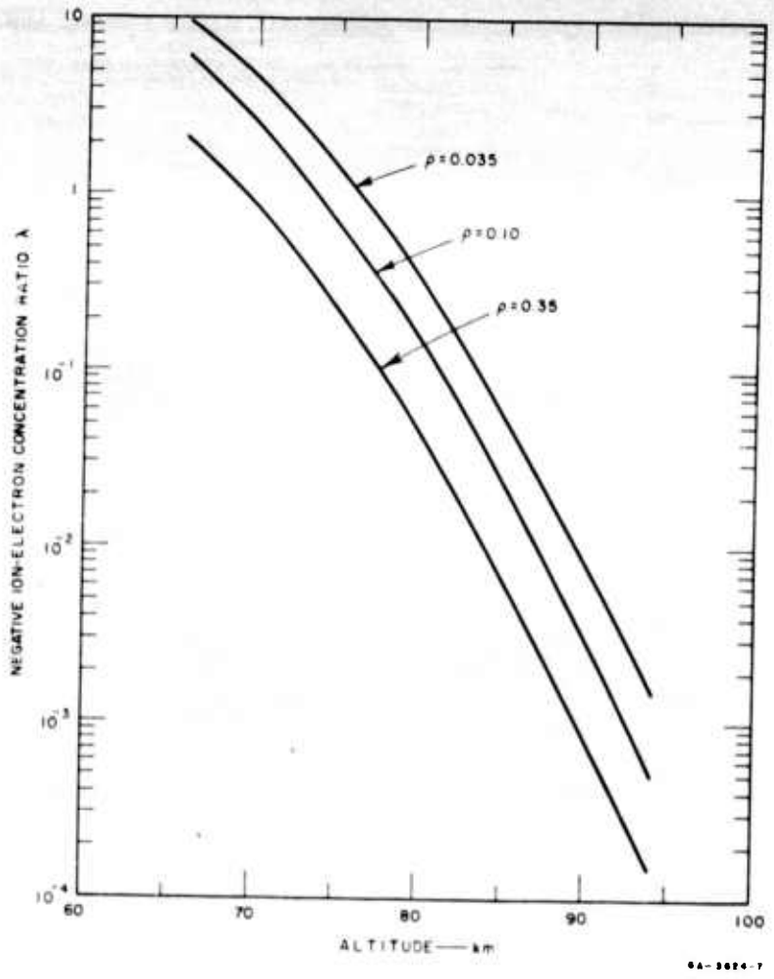

FIG. III-5 NEGATIVE ION-ELECTRON CONCENTRATION RATIO PROFILES FOR THREE POSSIBLE VALUES OF THE PHOTODETACHMENT RATE .

If the values of K, ρ, γ, α_D, α_i, the neutral particle concentration profile, and the functional relationship to altitude and time of the electron source function q(h,t) are known, it is possible to compute the electron concentration at any altitude h by means of the approximate form of equation (3):

$$\frac{dN_e}{dt} \approx \frac{q(h,t)}{1+\lambda} - (\alpha_D + \lambda\alpha_i)N_e^2 \qquad (3a)$$

Using the foregoing as a basis, we shall now construct a model of the D-region during sudden ionospheric disturbances. To facilitate this and to obtain an estimate of the dissociative recombination coefficient we shall utilize the NRL Sunflare II data and sudden cosmic noise absorption data presented in Figure III-4. In essence our task is to find a functional form for q and a value of the dissociative recombination coefficient α_D which, when inserted in equation (3a), yield electron concentration profiles at various times during the build-up phase that agree with the observed reduction in 18 Mc cosmic noise intensity. The mutual ionic neutralization coefficient α_i does not enter the computations because it is probably smaller than α_D (Crain, 1961) and because of the fact that the negative ion-electron concentration ratio at most is of order unity at altitudes of interest.

The relative cosmic noise intensity is given by the equation

$$\frac{I_d}{I_n} = \exp\left[-2 \int_D (k_d - k_n)\, dh\right] \qquad (6)$$

where I_d and I_n are the 18 Mc cosmic noise intensities corresponding to the disturbed and normal D-region, respectively, and $\int_D$ indicates integration over that segment of the ray path which lies in the D-region. The absorption coefficient k for the case in which $\omega >> \nu$ is given approximately by

$$k \approx \frac{5}{3} \frac{\omega_0^2}{2c\omega^2} \nu \qquad (7)$$

(Molmud, 1959), neglecting gyromagnetic splitting which is of little importance at 18 Mc; ω_0 is the plasma frequency, ω, the signal frequency, ν, the electron-neutral particle collision frequency, and c the velocity of light in free space.

In constructing this model we considered electron collision frequencies suggested by Phelps and Pack (1959), by Nicolet (1959), by Kane (1960), and by Barrington and Thrane (1962). Those proposed by Phelps and Pack were based on drift velocity measurements on electrons

in N_2 and probably constitute a lower limit, while those due to Nicolet were based on the results from a microwave interaction experiment carried out by Anderson and Goldstein (1956). The latter measurements undoubtedly corresponded to much larger electron temperatures than was realized at the time (Formato and Gilardini, 1959) and thus yielded collision frequencies which are too large. Lying between these models are the experimental results of Kane (1960) which were based on in situ measurements of high frequency radio wave absorption, and of the cross modulation results of Barrington and Thrane (1962). Since these results agree quite well for a quiet ionosphere, we employed them in the computation of the dissociative recombination coefficient.

The X-ray spectrum given in Figure III-1, together with equations (1) and (2), may be used to compute the electron production rate profile as a function of time if we assume a model for X-ray intensity time-dependence T(t).

Several simple functional forms of T(t), as well as several values of the dissociative recombination coefficient α_D, were used in equation (3a), which was then integrated numerically in order to obtain the electron concentration profiles at various times during the build-up phase. These profiles were then used in conjunction with equations (6) and (7) to compute the relative cosmic noise intensity I_d/I_n as a function of time. Upon comparson of $I_d(t)/I_n$ with the sudden cosmic noise absorption data presented in Figure III-1, it was immediately evident that only one of the trial analytical forms, i.e., $T(t) = at^m$, was a reasonably valid choice. After various values of m in the range $\frac{1}{4} \leq m \leq 1$ were tried, it was found that m = 1/2 best agreed with the sudden cosmic noise absorption data. The value of α_D that best agreed with the SCNA data was $\alpha_D = (2^{+3}_{-1} \times 10^{-7}$ cm^3/sec; the uncertainty in α_D reflects the uncertainties in the X-ray spectrum and the electron collision frequency profile.

The decay phase was then treated in a similar manner. It was found that the functional form $T(t) = a'(t_o - t)^2$ where $t_o = 11.7$ min, and a value of $\alpha_D = 2 \times 10^{-7}$ cm^3/sec were, when used to compute the relative cosmic noise intensity $I_d(t)/I_n$ in the manner outlined previously, in reasonable agreement with the sudden cosmic noise absorption observations until 15 minutes after commencement of the flare. The solid curve in Figure III-6 shows the analytical form for $T(t)$ used in these computations.

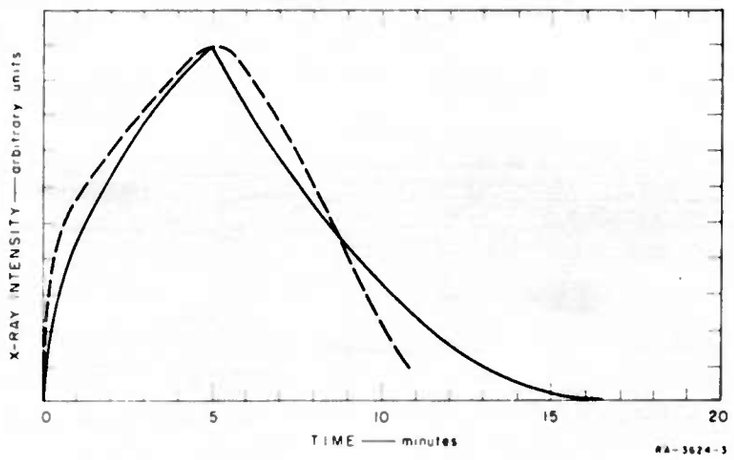

FIG. III-6 MODEL OF SOLAR RADIATION INTENSITY (λ = 2 to 8A) AS A FUNCTION OF TIME FOR THE FLARE OCCURRING ON 31 AUGUST 1959. THE SOLID LINE REPRESENTS THE FUNCTION $at^{1/2}$, $0 \leq t \leq 5$ MIN. AND $a'(11.7 - t)^2$, $t > 5$ MIN. THE BROKEN LINE REPRESENTS THE ESTIMATED X-RAY INTENSITY

The 18 Mc absorption exponent $2\int_D(k_d - k_n)dh$ is shown as a function of time in Figure III-7. The solid curve was obtained by substituting into equation (3a) the analytieal form of $T(t)$ and the values of α_D previously derived, then numerieally integrating the equation to obtain the electron concentration profile, and substituting the electron eoneentrations $N_e(h, t)$ so obtained into equation (7).

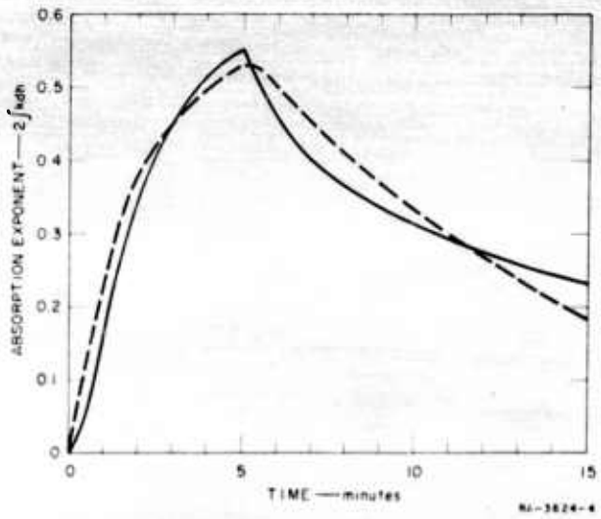

FIG. III-7 18-Mc COSMIC-NOISE-ABSORPTION EXPONENT 2 $\int kdh$ DURING THE BUILD-UP AND DECAY PHASES OF THE FLARE OCCURRING AT 22:50 UT ON 31 AUGUST 1959. THE BROKEN CURVE REPRESENTS THE OBSERVED ABSORPTION AND THE SOLID CURVE REPRESENTS THE COMPUTED ABSORPTION USING THE FUNCTIONS $at^{1/2}$ $(0 < t \leq 5$ min) AND $a'(11.7 - t)^2$ (5 min $< t <$ 11.7 min) TO REPRESENT THE ELECTRON PRODUCTION RATE. THE SYMBOL k IS EQUAL TO $k_d - k_n$

The profiles of $[k_d(t) - k_n]$ were then integrated over the ray path through the D-region to obtain the absorption exponent. It is evident from Figure III-7 that the functional relationship to time of X-ray intensity T(t) actually increased faster than $at^{1/2}$ during the initial portion of the build-up phase and decreased faster than $a'(t_0 - t)^2$ during the decay phase. This is indicated qualitatively by the broken curve in Figure III-6; the broken curve agrees qualitatively with X-ray intensity time-variation data obtained for two different flares by satellite 1960 eta 2(R. W. Kreplin, private communication). We wish to reiterate that the factorization of $Q(\lambda, h, t)$ in accordance with equation (2) is quite artificial. It is known, for example, that the X-ray sprectral form changes with time during the decay phase of a flare; this undoubtedly accounts for part of the disagreement between the observed and computed absorption exponents.

Figure III-8 shows the electron concentration profile at 22:54 UT as computed by the method outlined previously. The corresponding absorption coefficient obtained by substituting the data contained in Figure III-8 into equation (7) is presented in Figure III-9. This absorption coefficient profile is in rough agreement with the model proposed by Mitra (1960); the maximum at about 80 km occurs about 10 km higher than is proposed in the high frequency absorption model of Kanellakos and Villard (1962).

B. Ionization by Background Solar X-rays

The significance to normal D-region ionization of recently reported values of background solar X-ray fluxes (Kreplin, 1961) has largely been ignored. The purpose of this section is to present the results of a

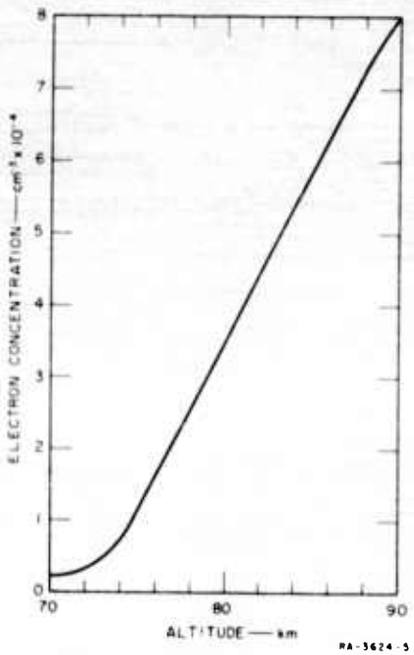

FIG. III-8 COMPUTED ELECTRON CONCENTRATION PROFILE AT TIME 22:54 UT

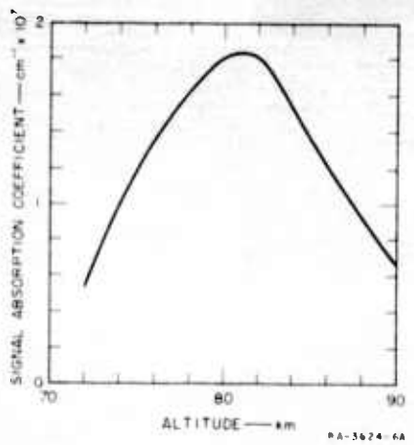

FIG. III-9 18 Mc ABSORPTION COEFFICIENT PROFILE CORRESPONDING TO THE ELECTRON CONCENTRATION PROFILE PRESENTED IN FIG. III-7

1961 study to assess the possible role of background solar radiation in the formation of the D-region.

Current concepts of normal D-region ionization processes seem to favor the model proposed by Nicolet and Aikin (1960), although other workers (Inn, 1961a, b; Bourdeau, 1961) have offered feasible alternative hypotheses. There seems to be little argument about the dominant role of cosmic radiation in the production of lower D-region ionization. The crux of the present controversy is the lack of verified data on the relative influence of solar Lyman-α radiation, nitric oxide, molecular oxygen, cosmic radiation, particulate matter, and X-radiation in producing upper D-region ionization. Nicolet and Aikin (1960) concluded that free-electron concentrations between approximately 80 and 85 km are produced principally as a result of the ionization of nitric oxide by solar Lyman-α radiation. This conclusion is the result of calculations employing a theoretical vertical distribution of nitric oxide, an assumed dissociative nitric oxide ion-electron recombination coefficient, and the solar radiation measurements available before 1960. Recent work by Gunton and Inn (1961) and by the authors (section IV C, this report) shows that the dissociative recombination coefficient assumed by Nicolet and Aikin may have been too small by two to three orders of magnitude. This means either that the nitric oxide concentrations are higher than those calculated by Nicolet and Aikin or that another ionization mechanism must be found.

Inn (1961a,b) suggests a mechanism based on the ionization of vibrationally excited ground-state oxygen molecules by solar Lyman-α. Bourdeau (1961) suggests that cosmic ray ionization modified by diffusion of ions to particulate material in the 60 to 80 km region can account for the observed conductivity profiles.

We should like to suggest another possibility by considering the X-ray spectra reported by Kreplin (1961) as being characteristic of background solar radiation, at least during periods of sunspot maxima.

Kreplin reports X-ray fluxes of the order of 10^{-3} erg/cm^2 sec in the 2-8 A range during quiescent solar conditions. These values are considerably higher (by two or three orders of magnitude) than those utilized for the quiet sun condition by Nicolet and Aikin; therefore, an evaluation of the possible effect of this level of solar radiation on the D-region seems appropriate. This suggestion was made years ago by Müller (1935), again by Rawer (1952), and more recently by Chamberlain (1961). Until now, however, data have not been available to substantiate the suggestion.

The data reported by Kreplin (1961) from flight NN 8.69 CF included values of solar X-radiation for three energy ranges and were, therefore, used to prepare an estimated quiet sun X-ray spectrum as shown in Figure III-10. The data from flight NN 8.68 CF, though not as complete, substantiate the data from flight NN 8.69 CF.

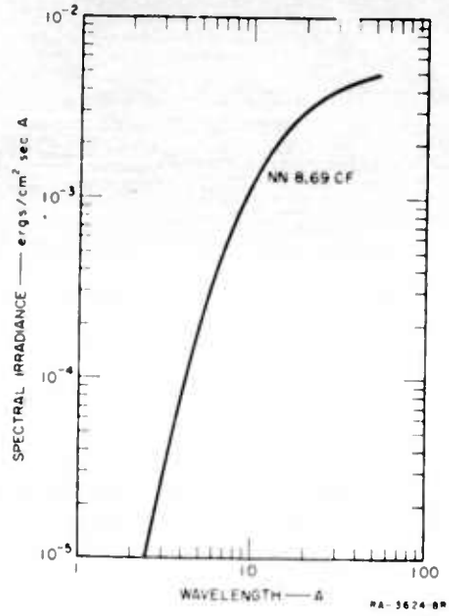

FIG. III-10 BACKGROUND SOLAR X-RAY SPECTRUM CONSTRUCTED FROM DATA OBTAINED BY SUNFLARE II PROBE NN 8.69 CF AT 15:59 UT ON 8 14 59

Measurements of background X-ray spectra and intensities at sunspot maximum reported by other observers tend to confirm the NRL data and our estimated spectrum. The spectrum measured by the SL 40 rocket (9/27/61) is in close agreement with our estimate in the 4-9 A region (Pounds, 1962). The measurement of intensities by Pounds and Sanford (1962) during the period 1959 to 1961 varies from 10^{-3} ergs cm^{-2} sec^{-1} in the 4-10 A range to 1.5×10^{-3} ergs cm^{-2} sec^{-1} in the 2-8 A range. Mandel'shtam, et al., (1962) report rocket measurements of 1.6×10^{-4} ergs cm^{-2} sec^{-1} in the 0-8 A range to 7.3×10^{-4} ergs cm^{-2} sec^{-1} in the 0-10 A range in 1959. Reported measurements of 0-10 A background X-radiation by satellite observatories in succeeding years vary from less than 0.6×10^{-3} ergs cm^{-2} sec^{-1} (Kreplin, Chubb, and Friedman, 1962) to 1.5×10^{-4} ergs cm^{-2} sec^{-1} (Neupert, et al., 1962). Note that all of these measurements are within the range found to be significant for D-region ionization by the calculations described in this section.

Using the spectrum of Figure III-10, the appropriate solar zenith angle (45^{o}), the appropriate X-ray cross sections, and ARDC 1959 model atmosphere, a profile of electron production rates was calculated. It is shown in Figure III-11.

Since the radiation measurements were made during quiet solar conditions, it is a good approximation to consider the D-region to have been in a steady state. The electron density $N_e(h)$ at altitude h is then given by

$$N_e(h) = \left[\frac{q(h)}{(1 + \lambda)(\alpha_D + \lambda\alpha_i)} \right]^{\frac{1}{2}} \qquad (1)$$

in which λ is the negative ion to electron concentration ratio, α_D is the dissociative recombination coefficient, and α_i is the mutual ionic neutralization coefficient. It can be shown that, if we restrict the discussion to altitudes above 70 km, omission of $\lambda\alpha_i$ will introduce an error of less than half an order of magnitude in $N_e(h)$ at the lower altitudes, thus simplifying equation (1). From our assumption that

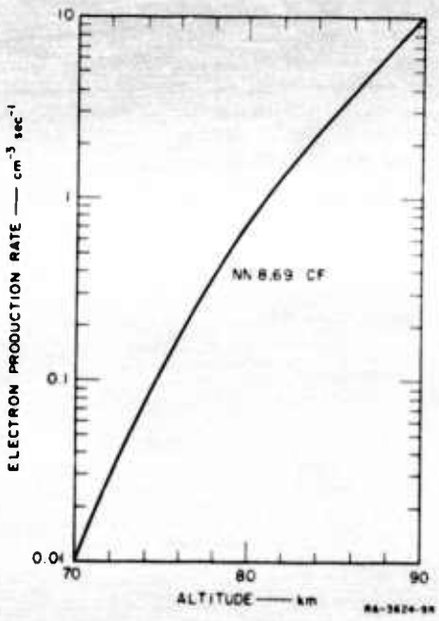

FIG. III-11 ELECTRON PRODUCTION RATE AND CONCENTRATION PROFILES CORRESPONDING TO THE X-RAY SPECTRUM SHOWN IN FIG. III-10

the ionization is caused by solar X-rays, it follows that the ionic processes would be similar to those in the same region produced by solar flare radiation. We considered this problem in an earlier paper (Whitten and Poppoff, 1961), deducing a value of $\alpha_D = 3 \times 10^{-7}$ cm^6/sec and a λ profile given by the curve labeled $\rho = 0.10$ in Figure III-5.

Using q(h) from Figure III-11, the λ profile referred to above, and the above value of α_D, the electron concentration profile of Figure III-11 is obtained. The values obtained are within the spread of observed values for D-region electron concentrations at these altitudes (Ratcliffe, 1960). The X-ray intensity could be an order of magnitude lower and still be adequate to account for some of the lower estimates of D-region electron concentrations. If the spectrum shown in Figure III-10 is 'softened' so that the X-ray intensity at $\lambda = 4$ A is about 10^{-5} erg/cm^2 sec A, the 100 cm^{-3} level in the electron-density profile (Figure III-11) is raised to about 76 km.

The electron concentration profile of Figure III-11 is not intended to serve as a model for the D-region. It does, however, illustrate the possible role of X-radiation in the altitude range 70 to 90 km. It also shows that, if the solar radiation flux measurements used for the calculations are representative (to within an order of magnitude), electron concentrations in the upper D-region can be accounted for without recourse to hypotheses requiring Lyman-α ionization. Preliminary calculations indicate that, if the electron concentrations estimated above are combined with estimates of ionization produced by cosmic radiation, the classical D-region electron profile can be obtained which includes a peak or inflection (depending on relative values of cosmic and X-ray fluxes) at middle D-region altitudes. A reasonable model must, of course, include all valid hypotheses of D-region electron production processes. The inclusion of Lyman-α ionization processes, as well as cosmic ray and X-ray ionization processes, would probably result in electron profiles with several inflections or peaks (or at least changes of gradient) whose position would vary with diurnal, seasonal, and solar-cyclical patterns.

C. Ionization by Auroral Electrons

1. Introduction

For many years, observations have been made of "soft" electromagnetic radiation at low altitudes in the auroral zone. Van Allen (1955) suggested that the observed radiation was bremsstrahlung generated by low energy electrons. Following this suggestion, Chapman and Little (1957) and Chapman (1959) prepared models of the lower ionosphere which showed that this interpretation was consistent with observations of radio absorption in the auroral zone. Meanwhile, observations were made by Anderson and Enemark (1960) of the bremsstrahlung spectrum which furnished the basis for estimates of the spectrum of the generating electrons. Although the source of the electrons is still somewhat controversial, it has been shown that qualitative correlations exist with geomagnetic activity and with solar activity.

Close correlations with cosmic noise absorption have been observed. This, of course, suggests a possible approach to the study of atmospheric relaxation processes, similar to the SID study made earlier in this project and described in III A (Whitten and Poppoff, 1961). However, the area of electron bombardment is relatively small and not stationary. Thus simultaneous observations of the radiation from balloons and of cosmic noise absorption by ground-based riometers were very difficult to obtain and, in fact, did not exist. Recently, however, Brown and Campbell (1962) reported simultaneous observations of radio noise absorption and radiation flux during a magnetic disturbance at College, Alaska on June 25, 1961. The existence of these observed data provided the opportunity to attempt the construction of a model of the ionization produced by auroral electrons and the resulting electron and ion profiles. Although the model could not be completed for this report, a considerable portion of the work has been done and will be described in this section.

2. Ionization by Electrons

The procedure followed was generally that suggested by Chamberlain (1961), which is essentially to consider the incident electrons as a plane source normally incident to the atmosphere. By making such an assumption, the extensive work of Spencer (1959) at the National Bureau of Standards could be utilized. The weakness of this assumption would seem to lie in the obvious fact that the electrons are not normally incident but arrive with an angle of incidence controlled by the geomagnetic field in the bombardment area. Quite obviously, a calculation that considered these factors would be beyond the resources of this study. However, calculations reported by Pedersen (1962) show that the penetration altitude would not change appreciably with angle of incidence. For example, he notes that 100 keV electrons at vertical incidence would penetrate to 80 km, whereas at angles of incidence 30^{o} and 60^{o} from the vertical, they would penetrate to 81 and 85 km, respectively.

Brown and Campbell (1962) reported an electron flux of 10^{8} per cm^{3} sec in the energy range greater than 50 keV at the peak of the

ionization event. In making their estimate an electron spectrum of $N_e = k\ E^{-5}$ was assumed and the computing procedure reported by Anderson and Enemark (1960) was utilized to obtain electron flux estimates from measured X-ray fluxes. An area of bombardment of 15,000 to 40,000 km^2 was estimated.

Using the above data, an extension of the National Bureau of Standards work, and the ARDC 1959 model atmosphere, an altitude profile of the peak ionization rate was computed. The energy range was extended to 10 keV in the low energy and to 200 keV in the high energy end of the reported spectrum. The results are illustrated in Figure III-12 and III-13.

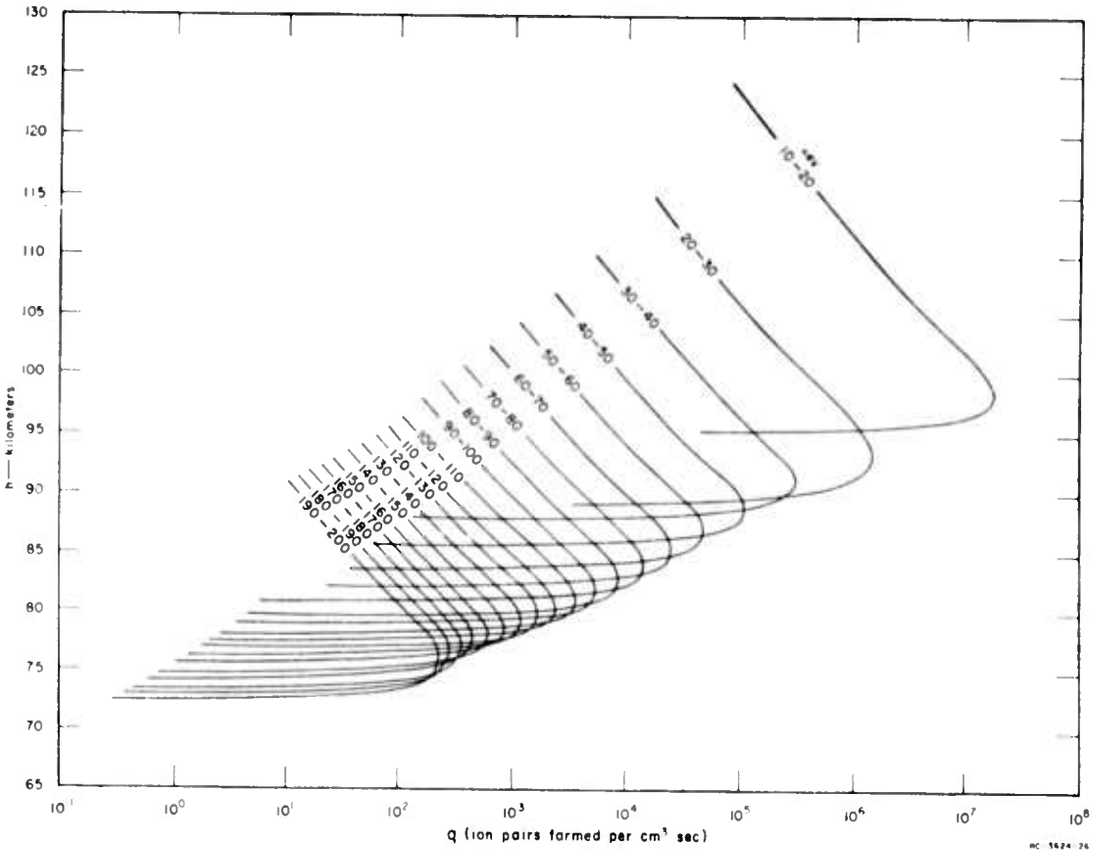

FIG. III-12 IONIZATION RATE vs. ALTITUDE (PER ENERGY INTERVAL)

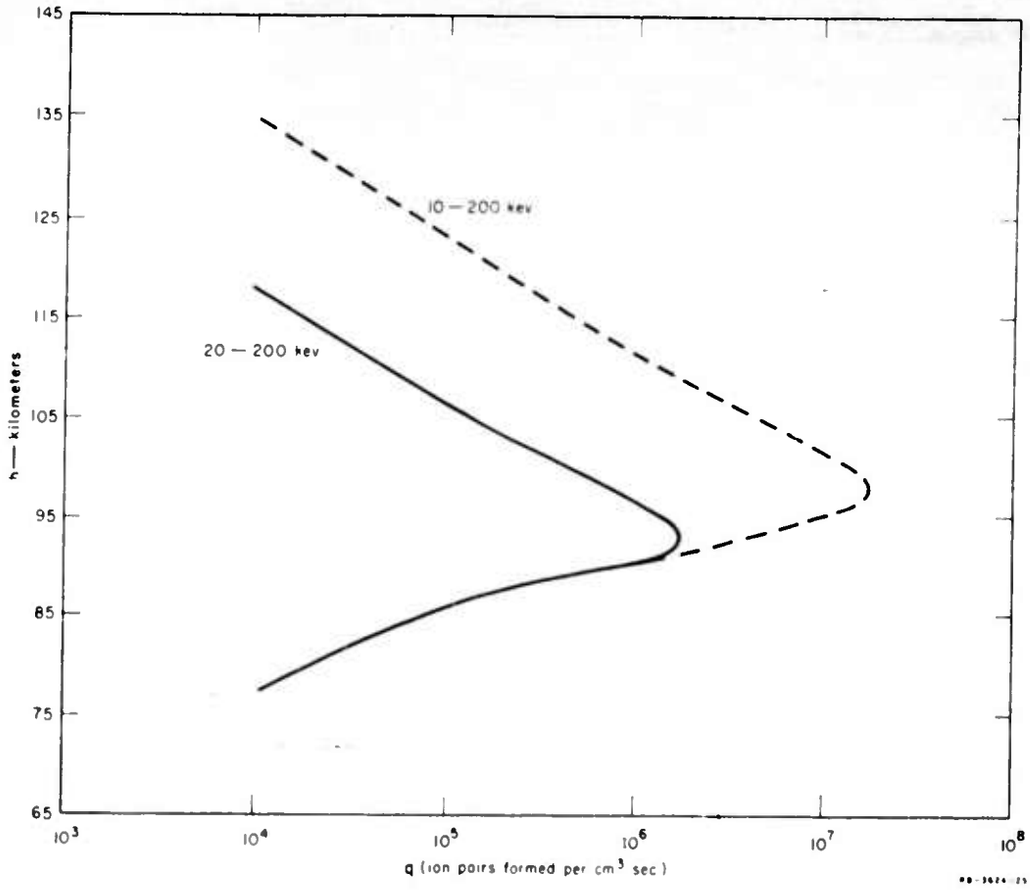

FIG. III-13 TOTAL IONIZATION RATE vs. ALTITUDE FOR LOW ENERGY CUTOFF AT 10 kev AND 20 kev

Study of the calculated curves immediately reveals an obvious difficulty. Because of the steep energy spectrum of the incident electrons, the lowest energy portion is always dominant in determining the peak in the ionization rate profile. Therefore, the low energy cutoff point should be considered very carefully in the preparation of an adequate model.

Although electrons have been detected with energies as low as 8 keV (Davis, Berg, and Meredith, 1960), recent analysis of auroral bremsstrahlung measurements by Winckler, Bhavsar, and Anderson (1962) suggests that the

electron energy is concentrated in the 20-100 keV region, with a maximum intensity in the 50-80 keV region of the electron energy spectrum.

The crux of the problem for this study would, of course, be the absorption of radio frequency energy by the D-region. The maximum in the ionization rate profile not only increases in magnitude with decreasing electron energy, but also in altitude. Since collision frequencies decrease with altitude, a compensating decrease should also occur in radio absorption coefficients. Thus, the effect of imprecise knowledge of the low energy cutoff may not be critical. Reid (1961), in studying proton ionization effects during polar radio blackout events, found that lack of knowledge of low energy proton cutoff points was not very important.

3. Ionization by Bremsstrahlung

Obviously (see Figure III-12) the altitudes at which incident primary electrons are absorbed and bremsstrahlung is produced vary greatly with energy, from about 75 to 100 km for the energy range considered. Inasmuch as the penetration altitude of the bremsstrahlung is a function of the source altitude, this should be considered in the calculation of bremsstrahlung ionization rate profiles. In these calculations, it was assumed that bremsstrahlung is produced at the altitude of peak absorption of the incident primary electrons in the energy ranges used in preparing the curves of Figure III-12.

Profiles of ionization produced by bremsstrahlung generated by electrons in each of the several electron energy ranges were computed. The calculated ionization rates were then summed for each altitude and a profile was prepared of ionization rates produced by bremsstrahlung generated by the entire spectrum of electrons.

Bremsstrahlung spectra were computed by following the treatment described by Anderson and Enemark (1960) which can be summarized as follows.

The number of photons produced by an electron of kinetic energy E in passing through a thickness $d\xi$ g cm^{-2} of material having radiation length L_R g cm^{-2} is

$$d\sigma_t(\xi) = \frac{d\xi}{L_R} \int_{\nu=\epsilon_a/h}^{\nu=\epsilon/h} \frac{d\nu}{\nu} = \frac{d\xi}{L_R} \ln \frac{E}{E_a}$$

ν = frequency of photon

E_a = chosen discrimination level or the lower limit of energy interval considered.

The number of photons with energies above the discrimination level E_a produced by an electron initially of energy E traversing its entire range is

$$n(E_a; E) = \int_{\xi_a}^{\xi} d\sigma_t(\xi) = \frac{1}{L_R} \int \ln \frac{E}{E_a} d\xi$$

Using the approximate range-energy relation R = E/2000, where E is expressed in keV and R in g cm^{-2}, the above equation can be integrated to give

$$n(E_a; E) = \frac{1}{2000\ L_R}[E(\ln E/E_a - 1) + E_a]$$

The expression for another, higher discrimination level, E_{a+1} would be identical except for the subscripts. The number of photons in the energy interval E_a to E_{a+1} produced by N electrons of energy E is

$$n(E_a; E_{a+1}) = \frac{N(E)}{2000\ L_R}[E \ln \frac{E_{a+1}}{E_a} - (E_{a+1} - E_a)]$$

The number of photons produced in each of a series of energy intervals from 1-2 keV up to the energy interval of the primary electrons was then computed for each electron energy interval used in Figure III-12.

The bremsstrahlung flux at the distance R from a large isotropic radiation can be computed as follows: (see Figure III-14). The contribution from each unit increment is

$$dI = \frac{2\pi i_0 r dr}{R^2} A B$$

where i_0 is the number of photons emitted per unit source area and r is the distance from the center of the source to the unit source. A and B are attenuation and scattering terms respectively.

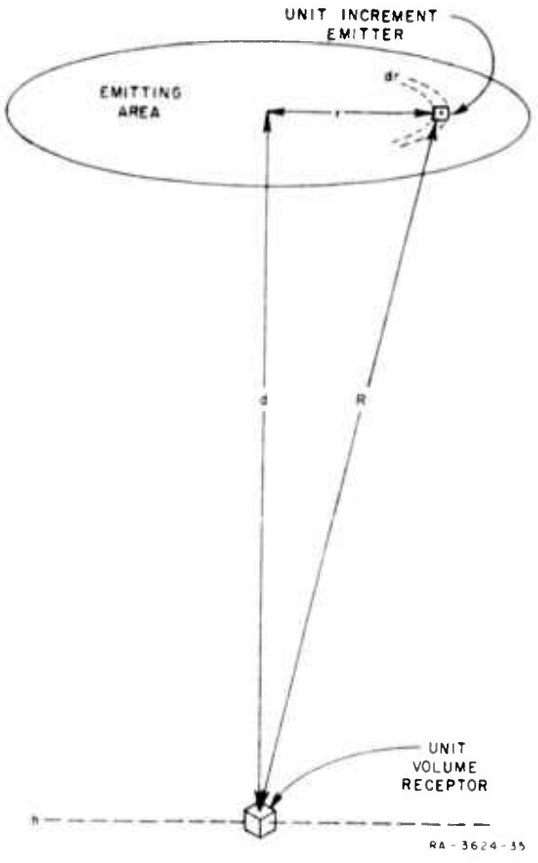

FIG. III-14 SCHEMATIC OF RADIATION GEOMETRY

The attenuation term,

$$A = \exp\left(- \int_{o}^{R} \mu_T(E)dR \right),$$

can, for this application, be expressed as

$$A = \exp\left(- \frac{\mu_T}{\rho_o} M \frac{R}{d}\right)$$

The scattering term is approximated as

$$B = 1 + \frac{\mu_s(E)}{\mu_a(E)} \int_{o}^{R} \mu_T(E)dR$$

and can, for this case, be expressed as

$$B = 1 + \frac{\mu_s}{\mu_a} \frac{\mu_T}{\rho_o} M \frac{R}{d}$$

where μ_a = linear absorption coefficient, μ_s is the linear scattering coefficient $\mu_T = \mu_s + \mu_a$ = total attenuation coefficient, M is the mass of atmosphere in a vertical column of unit cross section and d cm in length, ρ is the atmospheric density at altitude h and ρ_o is the density at N.T.P. conditions.

The total flux at altitude h produced by bremsstrahlung photons of energy E_p emitted from a source at altitude h + d is

$$I(h,E_p) = \int_{o}^{r >> R} dI$$

The ionization produced at h by the absorption of photons with energy E_p is

$$q(h, E_p) = I\ E_p\ \mu_a \frac{\rho}{\rho_o}\left(\frac{1000}{35}\right) \text{ ion pair/cm}^3 \text{ sec}$$

The total ionization rate at an altitude h is

$$q_h = \Sigma\ q(h, E_p)$$

where q is summed over the photon energy spectrum for the bremsstrahlung produced by primary electrons, in a particular energy interval E_e, absorbed at an altitude h + d; and then summed over the entire spectrum of primary electrons, absorbed over the entire altitude range of interest.

The results are presented in Figure III-15.

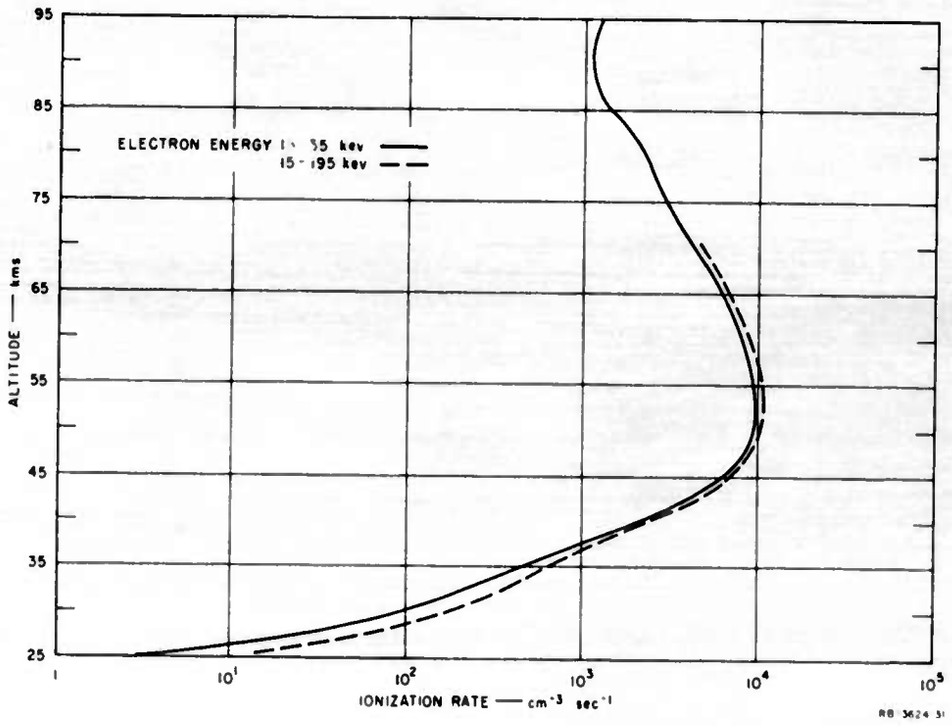

FIG. III-15 PEAK BREMSSTRAHLUNG IONIZATION RATE PROFILE

The combined electron-bremsstrahlung ionization rate profile for peak primary electron flux is presented in Figure III-16. The temporal

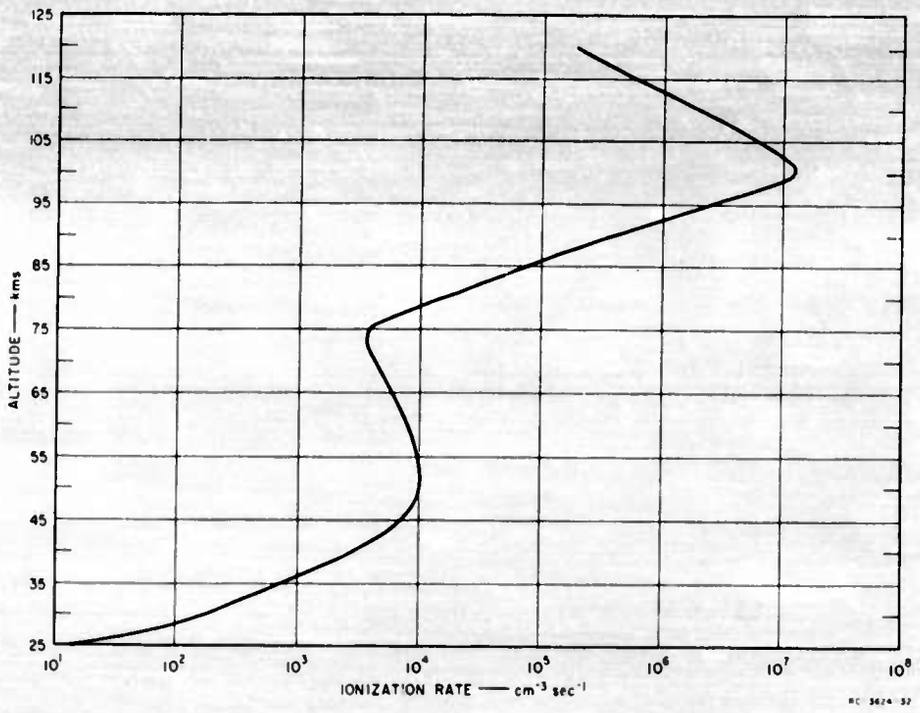

FIG. III-16 PEAK IONIZATION RATE PROFILE - ELECTRONS PLUS BREMSSTRAHLUNG

variation of the ionization rate q presented in Figure III-17 is a smoothed version of the bremsstrahlung curve recorded by Brown and Campbell (1962).

4. Electron and Ion Densities

Knowing the ionization rate, q, as a function of time and altitude, the free electron concentration, N_e, and the ratio of negative ions to electrons, λ, can be computed by utilizing the following well-known continuity equations (Mitra, 1952; Whitten and Poppoff, 1961)

$$\frac{dN_e}{dt} = \frac{q(t)}{1+\lambda} - (\alpha_D + \lambda\alpha_i)N_e^2 - \frac{N_e}{1+\lambda}\frac{d\lambda}{dt}$$

$$\frac{1}{1+\lambda}\frac{d\lambda}{dt} = \beta m - \lambda[\rho + \gamma n + N_e(\alpha_i - \alpha_D) + \frac{q(t)}{N_e(1+\lambda)}]$$

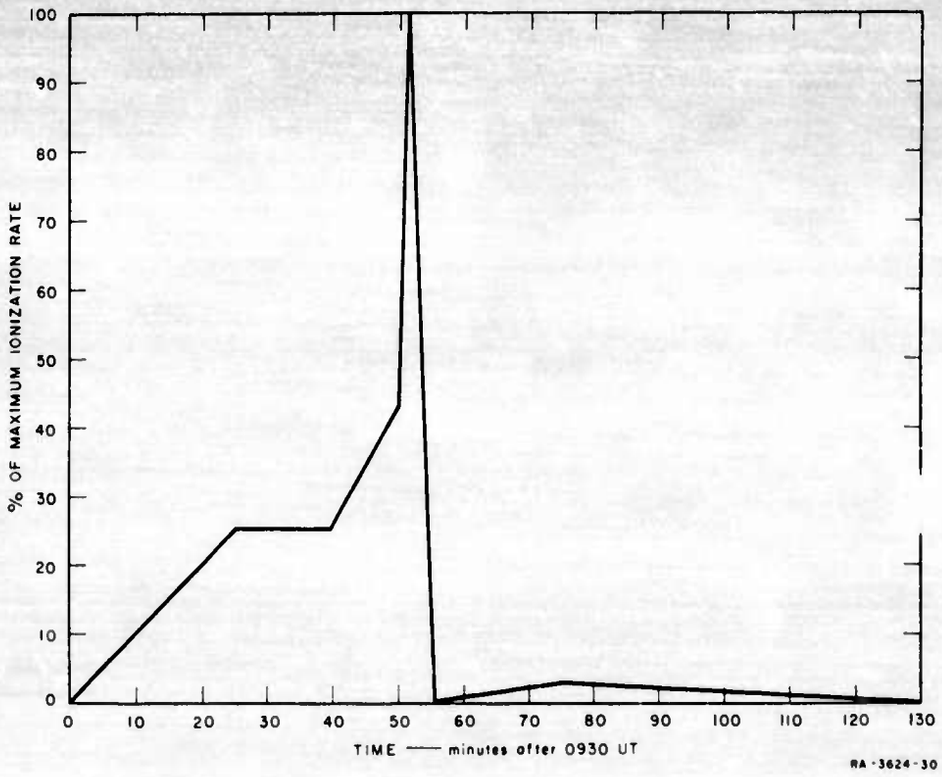

FIG. III-17 TEMPORAL VARIATION OF IONIZING PULSE

where α_D is the dissociative ion-electron recombination coefficient, α_i is the ion-ion mutual neutralization coefficient, β is the electron-oxygen attachment coefficient, ρ is the negative-ion photodetachment rate, γ is the negative-ion collisional detachment coefficient, m is the concentration of the attaching species (O_2 or O), and n is the concentration of the species causing collisional-type detachment.

Unfortunately, the computations of electron density profiles could not be completed in time for this report. Calculations of temporal variations in electron concentration were made for the altitude range 75 to 120 km and are presented in Figures III-18 and III-19. Calculation of an electron density profile was made for the peak ionization rate (51.6 minutes) for the range 40 to 120 km (Figure III-20); this can be

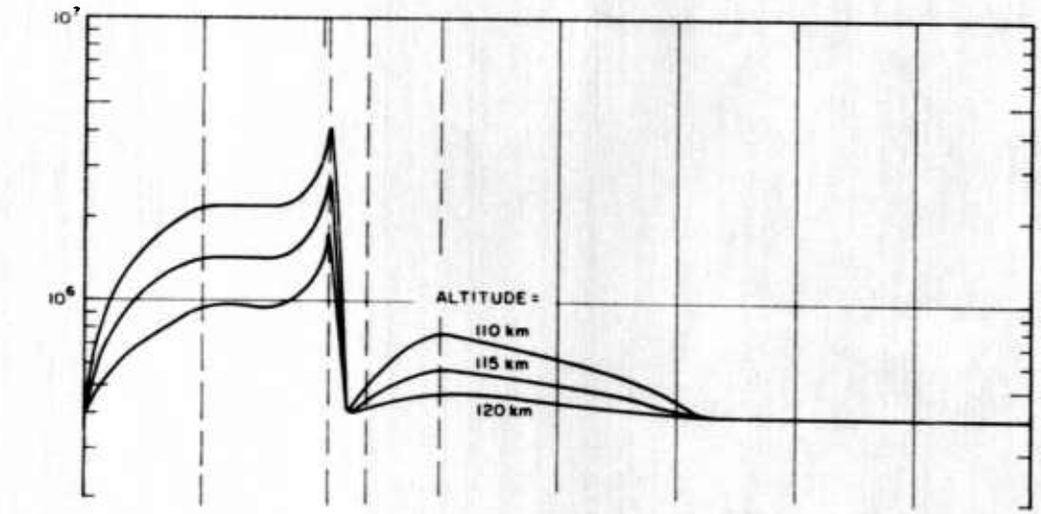
10^7
10^6
ALTITUDE =
110 km
115 km
120 km

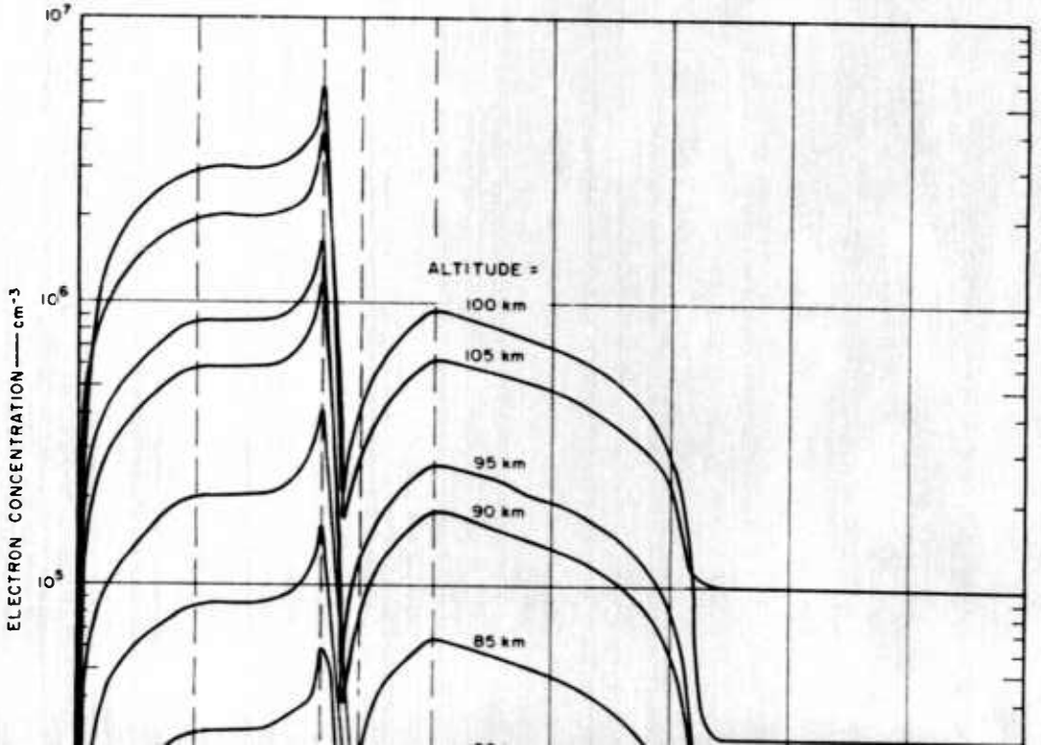
10^7
10^6
10^5
ALTITUDE =
100 km
105 km
95 km
90 km
85 km
ELECTRON CONCENTRATION —— cm^{-3}

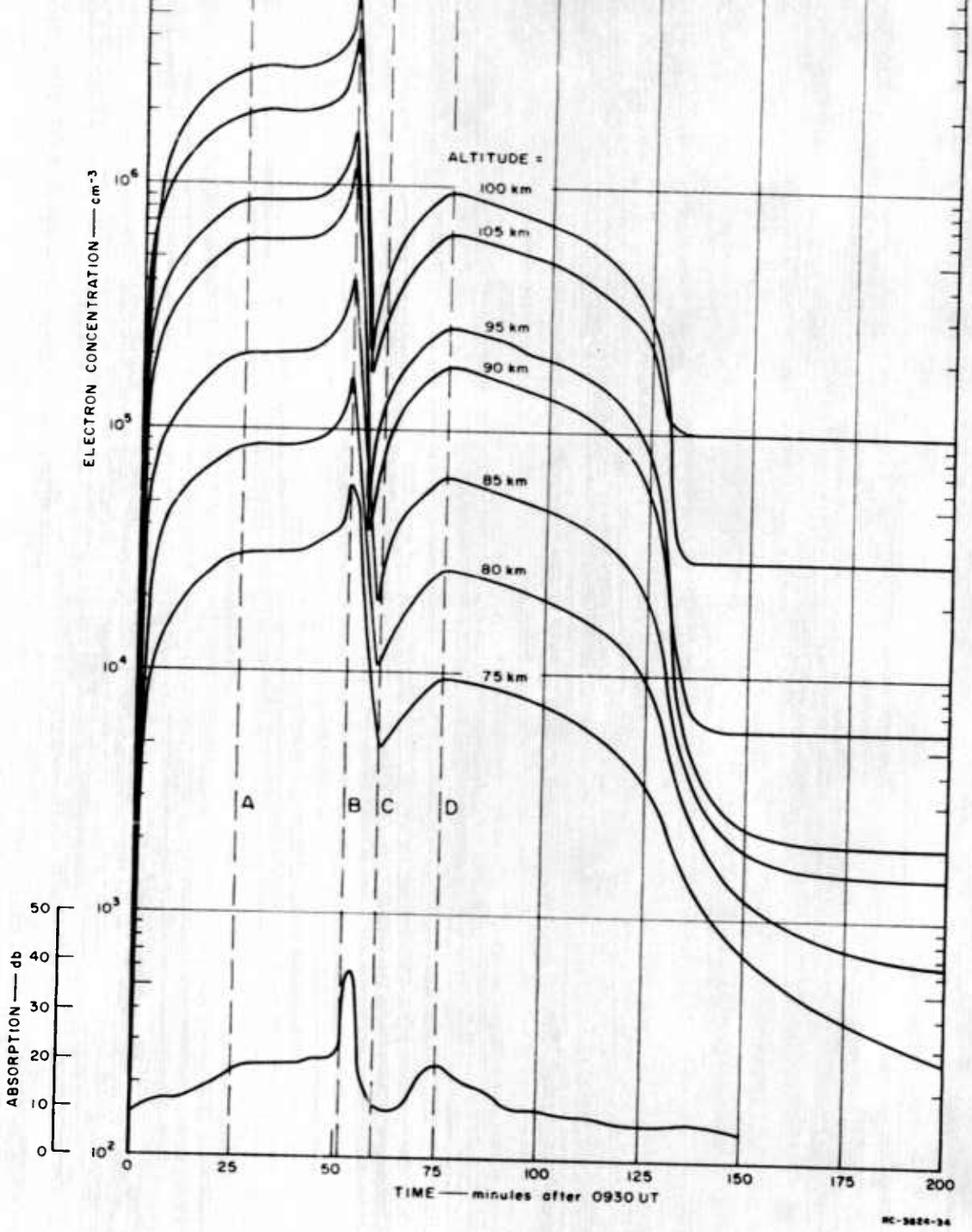

FIG. III-18 CALCULATED TEMPORAL VARIATIONS OF ELECTRON DENSITIES AND OBSERVED COSMIC NOISE ABSORPTION

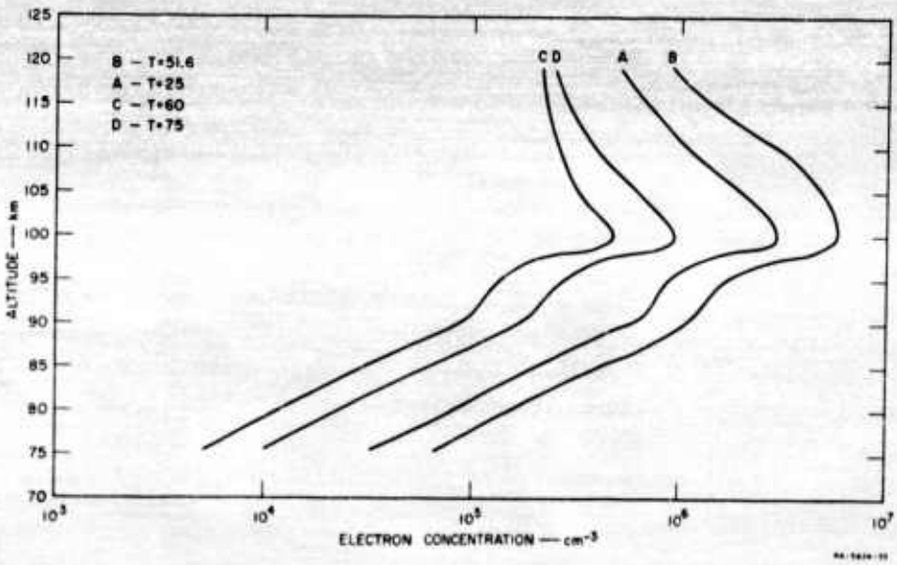

FIG. III-19 ELECTRON CONCENTRATION PROFILES FOR SEVERAL TIMES DURING THE EVENT

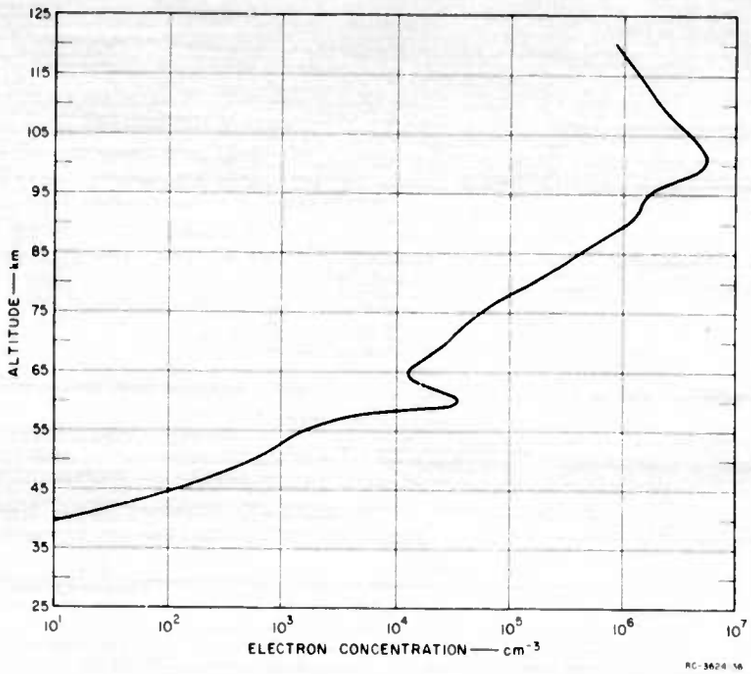

FIG. III-20 ELECTRON CONCENTRATION PROFILE AT PEAK IONIZATION (51.6 min)

compared with the peak ionization rate profile (Figure III-16). The coefficients for recombination, neutralization, attachment and detachment were taken from the appropriate sections of this report. The initial conditions for λ were also taken from this report (see section III A). The coefficients used for altitudes below 80 km become increasingly more speculative as the altitude decreases. The assumptions made in selecting coefficients for the lower altitude regions are noted in Table III-2.

Although the observations by Brown and Campbell (1962) were made in the vicinity of local midnight, calculations indicate that the atmosphere was illuminated throughout the observing period above at least 3 km. Therefore, there should be no question about the occurrence of photodetachment above the ozone layer.

In order to facilitate the calculations and provide rough estimates of electron concentrations for this report, simplifying assumptions were made in the continuity equations. For computations of electron concentrations above 75 km, λ was considered constant with respect to time. For computations below 75 km, α_i and α_D were considered equal. The results for altitudes above 75 km are considered to be good estimates in terms of the present state of knowledge. The results for altitudes below 75 km are much less defensible at this time and should be considered to be very provisional. The assumptions will be more carefully evaluated and better results should be obtained in the near future. Time-dependent solutions for λ will also be attempted.

Comparisons of the temporal-variation curves of electron densities (Figure III-18) and the temporal-variation of cosmic noise absorption (bottom of Figure III-18) are noteworthy. Inasmuch as cosmic noise absorption is dependent on free electron densities, the similarity between the shape of the electron concentration curves and the shape of the cosmic noise curve indicates that the auroral ionization model is at least partially valid. It is interesting to note that the decay of the electron density curves (after the two ionization maxima at 51.6

Table III-2

INITIAL CONDITIONS AND RECOMBINATION PARAMETERS

Altitude (km)	Recombination Parameters					Initial Conditions	
	α_D [a] cm^3/sec	α_i [b] cm^3/sec	β_m [c] sec^{-1}	ρ [d] sec^{-1}	γ_n [e] sec^{-1}	N_e cm^{-3}	λ [f]
25	2.0×10^{-6}	2.1×10^{-7}	3.6×10^{4}	0.1	1.6×10^{-2}	<1	3.6×10^{5}
30	2.0×10^{-6}	9.3×10^{-8}	8.1×10^{3}	0.1	1.5×10^{-2}	<1	8.0×10^{4}
35	2.0×10^{-6}	4.5×10^{-8}	1.7×10^{3}	0.1	8.5×10^{-3}	1	2.0×10^{4}
40	2.0×10^{-6}	1.8×10^{-8}	4.1×10^{2}	0.1	6.0×10^{-3}	8	4×10^{3}
45	2.0×10^{-6}	1.0×10^{-8}	9.7×10^{1}	0.1	4.0×10^{-3}	20	9.7×10^{2}
50	2.0×10^{-6}	1.0×10^{-8}	2.5×10^{1}	0.1	6.0×10^{-3}	30	250
55	2.0×10^{-6}	1.0×10^{-8}	9.5×10^{0}	0.1	4.0×10^{-3}	50	95
60	2.0×10^{-6}	1.0×10^{-8}	2.4×10^{0}	0.1	9.0×10^{-4}	2×10^{2}	24
65	1.5×10^{-6}	1.0×10^{-8}	6.9×10^{-1}	0.1	4.0×10^{-4}	2.5×10^{2}	6.9
70	1.0×10^{-6}	1.0×10^{-8}	2.0×10^{-1}	0.1	2.0×10^{-3}	4×10^{2}	2.0
75	8.0×10^{-7}	1.0×10^{-8}	4.5×10^{-2}	0.1	4.0×10^{-3}	6×10^{2}	0.3
80	6.0×10^{-7}	1.0×10^{-8}	9.0×10^{-3}	0.1	1.0×10^{-2}	6×10^{2}	4.5×10^{-2}
85	5.1×10^{-7}	1.0×10^{-8}	2.0×10^{-3}	1.0	1.5×10^{-2}	1.5×10^{3}	2×10^{-3}
90	5.0×10^{-7}	1.0×10^{-8}	4.0×10^{-3}	1.0	3.0×10^{-2}	2×10^{3}	4×10^{-3}
95	4.7×10^{-7}	1.0×10^{-8}	6.7×10^{-3}	1.0	5.0×10^{-2}	6×10^{3}	7×10^{-3}
100	4.2×10^{-7}	1.0×10^{-8}	2.7×10^{-3}	1.0	2.0×10^{-2}	3×10^{4}	2.7×10^{-3}
105	3.8×10^{-7}	1.0×10^{-8}	2.2×10^{-3}	1.0	1.6×10^{-2}	10^{5}	2.2×10^{-3}
110	3.4×10^{-7}	1.0×10^{-8}	1.3×10^{-3}	1.0	1.0×10^{-2}	2×10^{5}	1.2×10^{-3}
115	3.0×10^{-7}	1.0×10^{-8}	5.4×10^{-4}	1.0	4.0×10^{-3}	2×10^{5}	5.4×10^{-4}
120	2.6×10^{-7}	1.0×10^{-8}	2.7×10^{-4}	1.0	2.0×10^{-3}	2×10^{5}	2.7×10^{-4}

[a] Values of α_D below 75 km assume a clustering of molecules, values of α_D above 80 km are from curves of temperature dependence in this report, Chapt. IV.

[b] Three-body Thompson coefficient below 45 km.

[c] Above 85 km radiative attachment to O considered dominant, below 80 km three-body attachment to O_2 considered dominant.

[d] Above 85 km detachment from O^- considered dominant, below 80 km detachment from O_2^- considered dominant.

[e] Above 65 km associative detachment considered dominant, below 60 km collisional detachment considered dominant.

[f] Above 85 km initial λ considered equal to $\beta_r[O]/\rho(O^-)$
Below 80 km initial λ considered equal to $\beta[O_2]/\rho(O_2^-)$

where

β_r = radiative attachment coefficient for O
$[O]$ = concentration of atomic oxygen
β = three-body attachment coefficient for $O_2 = K[O_2]$ (see Sec. III A 3)
$[O_2]$ = concentration of molecular oxygen
$\rho(O^-)$ = photo detachment rate for O^-
$\rho(O_2^-)$ = photo detachment rate for O_2^-

and 75 mins) reassemble the decay of the cosmic noise absorption curve more closely as the altitude decreases. The results are not yet sufficiently complete to determine the altitude range that is most effective in producing this particular cosmic noise record. However, the data do seem to indicate that the lower altitude electron densities are important. Inasmuch as the collision frequency increases rapidly with decreasing altitude and the electron density in the range 75 km to 60 km decreases slowly with altitude, (and in fact increases to a maximum point at 60 km according to Figure III-20) it seems reasonable to expect that the electrons in this region are very important in producing cosmic nosie absorption.

Ionization in this region is caused by bremsstrahlung rather than primary electrons. (Compare Figures III-13 and III-16) Therefore, if the apparently important influence of lower altitude electron concentrations is confirmed by future results, the importance of bremsstrahlung will also be demonstrated.

D. Chemionization

Chemionization, which is the production of electron-ion pairs by means of chemical reactions, has been investigated in the laboratory only relatively recently (Kunkel and Gardner, 1955; Kunkel, 1956; Smith and Gatz, 1961). Since various reactants which can produce chemionization are present in the upper atmosphere, it is considered worthwhile to investigate the possible effects on ionization levels and relaxation times. Several energetically possible processes are:

$$N + N + NO \rightarrow NO^{+} + N_2 + e \qquad (1)$$

$$N + N + M \rightarrow N_2^{*} + M \qquad (2a)$$

$$N_2^{*} + NO \rightarrow N_2^{+} + NO + e \qquad (2b)$$

$$Na + O + O \rightarrow Na^{+} + O_2 + e \qquad (3)$$

where M represents an unspecified third body. Processes (1) and (2) are exothermic and (3) is endothermic by an amount approximately equal

to the mean kinetic energy of the reactants. In process (2) the intermediate excited state N_2^* can also decay by emission of radiation. Hence it must be metastable against radiation if the collisional mode (2b) dominates.

The corresponding electron production rates q are

$$q_1 = k_1 [N]^2 [NO] \tag{4}$$

$$q_2 = \frac{k_{2a} k_{2b} [N]^2 [NO][M]}{\frac{1}{\tau} + k_{2b} [NO]} \tag{5}$$

$$q_3 = k_3 [N_a] [O]^2 \tag{6}$$

where the k_α's are the rate constants of the corresponding processes listed above and τ is the lifetime of N_2^* with respect to radiation. The concentrations of the indicated atomic and molecular species at an altitude of 80 km are estimated to be of the order

$[N] \sim 10^6$ cm^{-3} (Barth, 1961)

$[NO] \sim 10^6$ cm^{-3} (Barth, 1961)

$[O] \sim 10^{12}$ cm^{-3} (Barth, 1961)

$[M] \sim 10^{14}$ cm^{-3} (Minzner, et al., 1959)

$[Na] \sim 10^4$ cm^{-3} (Bates, 1960)

Actually, Bates reports several measurements of the number of sodium atoms in a vertical column to be of the order 2-5 x 10^9 cm^{-2}. Since most of the sodium lies in the altitude range 80 to 100 km with a peak at 85 km, the concentration of sodium at 85 km is estimated to be $\sim 10^4$ cm^{-3} if we assume that all of it exists as free atoms.

Assuming (1) that the reaction rates are of the order 10^{-10} cm^3 sec^{-1} for two-body processes and $\sim 10^{-30}$ cm^6 sec^{-1} for three-body processes (these values are upper limits for the rate constants), (2) that the radiative lifetime of N_2^* is $\sim$ 1 sec, and (3) that no activation energy is required in the reactions, we obtain

$$q_1 \sim 10^{-12} \text{ cm}^{-3} \text{ sec}^{-1}$$

$$q_2 \sim 10^{-8} \text{ cm}^{-3} \text{ sec}^{-1}$$

$$q_3 \sim 10^{-2} \text{ cm}^{-3} \text{ sec}^{-1}$$

of which q_1 and q_2 are so small that equilibrium concentrations of electrons produced thereby are only of the order 10^{-2} and 1 cm^{-3}, respectively; we, therefore, neglect them. However, process (3) may be of marginal significance as a means of producing electrons at night in the region 80 to 90 km. In order to determine the nighttime contribution to the electron concentration from chemionization one must solve a number of first-order nonlinear differential equations with and without the chemionization source term; the equations containing the source term

$k_3 [Na] [O]$ are

$$\frac{d[e]}{dt} = k_3[Na][O]^2 - \alpha_D(NO^+)[NO^+][e] + \gamma [O][O_2^-] - \beta(\bar{O}_2)[O_2][e] - K[O_2]^2[e] \quad (7)$$

$$\frac{d[Na^+]}{dt} = k_3[Na][O]^2 - \alpha_i(Na^+, O_2^-)[Na^+][O_2^-] \quad (8)$$

$$\frac{d[NO^+]}{dt} = - \alpha_i(NO^+, O_2^-)[NO^+][O_2^-] - \alpha_D(NO^+)[NO^+][e] \quad (9)$$

$$\frac{d[O_2^-]}{dt} = K[O_2]^2[e] + \beta(O_2^-)[O_2][e] - (\alpha_i(Na^+, O_2^-)[Na^+] + \alpha_i(NO^+, O_2^-)[NO^+])[O_2^-] - \gamma[O][O_2^-] \quad (10)$$

where α_D and α_i are the dissociative and ion-ion recombination coefficients of the species indicated, K is the three-body and β the radiative electron attachment coefficient of O_2, and γ is the associative detachment coefficient of O_2. Actually negative ions other than O_2^- and positive ions other than NO^+ and Na^+ may also be important. Their inclusion would further complicate an already formidable set of equations. Not only is the solution difficult but, more important, the values of many of the rate constants are unknown.

One can arrive at rough estimates of the electron concentration at several hours after sunset by adding equations (7) and (10) and assuming that the negative ion-electron concentration ratio $\lambda = \frac{[O_2^-]}{[e]}$ is nearly constant in time.

$$\frac{d[e]}{dt} = \frac{q_3}{1+\lambda} - \lambda \left(\frac{\alpha_i(Na^+, O_2^-)[Na^+] + \alpha_i(NO^+, O_2^-)[NO^+]}{[Na^+] + [NO^+]} - \frac{\alpha_D(NO^+)[NO^+]}{[Na^+] + [NO^+]} \right)[e]^2 \quad (11)$$

We further assume that

$$\lambda \approx 1$$

$$\alpha_i(NO^+, O_2^-) \approx 10^{-8} \quad \text{(this paper)}$$

$$\alpha_i(Na^+, O_2^-) \approx 10^{-8} \quad \text{(Bates, 1960)}$$

$$\alpha_D(NO^+) \approx 10^{-7} \quad \text{(this paper)}$$

$$[e]_{initial} \approx 1300 \text{ cm}^{-3}$$

Electron concentrations at various times after sunset were computed using the values of the coefficients and concentrations given above for two cases: (1) without the occurrence of chemionization, and (2) with the occurrence of chemionization. The results are presented in Table IV-6.

Table IV-6

NIGHTTIME ELECTRON CONCENTRATIONS
(at 85 km)

Time after Sunset (hrs)	[e] Without Chemionization (cm^{-3})	[e] With Chemionization (cm^{-3})	$\alpha_{effective}$* ($cm^3\ sec^{-1}$)
1	900	1000	6.5×10^{-8}
2	670	800	6.4×10^{-8}
3	540	690	5.5×10^{-8}
4	440	600	5.5×10^{-8}
5	380	540	5.0×10^{-8}
6	340	500	4.2×10^{-8}
7	300	470	3×10^{-8}

*With chemionization occurring but not included in the calculation of $\alpha_{effective}$.

It is evident that even if the rather extreme value assigned to the electron production rate q_3 is correct, the effects of chemionization on the nighttime ionosphere are marginal at most. If chemionization is present and is not considered in deriving the effective nighttime recombination coefficient (from observation), the latter will appear to decrease steadily throughout the night; this is shown in the right-hand column of Table IV-6. Mitra (1957) has reported such an observed decrease in $\alpha_{effective}$ between 85 and 110 km altitude. He has attributed it to electron attachment. However, the lifetime of electrons with respect to attachment is only of the order of a few minutes in this region and the attachment process thus approaches equilibrium rapidly. Nevertheless, one cannot consider this evidence as definitely supporting the suggestion of chemionization, particularly since process (3) cannot be expected to be effective above 95 km. The question is open.

Chemionization is of potential importance in the ionosphere only when other sources of ionization are absent or very small. For example, the ultraviolet radiation from a nuclear explosion is expected to cause momentarily a very high degree of dissociation of N_2 and O_2 in the vicinity of the fireball, perhaps 10%. Large concentrations of NO will also form and the electron production rate from chemionization will be quite large--a value of $q_1 \approx 10^6$ cm^{-3} sec^{-1} would not be unreasonable. However, the local photoionization will be so large as to completely mask the chemionization effect. After the initial flash of ultraviolet radiation and X-rays, the atomic nitrogen and oxygen concentrations will rapidly decay to their normal values since radiation from fission fragments is not very effective in causing dissociation. Therefore one would expect chemionization to cease immediately after the initial radiation.

IV DE-IONIZATION PROCESSES

A. Negative Ions

1. Introduction

Existing knowledge of the nature of the neutral species present in the upper atmosphere appears to restrict the possible species of negative ions to O^-, O_2^-, O_3^-, H^-, NO_2^-, and OH^-. Which of these is the dominant negative ion is a question which can only be definitely answered by mass spectrometric measurements. It may even turn out that some species not considered heretofore is the most important one. Having no idea of the nature of such a species, however, we must of necessity restrict out discussion to the six previously mentioned.

The numerous processes involving the formation, destruction, and "shuffling" or interchange of negative ion species may be broadly classified as three-body attachment, radiative attachment, collisional type detachment, photodetachment, ion-ion recombination, charge transfer, and diffusion to dust. The following list does not exhaust all those possible but does include all processes considered potentially important (except diffusion to dust):

Three-body attachment

$$O_2 + O_2 + e \rightarrow O_2^- + O_2 \qquad (1a)$$

$$O_2 + O + e \rightarrow O_2^- + O \qquad (1b)$$

$$O_2 + O + e \rightarrow O_2 + O^- \qquad (1c)$$

Radiative attachment

$$O_2 + e \rightarrow O_2^- + h\nu \qquad (1d)$$

$$O + e \rightarrow O^- + h\nu \qquad (1e)$$

$$H + e \rightarrow H^- + h\nu \qquad (1f)$$

Photodetachment

$$O_2^- + h\nu \rightarrow O_2 + e \quad (1g)$$

$$O^- + h\nu \rightarrow O + e \quad (1h)$$

$$H^- + h\nu \rightarrow H + e \quad (1i)$$

$$NO_2^- + h\nu \rightarrow NO_2 + e \quad (1j)$$

$$OH^- + h\nu \rightarrow OH + e \quad (1k)$$

$$O_3^- + h\nu \rightarrow O_3 + e \quad (1\ell)$$

Collisional-type detachment

$$O_2^- + M \rightarrow O_2 + M + e \quad (1m)$$

$$O_2^- + O \rightarrow O_3 + e \quad (1n)$$

$$O_2^- + O \rightarrow O_3^- + h\nu;\ O_3^- + O \rightarrow O_2 + O_2 + e \quad (1o)$$

$$O^- + O \rightarrow O_2 + e \quad (1p)$$

$$H^- + H \rightarrow H_2 + e \quad (1q)$$

$$OH^- + H \rightarrow H_2O + e \quad (1r)$$

$$N + NO_2^- \rightarrow N_2 + O_2 + e \quad (1s)$$

$$O_3^- + O \rightarrow O_2 + O_2 + e \quad (1t)$$

Ion-ion recombination of the types

$$O_2^- + O_2^+ \rightarrow O_2 + O_2 \quad (1u)$$

$$O^- + N_2^+ \rightarrow NO + N \quad (1v)$$

$$O_2^- + O_2^+ + M \rightarrow O_2 + O_2 + M \quad (1w)$$

Charge transfer and ion-atom interchange

$$O_2^- + O \rightarrow O_2 + O^- \quad (1x)$$

$$O^- + NO_2 \rightarrow O + NO_2^- \quad (1y)$$

$$O_2^- + H \rightarrow O_2 + H^- \quad (1z)$$

$$O_2^- + OH \rightarrow O_2 + OH^- \qquad (1aa)$$

$$O^- + OH \rightarrow O + OH^- \qquad (1bb)$$

$$O_2^- + N_2 \rightarrow N + NO_2^- \qquad (1cc)$$

$$N + O_2^- + M \rightarrow NO_2^- + M \qquad (1dd)$$

$$O^- + O_2 + O_2 \rightarrow O_3^- + O_2 \qquad (1ee)$$

$$O_2^- + O + O_2 \rightarrow O_3^- + O_2 \qquad (1ff)$$

2. Electron Attachment

The formation of O_2^- by the three-body process (1a) has been investigated by Chanin and coworkers (1959) who found the rate constant to be sufficiently large to make the reaction of great potential importance in the D-region. For example at a temperature of $\sim 200^{\circ}K$ which is typical of D-region altitudes one obtains a value for the rate constant of $K = (1.4 \pm 0.5) \times 10^{-30}$ cm^3/sec. These investigators also found that N_2 is not an efficient "third body" in this type of reaction, being only about 2% as effective as O_2. The effectiveness of atomic oxygen as a "third body" has not been investigated. However, it is reasonable to assume that it is not more efficient than O_2 and we therefore neglect process (1b) because of the small (relative to O_2) concentrations of atomic oxygen in the D-layer.

Owing in part to obvious experimental difficulties, three-body attachment to atomic oxygen, process (1c), has never been investigated. However, we may arrive at a very rough estimate of the ratio of the rate constant to that of process (1b) from the work of Curran (1961) on dissociative attachment to ozone. Curran found that the branching ratio of the processes

$$O_3 + e \rightarrow O_2^- + O \qquad (2a)$$

$$O_3 + e \rightarrow O^- + O_2 \qquad (2b)$$

is about 7/11. If we assume that the rate of electron attachment to O_2 and O is about the same in the unbound state (processes (1b) and

(1c)) as in the bound state (process (2)), we can assign a branching ratio to processes (1b) and (1c) of order unity. We have already advanced arguments for neglecting process (1b) and thus we neglect (1c) also.

Branscomb and coworkers at the National Bureau of Standards (Branscomb, Burch, Smith and Geltman, 1958; Burch, Smith and Branscomb, 1958; Smith and Burch, 1959; Smith and Branscomb, 1960) have measured the photodetachment cross sections of O^-, O_2^-, and H^- for photon energies near threshold up to several electron volts (to be discussed in detail later). The radiative attachment cross section $\sigma_{att}(O^-)$ can be easily obtained from the photodetachment data by use of the principle of detailed balancing:

$$\sigma_{att}(O^-) = \left(\frac{\kappa}{k}\right)^2 \frac{g_-}{g_o} \sigma_{det}(O^-) \qquad (3)$$

where κ is the momentum of the incident photon divided by $\hbar$, k is the momentum of the incident electron divided by $\hbar$, $\frac{g_-}{g_o}$ is the ratio of the statistical weight of the O^- ground state to that of the oxygen atom ground state, and σ_{det} is the photodetachment cross section. One easily obtains the effective radiative attachment rate constant for any electron temperature by averaging the product of attachment cross section and electron speed over all electron energies:

$$\beta_r = \left(\frac{2}{kT}\right)^{3/2} \frac{1}{\sqrt{\pi m}} \int_0^\infty \sigma_{att} \, E \, e^{-E/kT} \, dE \qquad (4)$$

where T is the electron temperature, m the electron mass, E the electron energy, and k is Boltzmann's constant. Branscomb and coworkers (1958) found that the radiative attachment coefficient for atomic oxygen is a slowly varying function of electron temperature, decreasing from $\beta_r = 1.34 \times 10^{-15}$ cm^3/sec at an electron temperature of 250^o to $\beta_r = 1.25 \times 10^{-15}$ cm^3/sec at a temperature of 1000^oK. Actually use of the principle of detailed balancing for computation of σ_{att} is not fully justified for O^- in view of recent evidence (Schulz, 1962) that lower-lying energy states of the O^- ion may also exist. Hence the value of β_r given here must be recognized as provisional only.

In their experiment on O_2^- photodetachment cross sections Burch et al., (1958) found that the state of the O_2^- ion after attachment has "gerade" symmetry, thus permitting one to express the energy dependence (Geltman, 1958) of the cross sections as

$$\sigma_{det}(O_2^-) = E(E - E_0)^{3/2} [A_0 + A_1 (E - E_0) + A_2(E - E_0)^2 + \cdots] \tag{5}$$

where E is photon energy, E_0 is threshold energy, and the A_n are constants related to the electric dipole transition matrix elements. In practice the A_n are uncalculable to any acceptable degree of precision and must be found empirically. The first two were found to be $A_0 = 0.370 \times 10^{-18}$ cm^2 eV$^{-5/2}$, $A_1 = -0.071 \times 10^{-18}$ cm^2 eV$^{-7/2}$. The O_2^- created in the experiment apparently underwent very few collisions (of the order of one to ten per ion) (Smith and Branscomb, 1960) prior to electron detachment. We shall cite evidence later which seems to indicate that the O_2^- is formed in an excited state and then deactivated only after many collisions ($\gg 10$). Assuming that this interpretation is correct, the O_2^- ions must have remained essentially unchanged during the course of the experiment.

Invoking the principle of detailed balancing, one obtains the following equation for σ_{att} with the aid of (5)

$$\sigma_{att} = \frac{(\epsilon + E_0)^3 \epsilon^{1/2}}{2mc^2} [A_0 + A_1\epsilon + A_2\epsilon^2 + \cdots] \frac{g_-}{g_0} \tag{6}$$

where ϵ is the kinetic and mc^2 the rest energy of the electron. Equations (4) and (6) together with the previously stated values of A_0 and A_1 yield a value for $\beta_r(O_2^-)$ of $\sim 10^{-20}$ cm^3/sec at an electron temperature of 250°K.

Of course, the principle of detailed balancing is not really applicable here because neither O_2^- nor O_2 is necessarily left in the ground state after electron attachment and detachment; excited vibrational, rotational, and possibly electronic states can be occupied. In

other words, the process is not reversible and

$$\left| < O_2^-, h\nu \left| H^1 \right| O_2, e \left| \frac{1}{T} \right| O_2, e \left| H^1 \right| O_2^-, h\nu > \right|, \qquad (7)$$

where H^1 is the electric dipole operator. However, it is thought unlikely that the effect of such allowed excited states would increase the value of β_r by more than two to three orders of magnitude from that given above. In order to be of any importance in determining the rates of ionospheric processes we must have $\beta_r > 10^{-17}$ cm^3/sec. Hence it is unlikely (though not certain) that radiative attachment of electrons to O_2 is an important atmospheric reaction under normal conditions; this process may be of marginal significance at altitudes of 85 km and above. It can be shown that the radiative attachment coefficient increases with increasing temperature. At an electron temperature of 1000°K, for example, $\beta_r(O_2^-) \gtrsim 10^{-19}$ cm^3/sec, an increase of about a factor of ten over the value at a temperature of 250°K. Hence under disturbed conditions (e.g., SID or nuclear blackout) radiative attachment to O_2 may conceivably be of some importance. Further experimental investigation is definitely in order.

Smith and Burch (1959) have measured the photodetachment cross section of H^- for various electron energies above threshold. Use of the principle of detailed balancing (which can be justified as in the case of O^-) yields a radiative attachment coefficient of $\sim 10^{-16}$ cm^3/sec at a temperature of 200°K. Because of the relatively small concentrations ($n(H) \lesssim 10^9$ cm^{-3}) (Handbook of Geophysics, 1960) direct attachment to this species proceeds at a much smaller rate than direct attachment to atomic and molecular oxygen and hence process (1f) can be neglected.

We are thus left with processes (1a) and (1e) as the dominant direct attachment reactions. At an altitude of 85 km the rate of electron attachment to both atomic and molecular oxygen is about $\sim 10^{-3}$ sec^{-1}, assuming concentrations of $[O_2] \sim 3 \times 10^{13}$ cm^{-3} and $[O] \sim 5 \times 10^{11}$ cm^{-3} (Handbook of Geophysics, 1960). Below this altitude the rate of the three-body mode (1a) increases rapidly due to increasing concentration of O_2, while

the rate of process (1e) decreases slowly. Hence we conclude that radiative attachment of electrons to atomic oxygen is important only at the top of the D-region and that process (1a) provides the dominant attachment mechanism below.

It should be noted that we have excluded direct attachment to NO_2. Curran (1962) has apparently established this process to be forbidden.

3. Electron Detachment

Some of the electron detachment processes (1g, 1h, 1i, 1m) have also been investigated recently but the results have not been sufficient for the development of a reliable model of electron detachment in the ionosphere.

Photodetachment cross sections in the photon energy range 0 to 3 eV have been measured for O^- and O_2^- by Branscomb and coworkers (Branscomb, Burch, Smith and Geltman, 1958; Burch, Smith, and Branscomb, 1958) at the National Bureau of Standards. The O^- cross section was found to be a rapidly increasing function of photon energy between threshold (EA = 1.465 eV) and $\sim$ 1.6 eV ($\sigma = 5 \times 10^{-18}$ cm^2) after which it levels off, reaching 7×10^{-18} cm^2 at a photon energy of $\sim$ 3 eV. These results are in good agreement with the theory of photodetachment from negative atomic ions developed by Klein and Brueckner (1958). The ionospheric specific photodetachment rate is obtained from the equation

$$\rho = \int \sigma_{det} \left(\frac{dI}{d\lambda}\right) d\lambda \qquad (8)$$

where σ_{det} is the photodetachment cross section and $I(\lambda)$ is the solar photon number flux at wavelength λ incident on the ionosphere. The result for O^- is $\rho = 1.4$ sec^{-1} (Smith, Burch, and Branscomb, 1958).

Because of the possible presence of excited states, the situation for photodetachment from O_2^- is more complicated; one would in general expect to find different cross sections for detachment from ground and excited states, partly because of the difference in predicted threshold energies and partly because of different transition matrix elements

for the two cases. Geltman (1958) has computed the energy dependence near threshold of the photodetachment cross section of O_2^- and has obtained relation (5). In their investigation of the problem, Burch and coworkers (1958) were able to determine A_0 and A_1 as well as E_0 by a least squares fit of their experimental data to the theoretical form of σ_{det}. The value of the threshold energy ($E_0 = 0.15$ eV) was considerably smaller than that obtained by Phelps and Pack (1961) ($E_0 = 0.46$ eV) by means of collisional detachment experiments. This evidence seems to indicate that O_2^- is formed in an excited (probably vibrational) state. The gas pressures and ion residence times in the swarm experiments of Phelps and Pack were sufficiently large to permit collisional de-excitation to occur; they estimated that approximately 10^5 collisions of each O_2^- with neutral molecules occurred during the experiment. On the other hand, the gas pressures as well as the residence times in the photodetachment experiments (Smith and Branscomb, 1960) were so small that the mean number of collisions of each O_2^- ion with a neutral particle was only of the order of one to ten.

In contrast to the results of the experiments mentioned above, chemical experiments (Pritchard, 1953) seem to indicate an electron affinity of slightly less than 1 eV. A spectrophotometric measurement by Jortner and Sokolov (1961) and a measurement by Curran (1961) using data from an experiment on dissociative attachment to ozone yielded somewhat smaller values for the electron affinity, ~ 0.75 eV and > 0.58 eV, respectively. It is difficult to reconcile these results with those of Phelps and Pack (1961). A possible explanation is the existence of a metastable vibrational state at $E_0 \approx 0.46$ eV, the de-excitation from this to the ground state being of a high order of forbiddenness. In order to complete this explanation one must assume that in the experiments of Pritchard, Jortner, and Curran O_2^- is either formed in the low-lying state or undergoes relaxation in such a way as to avoid the metastable state.

It is expected that most of the O_2^- ions in the sunlit D-region will be in the ground state or a low-lying metastable excited state because of the relatively high gas pressures and long lifetimes (> 2 seconds) of the ions. If one approximates the solar radiation spectrum in the near infrared and visible regions by a black-body distribution and substitutes it for $\frac{dI}{d\lambda}$ in equation (8), one obtains an approximate threshold energy dependence of ρ

$$\frac{\rho(E_0)}{\rho(E_0')} \approx e^{-\frac{(E_0 - E_0')}{kT}} \frac{A_0(E_0)}{A_0(E_0')} \qquad (9)$$

For a solar surface temperature of 6000°K one obtains

$$\frac{\rho(0.45\ eV)}{\rho(0.15\ eV)} \approx 0.5\ \frac{A_0(0.46\ eV)}{A_0(0.15\ eV)} \qquad (10)$$

By substituting the observed solar spectrum, $\frac{dI(\lambda)}{d\lambda}$, in equation (8) Smith et al., (1958) obtained a value of $\rho(0.15\ eV) = 0.44\ sec^{-1}$. Making the reasonable assumption that $A_0(0.15\ eV) \geq A_0(0.46\ eV)$, we have $\rho(0.46\ eV) \lesssim 0.2\ sec^{-1}$. Further investigation of this problem is required before we can obtain a reliable D-region photodetachment rate. We shall provisionally adopt a value of $\rho(O_2^-) \approx 0.1\ sec^{-1}$.

Smith and Burch (1959) have investigated photodetachment from H^-. Their cross section data together with the solar spectral data used for the computation of $\rho(O^-)$ and $\rho(O_2^-)$ (Smith, Burch, and Branscomb, 1958) yield a detachment rate of $\rho \approx 8\ sec^{-1}$.

Photodetachment from NO_2^-, OH^-, and O_3^- has not been investigated although some idea of the electron affinities is available. Curran (1962) has shown that the electron affinity of NO_2^- is greater than 3.82 eV by causing NO_2 to undergo charge transfer with Cl^- (whose EA = 3.82 eV). The ion OH^- apparently has an electron affinity lying somewhere between 2 and 3 eV (Field and Franklin, 1957) while that of O_3^- is estimated to be of the order of 3 eV (Curran, 1961).

It has been proposed that NO_2^- may be the dominant negative ion in the D-region. This suggestion originated with the apparent observation by Johnson and coworkers (Johnson, Heppner, Holmes, and Meadows, 1958) of negative ions of mass number 46 in the E-region. The reliability of these measurements is uncertain; the NO_2^- may have been a product of the rocket exhaust.

It is known that just after sunset and just prior to sunrise when the sun's rays which illuminate the D-region must first pass through the ozone layer (Figure IV-1), the electrons in the D-region rapidly

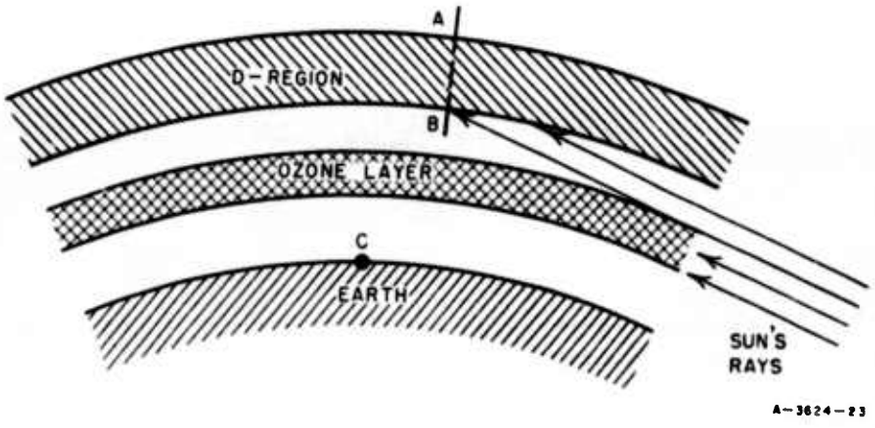

FIG. IV-1 SUNRISE-SUNSET EFFECT

At sunset the near UV solar radiation which would otherwise illuminate that part of the D-region lying to the left of line AB is absorbed by the ozone layer when the sun drops below the horizon with respect to an observer at C. Coincident with the absorption of this radiation is the rapid decrease in electron density (probably due to electron attachment) in the region to the left of line AB. The opposite effect (rapid detachment of electrons when the sun's rays pass above the ozone layer) occurs at sunrise.

attach to form negative ions (see, for example, Reid, 1961). This is called the "sunrise-sunset effect." One infers from this that the solar radiation responsible for photodetachment must be strongly absorbed by ozone and must therefore lie in the near UV spectral region. If one computes the spectral detachment rate for O^- and H^- by means of the

equation

$$\frac{d\rho}{d\lambda} = \sigma_{det} \frac{dI(\lambda)}{d\lambda} \qquad (11)$$

where the symbols have the same significance as in equation (8), one obtains the curves shown in Figure IV-2. The near UV obviously is of little importance in photodetachment from O^- and H^-. We conclude from this that O^- and H^- are not the dominant negative ions present in the D-region. If one then computes $\frac{d\rho}{d\lambda}$ for O_2^- using the cross sections reported by the NBS groups (Burch, et al., 1958) one also finds that this species is apparently in disagreement with the requirements of the "sunrise-sunset effect." If, however, the O_2^- just prior to

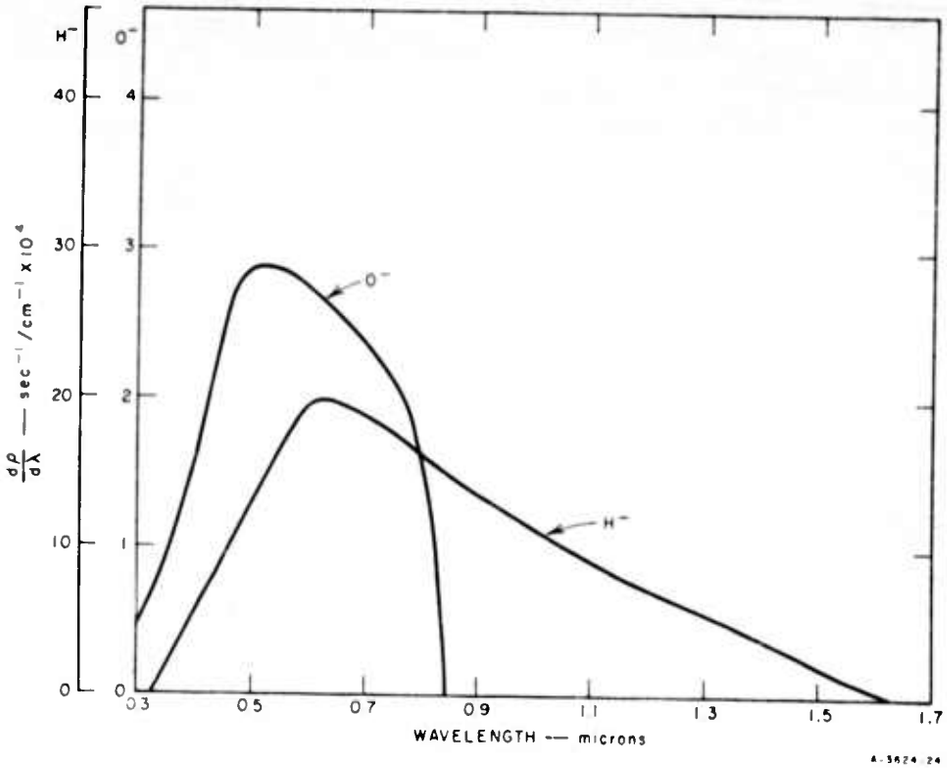

FIG. IV-2 SPECTRAL DETACHMENT RATE $d\rho/d\lambda$ OF O^- AND H^-

detachment is in a lower-lying state, e.g., EA = 0.46 eV, than that reported by the NBS groups, the photodetachment cross section could conceivably be very small in the spectral region above λ = 3500 A (~ 3.5 eV) and sufficiently large between 2500 to 3500 A that radiation in this spectral range is almost entirely responsible for the photodetachment. This hypothesis is not in disagreement with Geltman's theory of photodetachment from O_2^-.

If the electron affinity of NO_2^- is ~ 4 eV or perhaps even a little larger, photodetaching radiation is restricted to the near UV for this ion and it can meet the requirements of the "sunrise-sunset effect." Similarly, if the electron affinities of OH^- and O_3^- are ~ 3 eV as some measurements seem to indicate, these ions too can satisfy the "sunrise-sunset effect" requirements. Which, if any, of these negative ions is the dominant one in the D-region can be ascertained only by in situ experiments.

In the foregoing we have considered only solar radiation in the photodetachment process. The initial burst of radiation from a nuclear explosion is so intense that the negative ion concentration will be negligible at all altitudes for several seconds after detonation due to photodetachment. Subsequent to that time the only nuclear radiations which can detach electrons are β and γ rays. For reasonable beta particle/photon intensities (Poppoff, et al., 1961) (~ 10^6 to 10^8 cm^2/sec at 1 mev energy) the detachment cross sections (essentially the Møller and Compton scattering cross sections which are approximately equal to 10^{-23} and 10^{-18} cm^2, respectively) are much too small to yield more than an insignificant detachment rate. Hence we conclude that detachment of electrons from negative ions by delayed radiation from a nuclear burst is unimportant compared to solar photodetachment and detachment by collisions.

Collisional-type detachment from O_2^- and O^- was recently considered by Whitten and Poppoff (1962) who concluded on the basis of a study of polar cap absorption made by Bailey (1959), that associative detachment,

processes (1n), (1o), and (1p), is the dominant mechanism. Bailey's analysis of PCA events required a nighttime detachment rate of $\sim 10^{-2}$ sec^{-1}. Phelps and Pack (1961) found that the rate constant for process (1ℓ) was about 4×10^{-20} cm^3/sec at D-region temperatures and that molecular nitrogen is ineffective as a detaching agent. If we multiply the rate constant by the molecular oxygen concentration at an altitude of $\sim$ 70 km ($\sim 4 \times 10^{14}$ cm^{-3}), we obtain a detachment rate of only $\sim 10^{-5}$ sec^{-1}. Weber (1962) has suggested that process (1m) may be dominant by virtue of the fact that it is a rapidly increasing function of temperature. However, for reasonable values of the temperature at this altitude (250-300°K) it is too small to agree with the empirical value of the rate constant suggested by Bailey. Of course, NO_2^-, OH^-, or O_3^- may be the dominant negative ions in which case processes (1r), (1s) or (1t) rather than (1m), (1o) or (1p) are important.

The rate constants for processes (1n), (1o), and (1p) have been estimated by various workers to lie between 10^{-10} and 10^{-15} cm^3 sec^{-1} (Mitra, 1952; Dalgarno, 1961). Dalgarno's limiting estimate of 10^{-10} cm^3 sec^{-1} was presumably made under the assumption that almost every O_2^- - O and O^- - O collision results in a detaching reaction. This is, however, probably too optimistic.

The concentrations of atomic oxygen present in the daytime D-region have been computed by various workers (Barth, 1961; Handbook of Geophysics, 1960) and seem to be of the order of 10^{11} to 10^{12} cm^{-3} between 60 and 90 km. At night the atomic oxygen promptly combines with O_2 to form ozone by means of a three-body collision process at altitudes below 70 km. According to Barth (1961) the atomic oxygen concentration decreases by about a factor of 10 at an altitude of 70 km at night. It remains essentially constant in time at altitudes of 80 km and above. If our effective associative detachment coefficient is $\sim 10^{-13}$ cm^3 sec^{-1} and $[O] \approx 10^{11}$ cm^{-3} at 70 km at night, we see that the nighttime detachment rate is $\sim 10^{-2}$ sec^{-1} as required by Bailey's analysis.

In addition to processes (1n), (1o), and (1p), associative detachment from H^- and OH^- can also occur (processes (1q) and (1r)). Assuming an atomic hydrogen concentration at 70 km altitude of 10^9 cm^{-3} (Handbook of Geophysics, 1960), one must assign a rate constant to the processes of 10^{-11} cm^3 sec^{-1}

in order to obtain agreement with Bailey's analysis. Such values are not unreasonable. To our knowledge the ion OH^- has not heretofore been proposed as the dominant negative ion in the D-region but the considerations above seem to indicate that it cannot be excluded.

Nighttime detachment from NO_2^- can occur via process (1s) if the electron affinity of this ion is less than ~ 4.5 eV, otherwise, only the particles in the Maxwellian "tail" of the velocity distribution have sufficient energy to cause electron detachment. Nighttime detachment from O_3^- can occur via process (1t). The values of the associated rate constants are unknown but $k_{s,t} \times 10^{-12}$ cm^3 sec^{-1} is not unreasonable.

4. Charge Transfer and Ion-Atom Interchange

In addition to the processes of direct formation and destruction of negative ions (1a to 1w) there is the possibility of charge transfer and ion-atom interchange (1x to 1dd). All of these processes are energetically possible but their rates are completely unknown with the exception of (1y). Curran (1962) has estimated the value of the corresponding rate constant for (1y) to be of the order 10^{-10} to 10^{-9} cm^3 sec^{-1}, using the results of his mass spectrometer experiments. It is reasonable to assume that the coefficients corresponding to the other processes (except 1cc and 1dd) are of the same order of magnitude as the rate constants of positive ion charge transfer reactions, i.e., $\sim 10^{-13}$ to 10^{-10} cm^3 sec^{-1}. Processes (1cc and 1dd) involve the breaking and/or forming of chemical bonds and may thus have considerable activation energies. If so, they are expected to be slower than the charge transfer reactions. Actually, process (1cc) is energetically forbidden unless NO_2^- has an electron affinity greater than ~ 5.7 eV. However, it has been previously shown that nighttime detachment will not occur unless the electron affinity is less than ~ 4.5 eV. We therefore rule out reaction (1cc).

Similar processes (1ee and 1ff) can produce O_3^-; both are exothermic. Since molecular oxygen is much more effective than molecular nitrogen in three-body attachment (1a), it is probable that we can limit our consideration of third bodies to O_2.

5. Negative Ion Kinetics

In the foregoing we concluded, for various reasons, that many of the negative ion processes can probably be neglected. In addition, it can be shown that the ion-ion recombination processes above 80 km are probably much slower than the others listed. Those remaining are (1a), (1e), (1g), (1h), (1j), (1k), (1n) to (1p), (1r) to (1t), (1x), (1y), (1aa), (1bb), and (1dd) to (1ff); the kinetic equations for these processes can be written:

$$\frac{d[O_2^-]}{dt} = K[O_2]^2[e] - \rho(O_2^-)[O_2^-] - \gamma_{n,o}[O_2^-][O] - k_x[O_2^-][O] - k_{aa}[O_2^-][OH] - k_{dd}[O_2^-][N][N_2] - k_{ff}[O_2^-][O][O_2] \quad (12)$$

$$\frac{d[O^-]}{dt} = \beta[O][e] + k_x[O_2^-][O] - \rho(O^-)[O^-] - \gamma_p[O^-][O] - k_y[O^-][NO_2] - k_{bb}[O^-][OH] - k_{ee}[O^-][O_2]^2 \quad (13)$$

$$\frac{d[NO_2^-]}{dt} = k_y[O^-][NO_2] + k_{dd}[O_2^-][N][N_2] - \rho(NO_2^-)[NO_2^-] - \gamma_s[NO_2^-][N] \quad (14)$$

$$\frac{d[OH^-]}{dt} = k_{aa}[O_2^-][OH] + k_{bb}[O^-][OH] - \rho(OH^-)[OH^-] - \gamma_r[OH^-][H] \quad (15)$$

$$\frac{d[O_3^-]}{dt} = k_{ee}[O^-][O_2]^2 + k_{ff}[O_2^-][O][O_2] - \rho(O_3^-)[O_3^-] - \gamma_t[O_3^-][O] \quad (16)$$

where K is the rate constant for three-body electron attachment to O_2, β is the coefficient of radiative attachment to O, ρ is the photodetachment rate for the species indicated, e.g., $\rho(O_2^-)$, γ_σ are the collisional type detachment rates, and k_μ the rate constants for the charge transfer processes; e.g., k_y is the rate constant for process (1y), etc. Square brackets represent the concentrations of the various species.

The following values of some of the rate parameters are assumed:

$K = 1.5 \times 10^{-30}$ cm^3/sec (Chanin, et al., 1959)

$\rho(O_2^-) = 0.1$ sec^{-1} (this paper)

$\rho(O^-) = 1.4$ sec^{-1} (Branscomb, et al., 1958)

$\rho(NO_2^-) = 10^{-6}$ sec^{-1} (assumed)

$\beta = 1.34 \times 10^{-15}$ cm^3 sec^{-1} (Branscomb, et al., 1958)

$k_v = 3 \times 10^{-10}$ cm^3 sec^{-1} (Curran, 1962)

$k_{dd} = k_{ee} = k_{ff} = 10^{-28}$ cm^6 sec^{-1} (assumed)

In addition we assume daytime concentrations of N_2, O_2, O, NO_2, OH, H and electrons at 75 km altitude as follows:

$[N_2] = 8 \times 10^{14}$ cm^{-3} (Minzner, 1959)

$[O_2] = 2 \times 10^{14}$ cm^{-3} (Minzner, 1959)

$[O] = 2 \times 10^{11}$ cm^{-3} (Barth, 1961)

$[NO_2] = 10^2$ cm^{-3} (Barth, 1961)

$[OH] = 10^8$ cm^{-3} (Handbook of Geophysics, 1960)

$[H] = 10^9$ cm^{-3} (Handbook of Geophysics, 1960)

$[e] = 500$ cm^{-3} (day) (Galejs, 1962)

100 cm^{-3} (night) (Galejs, 1962)

The equilibrium concentrations of the various negative ions for possible values of γ_t, $\rho(OH^-)$, $\rho(O_3^-)$, and [N] are presented in Table IV-1. Although the set of values used is by no means exhaustive, it does give some idea of the range of negative ion concentrations which may be expected under daytime and nighttime conditions. It is apparent from the right-hand columns that OH^-, NO_2^-, and O_3^- may be of great importance in the D-region.

Table IV-1

EQUILIBRIUM CONCENTRATIONS OF NEGATIVE IONS
AT 75 KM ALTITUDE (cm^{-3})

$k_{x,aa,bb}$ $cm^3\ sec^{-1}$	$\gamma_{n,o,p,r,s}$ $cm^3\ sec^{-1}$	γ_t $cm^3\ sec^{-1}$	$\rho(OH^-)$ sec^{-1}	$\rho(O_3^-)$ sec^{-1}	[N] cm^{-3}	$[O^-]$ cm^{-3}	$[O_2^-]$ cm^{-3}	$[NO_2^-]$ cm^{-3}	$[OH^-]$ cm^{-3}	$[O_3^-]$ cm^{-3}
Day										
10^{-13}	10^{-13}	10^{-13}	10^{-3}	10^{-2}	10^6 (Barth, 1961)	1	200	15	2	150
10^{-13}	10^{-13}	10^{-14}	10^{-4}	10^{-3}	10^7	1	200	150	20	1500
10^{-11}	10^{-11}	10^{-12}	10^{-2}	10^{-2}	10^6	5	8	0.06	4	100
10^{-12}	10^{-12}	10^{-13}	10^{-2}	10^{-2}	10^6	8	60	2	7	500
Night										
10^{-13}	10^{-13}	10^{-13}	-	-	10^6 (Barth, 1961)	1/16	150	120	150	40
10^{-13}	10^{-13}	10^{-14}	-	-	10^7	1/16	150	1200	1500	400
10^{-11}	10^{-11}	10^{-12}	-	-	10^6	8	8	0.06	8	100
10^{-12}	10^{-12}	10^{-13}	-	-	10^6	8	8	5	70	800

The various rate constants suggested for OH^-, O_3^-, and NO_2^- are entirely reasonable. For example, the photodetachment rate for OH^- could well be 10^{-3} sec^{-1} if the electron affinity is as large as 3 eV. It is quite possible that all four species O_2^-, OH^-, O_3^-, and NO_2^- are important in the D-region, the relative importance of each varying with altitude and condition of daytime or nighttime. We re-emphasize that the foregoing are only plausibility arguments.

6. Conclusions

The following conclusions are drawn from the preceding arguments.

a. One cannot identify the species O^- and H^- with the dominant negative ions in the lower D-region, since they both conflict with the "sunrise-sunset effect." O^- may be important in the upper D-region.

b. O_2^-, OH^-, O_3^-, or NO_2^- may be the dominant species of negative ion without contradicting existing knowledge of the D-region. In fact they may all be important.

c. Radiative attachment to O_2 and three-body attachment to O are probably not important processes. Further investigation is required before this statement can be definitely established, however.

d. Associative detachment is probably the dominant nighttime mode of electron detachment from the species O_2^- and OH^-. Detachment from NO_2^- and O_3^- can occur via dissociative processes (1s and 1t).

e. Previously proposed values of the photodetachment rate for O_2^- are not reliable.

f. Diffusion to dust is an unimportant mode of negative ion removal (see Section VIII).

At the risk of seeming trite we reiterate the need for further measurements, both laboratory and in situ, if a reliable model of negative ion species and distribution is to be constructed.

B. Charge Transfer and Ion-Atom Interchange (Positive Ions)

In this section we shall investigate the importance of charge transfer and ion-atom interchange processes with respect to the ionic and electronic structures of the D- and E-regions. Specifically we shall show that these processes control the concentrations of the various ion species by "shuffling" them more rapidly than they can be created. The nature of the ionic species in turn has an important bearing on the rate of electron recombination and hence the electron density profile. There are many such processes which are possible in the altitude interval 80 to 150 km (Bortner, 1961a; Bortner and Baulknight, 1961b; Nawrocki, 1961a) but most can be eliminated for various reasons, e.g., a participating neutral species is present only in trace concentrations, reactions are highly endothermic, activation energies are too large for the process to be important at ordinary temperatures, etc. The following reactions are considered potentially important in the shuffling process.

$$O^+ + O_2 \rightarrow O + O_2^+ \qquad (1)$$

$$N_2^+ + O \rightarrow N_2 + O^+ \qquad (2)$$

$$N_2^+ + O_2 \rightarrow N_2 + O_2^+ \qquad (3)$$

$$N_2^+ + NO \rightarrow N_2 + NO^+ \qquad (4)$$

$$O_2^+ + NO \rightarrow O_2 + NO^+ \qquad (5)$$

$$O^+ + NO \rightarrow O + NO^+ \qquad (6)$$

$$O^+ + N_2 \rightarrow NO^+ + N \qquad (7)$$

$$O^+ + NO \rightarrow O_2^+ + N \qquad (8)$$

$$O_2^+ + N \rightarrow NO^+ + O \qquad (9)$$

$$N_2^+ + O_2 \rightarrow NO + NO^+ \qquad (10)$$

$$O_2^+ + N_2 \rightarrow NO + NO^+ \qquad (11)$$

$$N_2^+ + O \rightarrow N + NO^+ \qquad (12)$$

However, two of the processes [(10) and (11)] involve the breaking of two double bonds and hence are expected to have large activation energies. Bortner (1961a) has assigned rate constants of 7×10^{-15} and 3×10^{-17} cm^3/sec, respectively, but these are admittedly crude estimates only and are probably upper bounds on the actual values. In any event these estimates are sufficiently small that processes (10) and (11) can be neglected in any consideration of the ionosphere above 90 km. Fite and coworkers (Fite, Rutherford, Snow and van Lint, 1962) have found that the former is much slower than the charge transfer process (5). Nevertheless reaction (11) must be considered in ion shuffling kinetics at altitudes below 90 km. D. R. Bates (private communication) has concluded that process (12) is suppressed by virtue of the fact that an electronic transition is involved. We have therefore assumed it to be of negligible importance in our model.

The largest possible value of the rate constants for any of the processes (1) to (9) occurs if a reaction takes place during every collision; this value is of the order of 10^{-9} cm^3/sec if we equate the reaction cross section to the classical collision cross section (Eyring, Hirshfelder, and Taylor, 1936). For reasonable estimates of the concentration of nitric oxide in the upper atmosphere (see, for example, Handbook of Geophysics, 1960) the reaction rates of processes (4), (5), (6), and (8) are too small for these processes to be important in determining the equilibrium concentrations of the principal ion species. Process (9) is believed unimportant for a similar reason (small $[N]$). The remaining processes are (1), (2), (3), (7) and below 90 km, (11), and the equilibrium equations for the various ion species can be approximated by

$$q_a = \alpha_D^a [N_2^+][e] + k_2[N_2^+][O] + k_3[N_2^+][O] \qquad (13)$$

$$q_b = \alpha_D^b [O_2^+][e] - k_3[N_2^+][O_2] - k_1[O^+][O_2] + k_{11}[O_2^+][N_2] \qquad (14)$$

$$q_c = k_7[O^+][N_2] + k_1[O^+][O_2] - k_2[N_2^+][O] \qquad (15)$$

$$0 = \alpha_D^d [NO^+][e] - k_7[O^+][N_2] - k_{11}[O_2^+][N_2] \qquad (16)$$

where $q_{a,b,c}$ represent the production rates of N_2^+, O_2^+, and O^+, respectively, the k's are the rate constants corresponding to certain of the processes (as indicated by the subscripts) (1) to (9), the square brackets represent the concentrations of the indicated ions and neutral species, and $\alpha_D^{a,b,d}$ represent the dissociative recombination coefficients of N_2^+, O_2^+, and NO^+, respectively. We shall show in Section IV-D that ion-ion recombination can probably be neglected in the daytime at altitudes above 80 km. Obviously we must require that

$$[e] = [N_2^+] + [O_2^+] + [O^+] + [NO^+] \qquad (17)$$

and

$$q\ (\text{electron}) = q_a + q_b + q_c = q\ (\text{ion}) \qquad (18)$$

if electric charge is to be conserved.

In addition to the effects of recombination, two other electron-ion removal processes, diffusion and ionospheric currents, should in principle be included in the equilibrium equations. The effects of vertical diffusion were computed by finding the approximate value of the term $\frac{\partial}{\partial h}(N_+ W)$ where N_+ is the positive ion density, h refers to altitude and W is the diffusion velocity given by

$$W = -D\left(\frac{1}{N}\frac{\partial N}{\partial h} + \frac{1}{H}\right) \qquad (19)$$

In equation (19) D is the diffusion coefficient, N is the neutral species concentration and H is scale height. According to Nawrocki and Papa (1961b) the diffusion coefficient of NO^+ in air (at temperatures $> 300^\circ K$) is given approximately by

$$D = \frac{9 \times 10^{16}\ T^{\frac{1}{2}}}{N} \qquad (20)$$

where T is the temperature in $^\circ K$. Using reasonable values of T and N (Minzner, et al., 1959), it was found that the diffusion term was only about four percent of the magnitude of the recombination term at an altitude of 150 km. Hence the former is entirely neglected in this treatment since it rapidly decreases as one descends to lower altitudes.

The effects of the ionospheric current system on electron-ion removal have only recently been discovered (L. H. Brace, private communication). At the present time we do not have sufficient information for a quantitative study of its effects on the ion concentrations present in the E-region. Since the rate constants reported here are order of magnitude only, it is not likely that they would be greatly changed by inclusion of the current term. This point will be investigated in a future report when more data are available.

If the values of the various rate constants as well as the q's are known, the ion concentrations can be readily computed. Conversely, the rate constants k can be found if the ion concentrations, ion production rates, and dissociative recombination coefficients are known. Actually, sufficient knowledge of the upper atmosphere for the determination of precise values of any of these quantities does not exist. Nevertheless one can obtain order of magnitude estimates of the rate constants from mass spectrometric measurements of the relative concentrations of various ionic species between 100 and 200 km altitude together with estimates of the dissociative recombination coefficients $\alpha_D^{a,b,d}$ based on results obtained in the next section and the production rates of the various ionic species, $q_{a,b,c}$. The mass spectrometric measurements of the relative concentrations of the various species of positive ions at various altitudes (Johnson, Meadows, and Holmes, 1958; Meadows and Townsend, 1960; Taylor and Brinton, 1961; Istomin and Pokhunkov, 1962) are listed in Table IV-2. The values of the dissociative recombination coefficients presented in Table IV-3 are based on considerations discussed in the next section. The concentrations of N_2, O_2, and O at various altitudes according to a model developed at the National Bureau of Standards (Norton, van Zandt and Denison, 1962) are presented in Table IV-4. Production rates of N_2^+, O_2^+, and O^+ (Norton, van Zandt, and Denison, 1962) based on recently obtained solar ultraviolet spectra (Watanabe and Hinteregger, 1962) are listed in Table IV-5.

Table IV-2

RELATIVE CONCENTRATIONS OF POSITIVE ION SPECIES

Rocket Flight	Altitude (km)	Fraction of Total Positive Ions which are:			
		N_2^+	O_2^+	NO^+	O^+
NN 3.17 F[1]	150	<0.03	0.4	0.5	0.1
2321 CST	120	<0.03	0.2	0.8	<0.03
20 Nov. 56	100	<0.03	~ 0	1.0	~ 0
NN 3.18 F[1]	150	<0.03	0.1	0.8	0.1
2002 CST	120	<0.03	0.1	0.9	<0.03
21 Feb. 58	100	<0.03	0.1	0.9	~ 0
NN 3.19 F[1]	150	<0.03	0.3	0.6	0.1
1207 CST	120	<0.03	0.3	0.7	<0.03
23 Mar. 58	100	<0.03	0.4	0.6	~ 0
NASA 4.09[2]	150	~0.01	0.3	0.6	0.1
1047 EST	120	~0.01	0.1	0.9	<0.05
20 Apr. 60	100	~0.01	0.1	0.9	~ 0
NASA 4.14[2]	150	~0.01	0.4	0.4	0.2
1141 EST	120	~0.01	0.2	0.8	0.05
15 Nov. 60	100	~0.01	~ 0	1.0	~ 0
USSR[3]	150	--	0.1	--	--
h = -6°e	120	--	--	--	--
9 Sept. 57	100	--	--	--	--
USSR[3]	150	--	0.2	0.6	0.2
h = 36°m	120	--	0.3	0.7	~ 0
2 Aug. 58	100	--	0.2	0.8	~ 0
USSR[3]	150	--	0.4	0.6	0.05
h = 0°m	120	--	0.2	0.8	~ 0
13 Aug. 58	100	--	--	--	--
USSR[3]	150	--	0.3	0.7	0.05
h = 0°m	120	--	0.1	0.9	~ 0
22 July 59	100	--	--	--	--
USSR[3]	150	--	0.4	0.5	0.1
h = 15°m	120	--	0.3	0.7	~ 0
15 June 60	100	--	0.1	0.9	~ 0

[1]Johnson, Meadows, and Holmes, 1958; Meadows and Townsend, 1960

[2]Taylor and Brinton, 1961

[3]Istomin and Pokhunkov, 1962: h indicates altitude of sun above horizon, e and m denote evening and morning, respectively.

Table IV-3

DISSOCIATIVE RECOMBINATION COEFFICIENTS
($cm^3\ sec^{-1}$)

Altitude (km)	$\alpha_D(N_2^+)$	$\alpha_D(O_2^+)$	$\alpha_D(NO^+)$
150	2×10^{-7}	9×10^{-8}	7×10^{-9}
120	4×10^{-7}	2×10^{-7}	2×10^{-8}
100	9×10^{-7}	5×10^{-7}	8×10^{-8}
80	9×10^{-7}	5×10^{-7}	8×10^{-8}

Table IV-4

CONCENTRATIONS OF NEUTRAL SPECIES[a]
(cm^{-3})

Altitude (km)	$[N_2]$	$[O_2]$	$[O]$
200	1.5×10^{9}	6×10^{7}	6×10^{9}
150	2×10^{10}	1×10^{9}	3×10^{10}
120	4×10^{11}	3×10^{10}	2.5×10^{11}
100	7×10^{12}	6×10^{11}	3×10^{12}
80	5×10^{14}	1×10^{14}	1×10^{12}

[a] Norton, van Zandt, and Denison, 1962

Table IV-5

ION PRODUCTION RATES[a]
(cm^{-3} sec^{-1})

Altitude (km)	N_2^+	O_2^+	O^+
200	450	~ 0	800
150	2000	160	1700
120	1200	600	800
100	400	1100	160
80[b]	50	50	~ 0

[a] Norton, van Zandt, and Denison, 1962

[b] Estimated ionization rates under disturbed solar conditions.

In order to arrive at estimates of the rate constants k_1, k_2, k_3, and k_7 it was first necessary to compute the electron concentration at the altitudes considered. This was done by setting the sum of the right-hand members of equations (13) to (16) equal to the total ion production rate, expressing the various ion concentrations in terms of the electron concentration (from Table IV-2) and solving for [e]. The rocket data employed in the computations were taken from flights NN 3.19 (solar zenith angle: $\chi = 32^{\circ}$), NASA 4.09 ($\chi = 28^{\circ}$), and the Soviet flight of 2 August 1958 ($\chi = 54^{\circ}$). Although the solar zenith angle in these flights was not equal to the $\chi = 34^{\circ}$ for which the ion production rates were computed, this discrepancy introduces very little error, particularly in the case of the American observations. The solar zenith angles of the other observations were so large that one could not justify their use.

Values of the rate constants at an altitude of 150 km were computed by substituting the values of the estimated ion and electron concentrations and the ion production rates from Table IV-5 together with the

appropriate dissociative recombination coefficients (Table IV-3) and neutral species concentrations (Table IV-4) into equations (13) to (16). The values which best fit the data were found to be

$$k_1 \sim 2 \times 10^{-11} \text{ cm}^3 \text{ sec}^{-1}$$

$$k_2 \sim 2 \times 10^{-11} \text{ cm}^3 \text{ sec}^{-1}$$

$$k_3 \sim 2 \times 10^{-10} \text{ cm}^3 \text{ sec}^{-1}$$

$$k_7 \sim 6 \times 10^{-13} \text{ cm}^3 \text{ sec}^{-1}$$

Of these, k_1, k_3, and k_7 have recently been measured in the laboratory by various workers. The results are

k_1	Dickinson and Sayers (1960)	2.5×10^{-11} cm^3/sec
	Sayers (1962)	1.6×10^{-11}
	Langstroth and Hasted (1962)	1.8×10^{-12}
	Fite, Rutherford, Snow, and van Lint (1962)	(1 to 15) $\times 10^{-11}$
k_3	Fite, Rutherford, Snow, and van Lint (1962)	2×10^{-10}
k_7	Talrose, Markin, and Larin (1962)	$\leq 6.7 \times 10^{-12}$
	Sayers (1962)	2.5×10^{-11}
	Langstroth and Hasted (1962)	4.7×10^{-12}

It is evident that our estimates of k_1 and k_3 are in quite good agreement with the laboratory measurements. In fact the agreement is perhaps misleading, since our estimates are order of magnitude values only. On the other hand, our estimate of k_7 is in very poor agreement with the laboratory measurements. Since the estimated uncertainty in our computations is only about half an order of magnitude, the ohvious conclusions are (if the laboratory measurements are correct) that we are using too small a value for the dissociative recombination coefficient

of NO^+ or that another charge transfer process for conversion of NO^+ into a different ion is effective. However, it is believed highly improbable that $\alpha_D(NO^+)$ is in error by more than half an order of magnitude. Nor can we find an exothermic charge transfer process which will remove the NO^+; all such exothermic processes involving NO^+ are ones which produce NO^+. Hence, the discrepancy remains unresolved.

The concentrations of N_2^+, O_2, O^+, and NO^+ at various altitudes have been computed using our estimated rate constants and the means of the laboratory-determined values listed above. They are shown in Figures IV-3

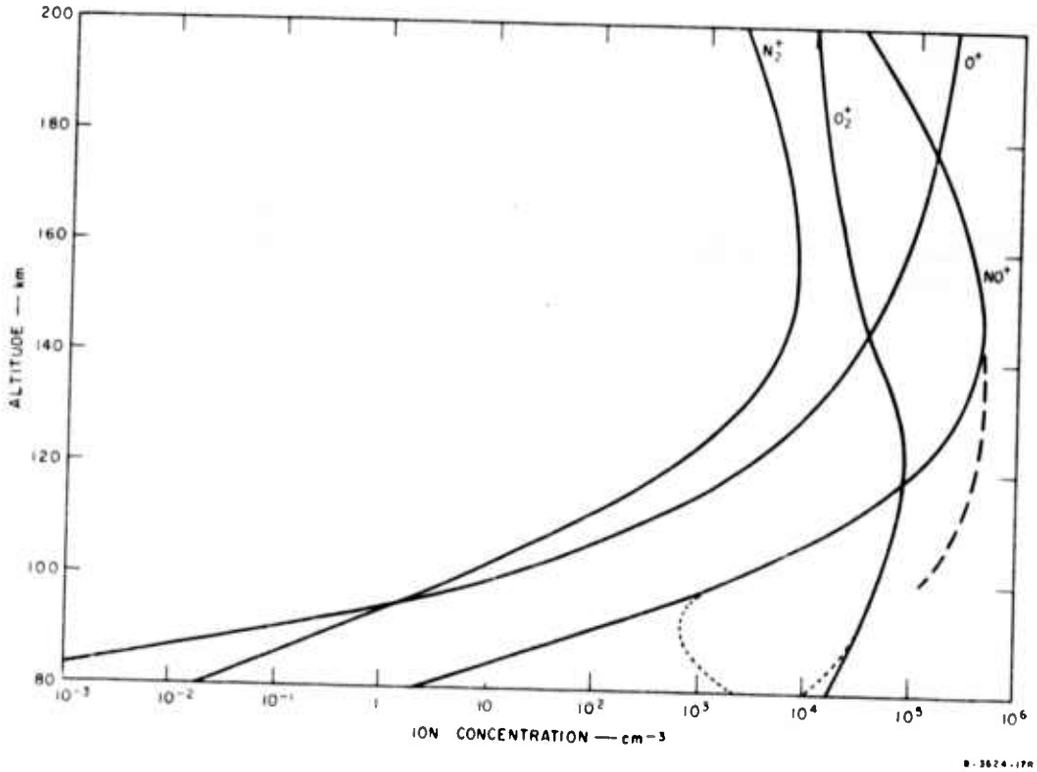

FIG. IV-3 ION CONCENTRATIONS ABOVE 80 km. THESE CONCENTRATIONS WERE COMPUTED USING THE VALUES OF THE RATE CONSTANTS k_1, k_2, k_3, AND k_7 OBTAINED FROM THE MASS SPECTROMETRIC OBSERVATIONS. THE BROKEN LINE REPRESENTS THE OBSERVED CONCENTRATION OF NO^+

and IV-4, respectively. The broken line in Figure IV-3, which was obtained from the observed relative concentration of NO^+, illustrates the discrepancy between the computed ion concentrations using our set of rate constants and the observed relative ion concentrations at altitudes

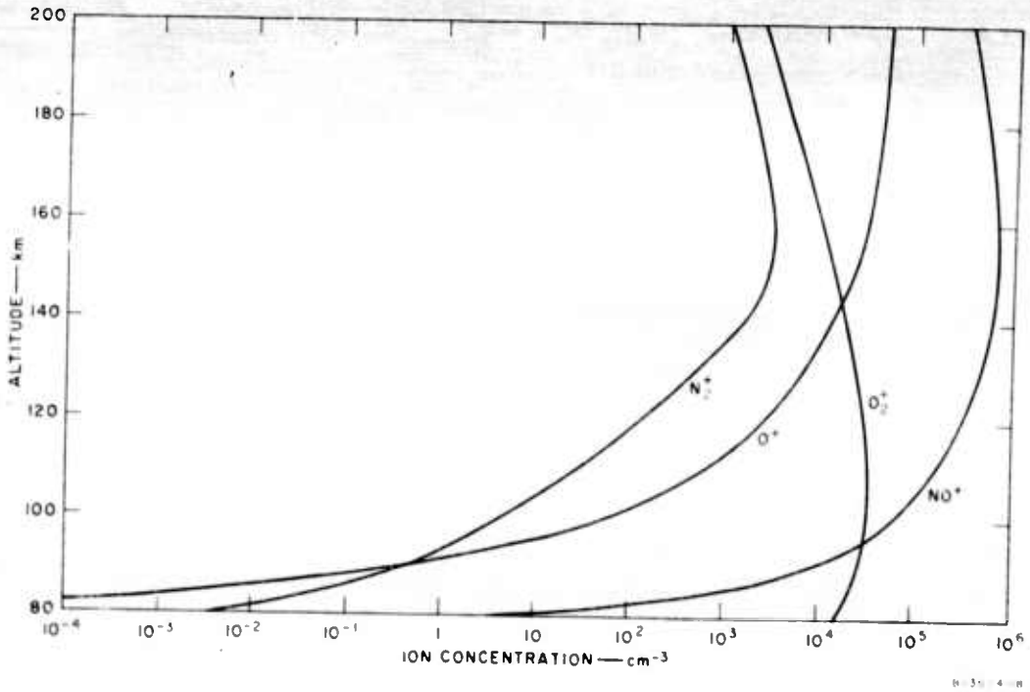

FIG. IV-4 ION CONCENTRATIONS ABOVE 80 km. THESE CONCENTRATIONS WERE COMPUTED USING THE MEANS OF RECENT LABORATORY MEASUREMENTS OF k_1, k_3, AND k_7. OUR VALUE OF k_2 WAS USED IN THE COMPUTATIONS

below 150 km. Comparison of the NO^+ curve in Figure IV-4 with the observed relative NO^+ concentrations reveals the disagreement between observation and our model when the rate constant k_7 and Sayers (1962) is used in the computations.

It is evident from Figures IV-3 and IV-4 that the dominant ion in the D-region under disturbed conditions must be O_2^+. NO^+ is quite unimportant unless it is produced directly, e.g., ionization of NO by Lyman α. This model cannot be extended to the lower D-region ($<$ 75 km) because of the possible importance of such exotic ions as N_3^+, N_4^+, and O_3^+. Kasner, et al. (1961) have observed such ions at gas pressures of about 0.1 mm of Hg, obtaining a value of $\alpha_D(N_3^+/N_4^+) \approx 2 \times 10^{-6}$ cm^3 sec^{-1} at this pressure. However, the pressure at which such ions gain significance as well as the effects at higher pressures (e.g., formation of N_5^+, etc.) are not known.

C. Dissociative Recombination

Numerous laboratory measurements (see Table IV-6) of the dissociative recombination coefficients of N_2^+ and O_2^+ have been made during the last decade with somewhat conflicting results. In addition, three measurements of the recombination coefficient of NO^+ have been carried out recently; one of these was a shock tube measurement (at a temperature of 5000°K), and the others were low temperature, i.e., room temperature, plasma experiments. Since most of these laboratory values were discussed earlier by Bortner and Baulknight (1961), the purpose of this report is to include some new results (Kasner, et al., 1961; Gunton and Inn, 1961; Doering and Mahan, 1962) together with the results of various ionospheric measurements (McElhinny, 1959; Bowhill, 1961; Whitten and Poppoff, 1961) and to develop from them a model of the daytime effective recombination coefficients in the altitude interval 80 to 150 km.

The recent measurement of $\alpha_D(N_2^+)$ and $\alpha_D(O_2^+)$ by Biondi's group involved the use of a mass spectrometer. They found that at low gas pressures, i.e., $\lesssim 0.01$ mm Hg of N_2 and O_2, the dominant positive ions were N_2^+ and O_2^+, but at higher pressures, i.e., $\gtrsim 0.1$ mm Hg of N_2 and O_2, the dominant positive ions were N_3^+, N_4^+, and O_3^+. This was in good agreement with the earlier results of mobility experiments conducted by Saporaschenko (1958) and Kovar and coworkers (1957). The latter investigators also found a strong temperature dependence for the formation of N_4^+: its formation is greatly inhibited by high temperatures. This is readily understandable in view of the low binding energy of N_4^+, about 0.14 eV.

Measurements of the decrease in the E-region critical frequency during solar eclipses have been used by McElhinny (1959) to obtain effective daytime recombination coefficients at E-region altitudes. Bowhill (1961) has, by use of a two-ion model and McElhinny's effective coefficients, derived component recombination coefficients. The values were $\alpha_D^1 = 10^{-7}$ cm^3 sec^{-1} and $\alpha_D^2 = 5 \times 10^{-9}$, $\alpha_D^2 = 1 \times 10^{-9}$ cm^3 sec^{-1},

Table IV-6

LABORATORY MEASUREMENTS OF DISSOCIATIVE RECOMBINATION COEFFICIENTS α_D

Investigators	$\alpha_D(N_2^+)$ ($cm^3\ sec^{-1}$)	$\alpha_D(O_2^+)$ ($cm^3\ sec^{-1}$)	$\alpha_D(NO^+)$ ($cm^3\ sec^{-1}$)
Kasner, Rogers, and Biondi, 1961	[a] $(5.9\pm1) \times 10^{-7}$	[a] $(3.8\pm1) \times 10^{-7}$	
	[b] 2×10^{-6}		
Holt, 1959		3×10^{-7}	
Faire and Champion, 1959	4.0×10^{-7}		
Biondi and Brown, 1949	1.4×10^{-6}		
Faire, Fundingsland, Aden, and Champion, 1958	1.4×10^{-6}		
Bialecki and Dougal, 1958	[c] 6.7×10^{-6}		
	[d] 8.7×10^{-7}		
Sayers, 1956	[e] 1.1×10^{-7}	[f] 4×10^{-8}	
Lin, 1960			[g] 10^{-9}
Gunton and Inn, 1961			[h] 1.3×10^{-8}
Doering and Mahan, 1962			$(3^{+17}_{-2}) \times 10^{-7}$

[a] for pressures $\lesssim$ 0.01 mm Hg; temp $\sim 300^\circ K$

[b] for pressures $\gtrsim$ 0.1 mm Hg; temp $\sim 300^\circ K$

[c] at $92^\circ K$

[d] at $300^\circ K$

[e] at $3200^\circ K$

[f] at $2500^\circ K$

[g] at $500^\circ K$

[h] for pressures > 0.1 mm Hg; temp $\sim 300^\circ K$

presumably representing recombination of O_2^+ and NO^+, respectively; the two values of α_D^2 correspond to different assumptions as to the altitude of emission of ionizing radiation from the solar corona. In his (1961) paper Bowhill also computed values of α_D^1 and α_D^2 using measurements of the diurnal variation of the E-region critical frequency together with his two-ion model. The component recombination coefficients were found to be $\alpha_D^1 = 10^{-7}$ cm^3 sec^{-1} and $\alpha_D^2 = 6 \times 10^{-9}$ cm^3 sec^{-1}. This value of α_D^2 tends to support the first one listed above for eclipse observations.

The computation of an effective dissociative recombination coefficient for the D-region during sudden ionospheric disturbances was presented in III-A: $\alpha_D = 2^{+3}_{-1} \times 10^{-7}$ cm^3 sec^{-1}. It was shown in the preceding section that we do not know whether the dominant ion in the disturbed D-region is O_2^+ or NO^+. Hence we do not know what ratio of $[O_2^+]/[NO^+]$ is represented by our value of the recombination coefficient.

Dissociative recombination coefficients are temperature-dependent, decreasing with increasing temperatures. Several years ago Bates (1950) derived the well-known form for general temperature dependence, $\alpha_D \propto T^{-\frac{1}{2}}$. Recently a more general form was derived under the assumption of thermal equilibrium (Bates and Dalgarno, 1962) which indicates that the temperature dependence of α_D is much more complicated. As they point out, the transition may occur with or without emission of radiation, the latter case being the more common. Their form of the dissociative recombination coefficient is

$$\alpha_D = C_1 \, T^{3/2} \, \frac{\omega_{AB}}{\omega_{AB^+}} \, A_0 \, (T) \qquad (1)$$

where ω_{AB} and ω_{AB^+} are the statistical weights of the relevant electronic states of the neutral molecule and the molecular ion, and C_1 is a constant:

$$C_1 = \frac{h^3}{2(2\pi mk)^{3/2}} \qquad (2)$$

in which h, k, and m are Planck's and Boltzmann's constants and the mass of the electron, respectively. $A_0(T)$ is a temperature-dependent function

related to the oscillator strength of the transition, $f_o(\epsilon)$, and to the lifetimes of the radiation emission and radiationless modes (τ_p and τ_a) by the equation

$$A_o(T) = \frac{g_o(T)}{\tau_a + \tau_p\, g_o(T)} \qquad (3)$$

where

$$g_o(T) = \int_o^\infty f_o(\epsilon)\, e^{-\frac{\epsilon}{kT}}\, d\epsilon \qquad (4)$$

The subscript zero affixed to the oscillator strength indicates that we are considering the system to be in the ground vibrational state. If the temperature is high, excited vibrational states ν must be considered; the function g_o must then be replaced by an average

$$\bar{g}\,(T) = \sum_\nu g_\nu(T)\, e^{-\epsilon_\nu/kT} \Big/ \sum_\nu e^{-\epsilon_\nu/kT} \qquad (5)$$

For E-region temperatures, excited vibrational states cannot always be neglected.

According to Bates and Dalgarno, the case in which $\tau_p\, g_o(T) \ll \tau_a$ is the more common. Then A_o takes the form

$$A_o(T) \approx \frac{1}{\tau_a} \int_o^\infty f_o(\epsilon)\, e^{-\epsilon/kT}\, d\epsilon \qquad (6)$$

The temperature dependence of α_D is thus dependent in turn upon the functional form of $f_o(\epsilon)$. For example, if the latter is $\sim \epsilon^{-\frac{1}{2}}$, then $\alpha_D \propto T^{-1}$. In general, however, one would expect the energy dependence of $f_o(\epsilon)$ to be more complex than a power law in which case the dissociative recombination coefficient would not be related to the temperature by any simple expression, particularly at elevated temperatures. Nevertheless, values of the exponent n in the range $-3/2 \leq n \leq -1/2$ seem to fit the existing experimental data fairly well. This is shown in Figures IV-5, 6 and 7 which indicate that $n \approx -3/4$ for $\alpha_D(N_2^+)$ and $n \approx -1$ for $\alpha_D(O_2^+)$ are the best fits to the most reliable data. Actually the temperature exponent

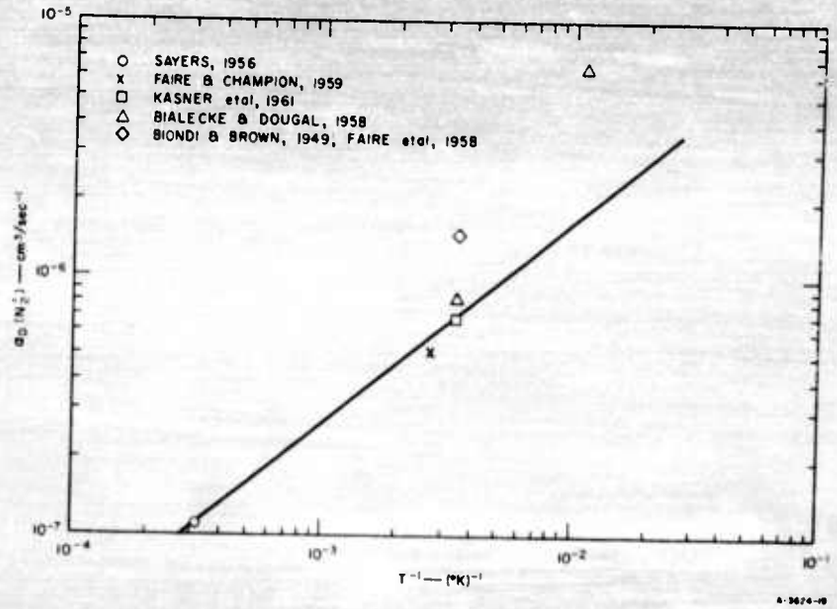

FIG. IV-5 DISSOCIATIVE RECOMBINATION COEFFICIENT OF N_2^+ AT VARIOUS TEMPERATURES T

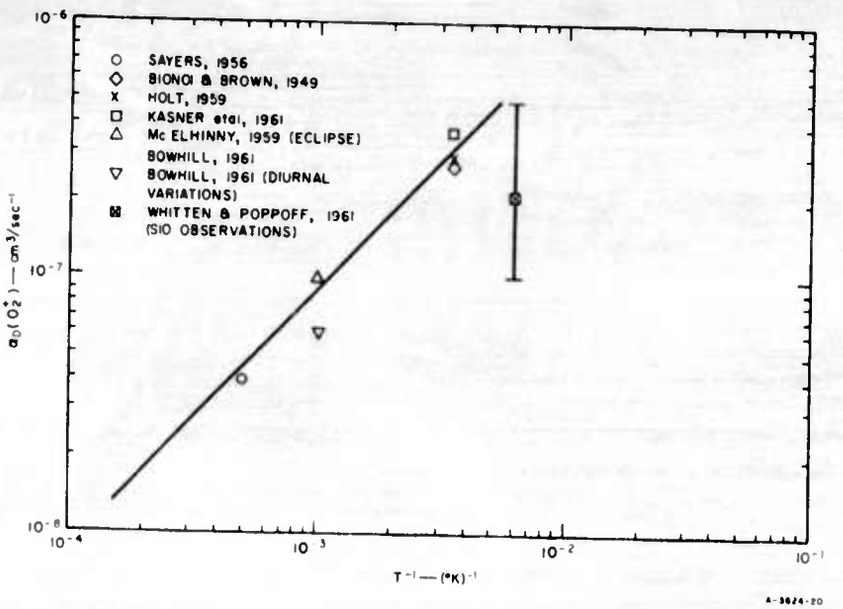

FIG. IV-6 DISSOCIATIVE RECOMBINATION COEFFICIENT OF O_2^+ AT VARIOUS TEMPERATURES T

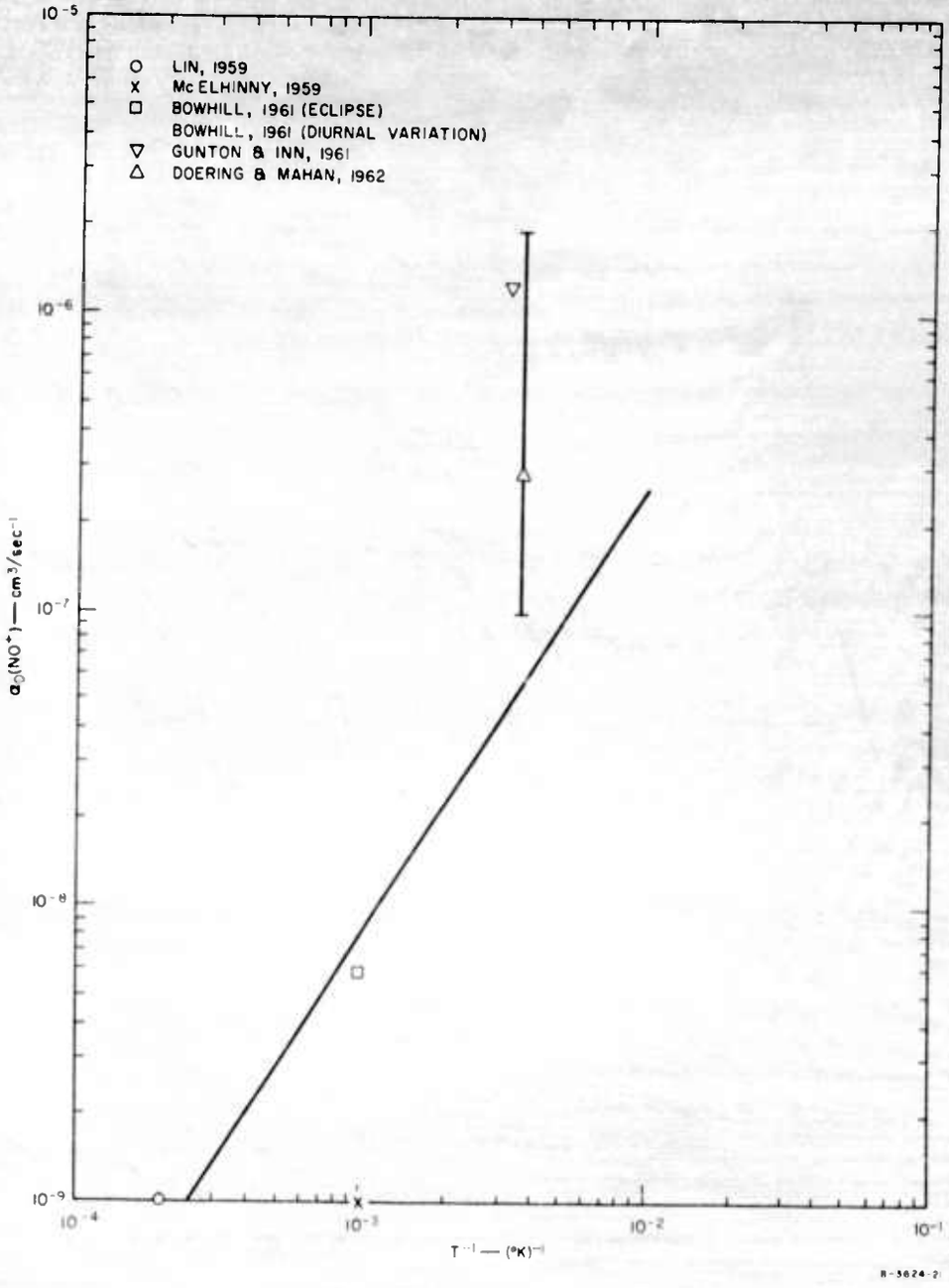

FIG. IV-7 DISSOCIATIVE RECOMBINATION COEFFICIENT OF NO^+ AT VARIOUS TEMPERATURES T

corresponding to N_2^+ may be as small as -1 or as large as -1/2. In view of Kasner's results it would appear that the poor agreement of the data of Bialecki and Dougal (1958) is due to the formation of relatively large concentrations of N_3^+ and N_4^+ in their experiments. Figure IV-6 also presents the previously mentioned values of α_D, presumably corresponding to recombination with O_2^+, obtained from eclipse and diurnal variation observations (McElhinny, 1959; Bowhill, 1961). The temperature to which this value corresponds can only be estimated but the agreement with laboratory measurements is quite good.

Derivation of the temperature dependence of $\alpha_D(NO^+)$ is much more tenuous and is based on the value obtained by Lin (1960) and Doering and Mahan (1962) as well as on solar eclipse data (McElhinny, 1959; Bowhill, 1961). An approximate value of n for $\alpha_D(NO^+)$ is $n \approx -3/2$. Again the temperatures to which the values obtained from ionospheric observations correspond must be estimated ($\sim 1000^{\circ}K$ for the E-region). Gunton and Inn (1961) have obtained a value for $\alpha_D(NO^+)$ of 1.3×10^{-6} cm^3/sec at room temperature and at nitric oxide pressures of several tenths of one mm of Hg. This value seems too large to correspond to the dissociative recombination of NO^+ and may correspond to recombination of complex ions such as $(NO)_2^+$. Somewhat similar results were obtained by Doering and Mahan who estimated the experimental upper limit as $\sim 2 \times 10^{-6}$ cm^3/sec and the lower limit as $\sim 10^{-7}$ cm^3/sec. The nitric oxide partial pressure was of the order of 0.1 mm of Hg.

The conclusions concerning dissociative recombination can be summarized as follows:

1. On the basis of existing data, probable values of the important dissociative recombination coefficients in the D- and E-regions are $\alpha_D(N_2^+) = 5 \times 10^{-5}\ T^{-3/4}$ $cm^3\ sec^{-1}$; $\alpha_D(O_2^+) = 9 \times 10^{-5}\ T^{-1}$ $cm^3\ sec^{-1}$; $\alpha_D(NO^+) = 2.6 \times 10^{-4} T^{-3/2}$ $cm^3\ sec^{-1}$.

2. It is evident from the results of the preceding section that the most important coefficients in the upper D-region and in the E-region are $\alpha_D(O_2^+)$ and $\alpha_D(NO^+)$; $\alpha_D(N_2^+)$ is at most of marginal significance.

3. The identities of the dominant positive ions in the lower D-region are not known. This arises from ignorance of the role played by the ions N_4^+, N_3^+, and O_3^+ at these altitudes. (See Section IV-B, ion-atom interchange processes.)

A model of the effective daytime ionospheric electron dissociative recombination coefficient in the altitude range 80 to 150 km is shown in Figure IV-8. The profiles A_1 and A_2, which merge at about 110 km altitude, correspond to the normal and disturbed D-regions,* respectively.

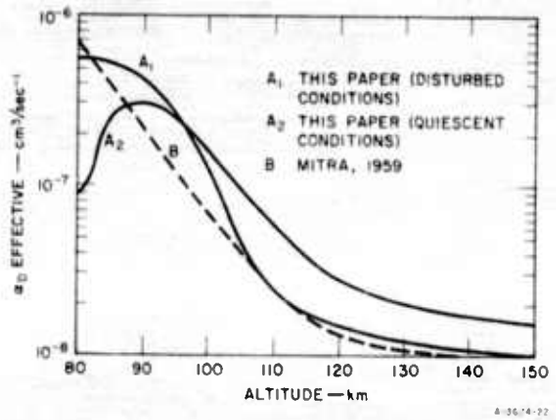

FIG. IV-8 MODELS OF THE DAYTIME IONOSPHERIC ELECTRON RECOMBINATION COEFFICIENT ABOVE 80 km ALTITUDE

*It is assumed that the quiescent D-region ion above 80 km is NO^+ and that the disturbed D-region ion is in general a mixture of NO^+ and O_2^+; the first assumption may not always be justified (Poppoff and Whitten, 1962)

This model is based on the values of α_D for the various ionic species given above, on the middle latitude temperature profiles corresponding to quiescent and disturbed conditions found by Spencer, Brace, and Carignan (1962), and on the relative concentrations of ionic species as reported by Taylor and Brinton (1961). It was constructed under the assumption that dissociative recombination is dominant in this altitude interval. We justify this by comparing the estimated value of $\alpha_D(NO^+)(\sim 10^{-7}\ cm^3\ sec^{-1})$ with the estimated value of the product of the negative ion concentration ratio (~ 0.02, see Section IV-A), and the ion-ion recombination coefficient ($\sim 2 \times 10^{-8}\ cm^3\ sec^{-1}$, see Section IV-D); obviously $\alpha_D(NO^+) \gg \lambda \alpha_i$ - and we thus neglect the ion-ion recombination processes in our model. For this reason the α_D profiles also serve as models of the effective recombination coefficient. The sharp rise in curve A_2 between 80 and 85 km is a result of our assumption that NO^+ is the dominant ion below 85 km under quiescent conditions (Nicolet and Aikin, 1960). If O_2^+ should prove to be dominant in this interval, curve A_2 will coincide with curve A_1 below 100 km. It is apparent from the dotted curve that for $k_{11} \leq 10^{-18}\ cm^3\ sec^{-1}$, reaction (11) will not have an important bearing on α_D above 80 km. The difference between the curves corresponding to disturbed and quiescent conditions at higher altitudes is due to higher electron temperatures expected under disturbed conditions (Spencer, et al., 1962). Mitra's (1959) noontime (quiescent) model for middle latitudes is also presented. It is evident that above 90 km the two quiescent models agree to within a factor of two. The poor agreement at lower altitudes is due in part to (in our opinion) Mitra's probable over-estimation of the importance of electron attachment and ion-ion recombination.

In the altitude range 80 to 60 km the pressure rises to ~ 0.1 mm Hg and the dissociative recombination coefficients of ionized molecular oxygen is expected to rise to 10^{-6} cm^3/sec (Kasner, et al., 1961) as the O_3^+ and perhaps O_4^+ ions become significant and then dominate. Whether or not such clustering occurs in the nitric oxide ion is unknown at present. Its discovery should occasion no surprise.

D. Ion-Ion Recombination

Ion-ion recombination is of potential importance in the D-region under both day and night conditions; the altitudes at which one must begin to consider it are of the order of 70 to 75 km during the day and 80 to 85 km at night. For ionospheric disturbances which result in large ionization rates at low altitudes ($\sim$ 30 to 60 km) such as polar cap events and nuclear bursts, ion-ion recombination will be the dominant recombination mechanism and must be included in the kinetics of the ionic reactions.

The ion-ion neutralization reactions are basically of two types, two-body and three-body. Typical examples are

Two Body

$$N_2^+ + O_2^- \rightarrow N_2 + O_2 \quad (1)$$

$$O_2^+ + O_2^- \rightarrow O_2 + O_2 \quad (2)$$

$$NO^+ + O_2^- \rightarrow NO + O_2 \quad (3)$$

$$O_2^+ + O_2^- \rightarrow O + O + O_2 \quad \text{(ion-ion dissociative recombination)} \quad (4)$$

Three Body

$$N_2^+ + O_2^- + M \rightarrow N_2 + O_2 + M \quad (5)$$

where M is an unspecified third body. Neither mode has been extensively investigated.

Yeung (1958) measured the rate constants for the processes

$$I_2^+ + I_2^- \rightarrow I_2 + I_2 \quad (6)$$

$$Br_2^+ + Br_2^- \rightarrow Br_2 + Br_2 \quad (7)$$

and found values of 1.47×10^{-8} and 1.85×10^{-8} cm^3 sec^{-1}, respectively, at temperatures of the order of $300^{\circ}K$. His attempt to obtain the temperature dependence of the reaction was unsuccessful although he did find that the rate constant decreased with increasing temperature. In spite of great care in carrying out his investigations Yeung may have used a defective amplifier in his experimental apparatus (Sayers, 1962). According to Sayers the necessary correction under these conditions would raise the experimental values of the two coefficients to $\sim 10^{-7}$ cm^3 sec^{-1}. Unfortunately, no experimental work has yet been done on the very important reactions (1) to (4). Nawrocki and Dalgarno (Nawrocki, 1961a) have suggested the adoption of a mean atmospheric ion-ion recombination coefficient of $\bar{\alpha}_i \approx 10^{-8}$ cm^3 sec^{-1}.

Many years ago Thomson obtained a semi-empirical equation for the three-body ion-ion recombination process

$$\alpha_T = \pi d_D^2 \epsilon (\bar{C}_+^2 + \bar{C}_-^2)^{\frac{1}{2}} \qquad (8)$$

where d_D is the effective radius of coulombic attraction, ϵ is a probability function, and $\bar{C}$ is the mean ion velocity. More recently Massey (1952) showed that for air at pressures $<$ 300 mm of Hg equation (8) can be expressed in the more useful form

$$\alpha_T = 8 \times 10^{-3} \, p \, T^{-5/2} \qquad (9)$$

where p is pressure in mm of Hg and T is temperature in $^{\circ}K$. Because the rate of two-body ion-ion recombination exceeds that of the three-body mode at altitudes above 45 km, the latter mechanism is of no importance in the normal ionosphere. It may, however, play an important role at relatively low altitudes during a polar cap absorption event or during a nuclear explosion-induced ionospheric disturbance.

E. Diffusion to Dust

Several years ago Bourdeau, Whipple, and Clark (1959) measured atmospheric conductivities (both positive and negative) in the altitude range 35 to 80 km by means of a Gerdien condenser flown by a Viking rocket. Below 50 km the results contained no surprises, but the behavior of the measured conductivities was quite anomalous between 50 and 80 km. The positive ion conductivity was found to increase more slowly than one would normally expect, while the negative conductivity was found to increase in the predicted manner to an altitude of about 70 km after which it decreased. Bourdeau and co-workers were able to explain their results by assuming a layer of particulate matter, with a number density of ~ 1 particle/cm^3 and a particle radius of $\sim 10^{-5}$ cm, to be present in the region 50 to 80 km. The occurrence in this region of dust layers with similar properties has been proposed by investigators of the nature of noctilucent clouds (Ludlam, 1957) and twilight scattering (Bigg, 1956). Recent studies by Volz and Goody (1962), however, imply that the normal concentration of dust at about 65 km is several orders of magnitude smaller than one finds in noctilucent clouds.

One can include the effects of diffusion to dust in the ion rate equations by introduction of appropriate diffusion terms, typically of the form

$$\pi a^2 \bar{C}_{\pm} N_0 N_{\pm}$$

where a is the particle radius, N_0 the particle concentration, $N_{\pm}$ the ($\pm$) ion concentration, and $\bar{C}_{\pm}$ the ($\pm$) ion rms velocity. The rate equations are written

$$\frac{dN_+}{dt} = q - \alpha_D N_+ N_e - \alpha_i N_- N_+ - \pi a^2 \bar{C}_+ N_0 N_+ - \pi a^2 \bar{C}_+ N_+ N_-^d \qquad (1)$$

$$\frac{dN_-}{dt} = \mu N_e - \alpha_i N_+ N_- - (\rho_{coll} + \rho_{photo}) N_- - \pi a^2 N_0 \bar{C}_- N_- - \pi a^2 \bar{C}_- N_- N_+^d \qquad (2)$$

$$\frac{dN_e}{dt} = q + (\rho_{coll} + \rho_{photo})N_- + \delta N_-^d - \alpha_D N_+ N_e - \mu N_e - \pi a^2 \bar{C}_e N_+^d N_e - \pi a^2 \bar{C}_e N_0 N_e \qquad (3)$$

$$\frac{dN_+^d}{dt} = \pi a^2 \bar{C}_+ N_0 N_+ - \pi a^2 \bar{C}_e N_+^d N_e - 2\pi a^2 \bar{C}_d N_+^d - \pi a^2 \bar{C}_- N_- N_+^d \qquad (4)$$

$$\frac{dN_-^d}{dt} = \pi a^2 \bar{C}_- N_0 N_e + \pi a^2 \bar{C}_e N_0 N_e - 2\pi a^2 \bar{C}_d N_+^d N_-^d - \delta N_-^d - \pi a^2 \bar{C}_+ N_+ N_-^d \qquad (5)$$

assuming that every ion-particle collision results in charge capture by the dust particle. The symbols have the significance

N_e = electron concentration

q = electron production rate

α_D = dissociative recombination coefficient

α_i = two-body ion-ion recombination coefficient

μ = specific electron attachment rate

ρ_{coll} = specific electron detachment rate (collisional-type)

ρ_{photo} = specific electron photo detachment rate

δ = rate of electron detachment from negatively charged dust particles

$\bar{C}_e$ = electron rms velocity

$N_{\pm}^d$ = concentration of positive (negative) charges residing on dust particles (electronic charges per cm^3)

$\bar{C}_d$ = dust particle rms velocity.

The third terms appearing on the right-hand sides of (4) and (5) can be neglected because of the very small velocity of the dust particles.

Under equilibrium conditions the concentration of positive charges residing on dust particles is given approximately by

$$N_+^d \approx \frac{\bar{C}_+ N_0 N_+}{\bar{C}_e N_e + \bar{C}_- N_-} \qquad (6)$$

Assuming a temperature of 200°K, a dust particle concentration and mean radius of $N_o \sim 1$ cm^{-3} and $a \sim 10^{-5}$ cm, respectively, and an electron concentration of $N_e \sim 10^4$ cm^{-3}, we find that according to equation (6) $N_+^d \sim 200$ cm^{-3}. Actually it is not likely that a dust particle of this size could accumulate more than a few electronic charges because of coulomb repulsion of positive ions by the positively charged dust particles.

The electron concentration at any altitude under conditions of equilibrium is obtained by adding equations (2) and (3)

$$q + \delta N_-^d = (1+\lambda)(\alpha_D + \lambda\alpha_i)N_e^2 + \pi a^2 \bar{C}_e N_+^d N_e + \pi a^2 (C_e + \lambda^d \bar{C}_-) N_o N_e + \pi a^2 \bar{C}_- N_- N_+^d \quad (7)$$

where $\lambda = \frac{N_-}{N_e}$. In order to gain some idea of the effects of diffusion to dust we compute N_e at several altitudes under the assumption that $a = 10^{-5}$ cm, $N_o = 1$ cm^{-3}, $N_d^+ = 1$ cm^{-3}, $\alpha_D = 10^{-7}$ cm^3 sec^{-1}, and $\alpha_i = 10^{-8}$ cm^3 sec^{-1}. We further assume that the negative ion terms in (7) are independent of the terms containing electron concentrations. The results are shown in Table IV-7.

It is evident that particulate matter can, if present in even minuscule quantities, be very effective in electron removal. In view of the results of Volz and Goody (1962) it is doubtful that the mechanism is normally of importance in the D-region.

It is easily shown that as the electron concentration is substantially raised, perhaps several orders of magnitude in the case of a high altitude nuclear burst, diffusion to dust becomes an even less important electron removal mechanism unless the dust concentration is simultaneously increased by many orders of magnitude. The increase of the dust concentration to $N_o = 10$ cm^{-3} in a 10-km cube requires the proper dispersal of 40 kg of material. Hence it is not considered likely that after such a burst, diffusion of electrons will be important outside the locale of the explosion. Inside this region it may be of some significance, depending upon the degree of dispersal of particulate matter.

Table IV-7

ELECTRON CONCENTRATIONS WITH AND WITHOUT DIFFUSION TO DUST
(daytime)

Altitude (km)	β	q ($cm^{-3}\ sec^{-1}$)	N_o (cm^{-3})	N_e (without diffusion) (cm^{-3})	N_e (with diffusion) (cm^{-3})
90	10^{-2}	10	1	10^4	5×10^3
80	10^{-1}	0.1	1	10^3	100
70	2	4×10^{-3}	1	10^2	1
60	30	10^{-3}	1	10	0.3
90	10^{-2}	10	0.01	10^4	10^4
80	10^{-1}	0.1	0.01	10	500
70	2	4×10^{-3}	0.01	10^2	25
60	30	10^{-3}	0.01	10	4

F. Effects of Chemical Reactions

1. Introduction

The chemical composition of the upper atmosphere determines in part the nature of the ionic species produced by ionizing radiation, as well as the "shuffling" of the ionic species by means of charge transfer and ion-atom interchange. Since the identity of the ionic species in turn fixes the rate of electron removal, chemical composition can be seen to have a most important bearing on ionospheric relaxation.

The normal composition of the upper atmosphere is dependent not only upon the chemical reactions including photo-reactions but also upon diffusion and, to some extent, ionic reactions. For example, at altitudes above 100 to 110 km the recombination lifetime of oxygen atoms is of the order of several months. Instead of recombining at these altitudes after formation by photo-dissociation, they diffuse downward and recombine below 100 km altitude (Nicolet, 1959). Meanwhile, oxygen molecules diffuse upward, the net effect being the establishment of diffusive equilibrium at an altitude probably not greater than 120 km. At lower altitudes, i.e., below ~ 90 km, oxygen atoms recombine as fast as they are photo-dissociated or diffuse into the region and we have a condition of photo-chemical equilibrium. The altitude at which turbulent mixing ceases and the atmospheric composition begins to depart from photo-chemical equilibrium (turbopause), and the altitude at which diffusive equilibrium is attained are functions of the rate of dissociation and scale height. These quantities also fix the time required for the attainment of diffusive equilibrium starting from an initial state of photo-chemical equilibrium (Nicolet, 1960).

If the system is to be maintained in photo-chemical equilibrium conditions must be such that diffusive equilibrium would be attained in a time interval greater than 2 to 3 days; this requirement is due to the varying rate of oxygen dissociation throughout the day (Nicolet, 1960).

Recently several model atmospheres have been developed on the bases of satellite drag measurements, measurements of the absorption of solar radiation, and estimates of the heating effect. The one presented in Figure IV-9 is due to Norton, Van Zandt, and Denison (1962) for altitudes above 100 km and the Handbook of Geophysics (1960) for altitudes below 100 km, while that presented in Figure IV-10 is taken from a paper by Barth (1961) and is based on the work of Kallman-Bijl (1961) and Nicolet (1959). The former (Figure IV-9) is probably the more reliable since it is based in part on measurements of the absorption of solar radiation. The Handbook of Geophysics model atmosphere was selected for the lower altitudes in Figure IV-9 because it joins smoothly with

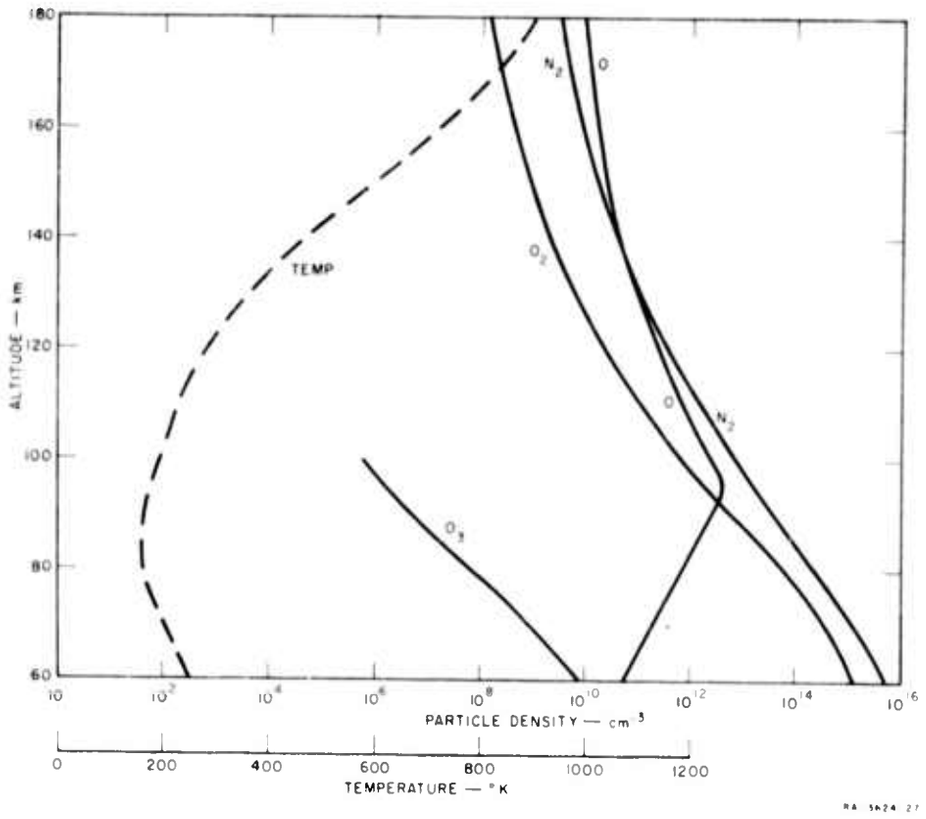

FIG. IV-9 ATMOSPHERIC NEUTRAL CONSTITUENTS AND TEMPERATURE, 60 TO 180 km ALTITUDE (Norton, et al, 1962 and Handbook of Geophysics, 1960)

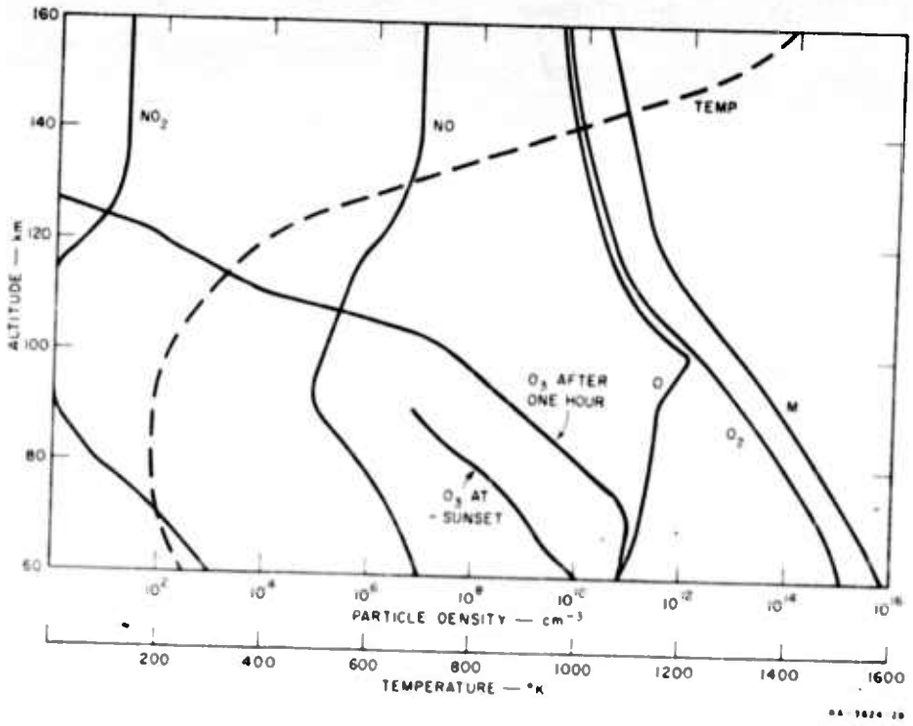

FIG. IV-10 ATMOSPHERIC NEUTRAL CONSTITUENTS AND TEMPERATURE, 60 TO 160 km ALTITUDE (Barth, 1961)

the model atmosphere of Norton, et al. at 100 km, the lowest altitude to which the latter was extended.

2. Basic Chemical Reactions

Barth (1961) has thoroughly discussed the chemical reactions in the upper atmosphere which control the concentrations of atomic and molecular oxygen and nitrogen, nitric oxide, nitrogen dioxide, and ozone. These reactions can be summarized as follows

$$N + N + M \rightarrow N_2 + M \quad (1)$$

$$N + O + M \rightarrow NO + M \quad (2)$$

$$O + O + M \rightarrow O_2 + M \quad (3)$$

$$N + NO \rightarrow N_2 + O \quad (4)$$

$$N + O_2 \rightarrow NO + O \quad (5)$$

$$O + O_2 + M \rightarrow O_3 + M \quad (6)$$

$$O + O_3 \rightarrow O_2 + O_2 \quad (7)$$

$$NO + O + M \rightarrow NO_2 + M \quad (8)$$

$$NO_2 + O \rightarrow NO + O_2 \quad (9)$$

with the corresponding rate constants obtained by various investigators shown in Table IV-8. In addition, Table IV-8 contains in the right-hand

Table IV-8

RATE CONSTANTS CORRESPONDING TO PROCESSES (1) TO (9)

Rate Constant	Barth (1961)‡	Bortner and Baulknight
k_1	7×10^{-33} cm^6 sec^{-1} (300°K)	$1.7 \times 10^{-30} T^{-\frac{1}{2}}$ cm^6 sec^{-1}; ($M = N_2$)•
		$2 \times 10^{-31} T^{-\frac{1}{2}}$ cm^6 sec^{-1}; ($M = N$)•
		$3 \times 10^{-31} T^{-\frac{1}{2}}$ cm^6 sec^{-1}; ($M \neq N_2, N$)•
k_2	1.5×10^{-32} cm^6 sec^{-1} (300°K)	$5 \times 10^{-31} T^{-\frac{1}{2}}$ cm^6 sec^{-1}•
k_3	8.0×10^{-33} cm^6 sec^{-1} (300°K)	$6 \times 10^{-32} T^{-\frac{1}{2}}$ cm^6 sec^{-1}; ($M = O_2$)†
		$2 \times 10^{-31} T^{-\frac{1}{2}}$ cm^6 sec^{-1}; ($M = O$)†
		$1 \times 10^{-32} T^{-\frac{1}{2}}$ cm^6 sec^{-1}; ($M \neq O, O_2$)†
k_4	8.3×10^{-11} cm^3 sec^{-1} (300°K)	$2.2 \times 10^{-13} T^{-\frac{1}{2}}$ cm^3 sec^{-1}•
k_5	$3.3 \times 10^{-12} e^{-\frac{3100}{T}}$ cm^3 sec^{-1}	$4 \times 10^{-13} T^{\frac{1}{2}} e^{-\frac{6600}{RT}}$ cm^3 sec^{-1}†
k_6	$6.8 \times 10^{-38} e^{\frac{300}{T}}$ cm^6 sec^{-1}	$4 \times 10^{-34} e^{-\frac{150}{T}}$ cm^6 sec^{-1}•
k_7	$5.0 \times 10^{-11} e^{-\frac{3000}{T}}$ cm^3 sec^{-1}	$7 \times 10^{-12} e^{-\frac{1600}{T}}$ cm^3 sec^{-1}•
k_8	5.2×10^{-32} cm^6 sec^{-1} (300°K)	5×10^{-32} cm^6 sec^{-1}•
k_9	3.5×10^{-12} cm^3 sec^{-1} (300°K)	2.5×10^{-12} cm^3 sec^{-1}•

†Bortner and Baulknight (1961)

•Bortner and Baulknight (1962)

‡For specific references see Barth's (1961) paper.

column a set of rate constants proposed by Bortner and Baulknight (1961, 1962) which are somewhat different from those of Barth.

3. Chemistry of the Normal Atmosphere

In order to write and solve differential equations for the rates of change of the concentrations of the various species, one must know the rates of dissociation of nitrogen and oxygen. The dominant mechanism for the formation of atomic oxygen in the upper atmosphere is photo-dissociation of O_2 by solar radiation in the Schumann-Runge continuum (1300-1750 A). The photo-dissociation cross section in this region is of the order of 5×10^{-18} cm^2 (Watanabe, 1958) and the solar photon flux $\sim 5 \times 10^{13}$ cm^2 sec^{-1} (Mitra, 1952). Using the concentration of O_2 given in Figure IV-10, and neglecting attenuation of the photon flux by absorption, one finds an approximate value of the rate of dissociation of O_2 of 5×10^8 cm^{-3} sec^{-1}.

On the other hand photo-dissociation of N_2 is a very weak process The N_2 molecule is apparently dissociated by absorption in the Lyman-Birge-Hopfield band at 1226 A, for which the estimated cross section is about 10^{-21} cm^2 Since the photon flux is $\sim 10^9$ cm^{-2} sec^{-1} (Barth, 1961) we obtain a photo-dissociation rate at 100 km of only 10 cm^{-3} sec^{-1}. A process which promises a much larger rate of formation of nitrogen atoms is the dissociative recombination of N_2^+ or NO^+. In order to obtain an estimate of the effective dissociation rate of NO^+ at 100 km we estimate that $[e] \approx 2 \times 10^5$ cm^{-3}, $[NO^+] \approx 10^5$ cm^{-3} and $\alpha_D(NO^+) \approx 5 \times 10^{-8}$ cm^3 sec^{-1}. Then the rate of formation of nitrogen atoms from the process

$$NO^+ + e \rightarrow N + O \qquad (10)$$

is $\alpha_D(NO^+)[NO^+][e] \approx 10^3$ cm^{-3} sec^{-1}, a much larger value than that arising from photo-dissociation of N_2.

It is in principle now possible to compute the chemical composition of the upper atmosphere if one knows how to handle the diffusion problem. In practice this is a formidable problem and Barth contented himself

with starting with the initial (daytime) conditions shown in Figure IV-10 and computing the concentrations of various constituents at various times after sunset. It was found that the concentration of atomic oxygen was quite constant during the night for altitudes above 70 km while the concentration of atomic nitrogen remained constant at altitudes of 80-120 km but decreased rapidly during the night at altitudes above or below this range. The decrease of [O] and [N] during the period between sunset and one hour thereafter are shown in Figure IV-11, under the

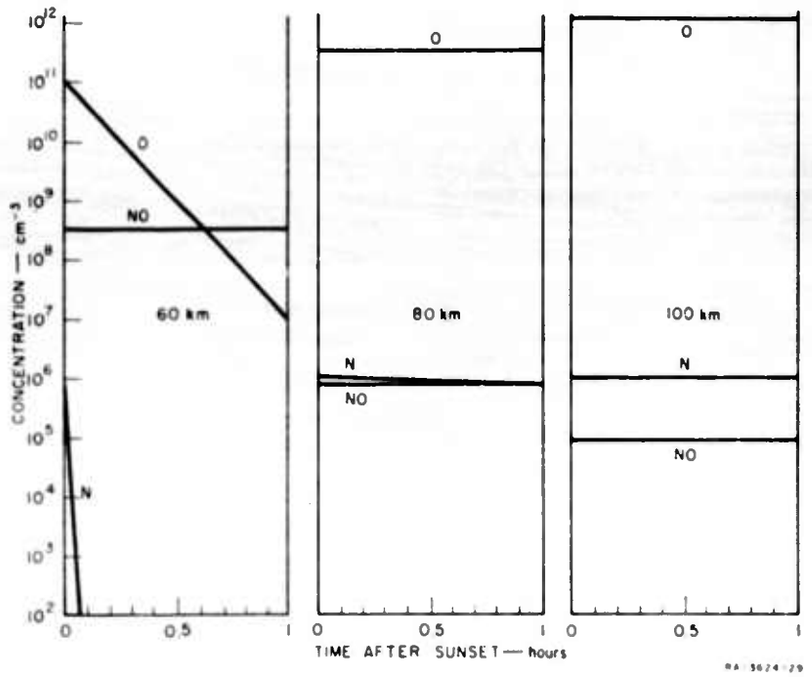

FIG. IV-11 CHANGES IN CONCENTRATION OF O, N, AND NO AFTER SUNSET AT ALTITUDES OF 60, 80, AND 100 km

assumption that during the daytime $[N] \approx 10^6$ cm^{-3}.

Formation and destruction of nitric oxide result primarily from reactions (5) and (4) respectively. These processes together with diffusion yield the daytime NO concentration curves shown in Figure IV-10.

The decrease of [NO] during the first hour after sunset is shown in Figure IV-11.

The composition of the upper atmosphere has, of course, a pronounced effect on ionospheric structure since it determines to a large extent the nature of the ions present, the ionization rate, and the rate of electron removal. However, this composition is nearly constant under normal conditions, the concentrations of a few of the minor constituents at certain altitudes decreasing after sunset. The only change of this kind which may significantly alter the electron removal rates is the combination of atomic and molecular oxygen to form ozone at altitudes below 70 km. Specifically, such a reduction in the atomic oxygen concentration will result in a smaller rate of associative detachment of electrons from negative ions (e.g., O_2^-) at night than in the daytime.

The change of the solar spectrum between maximum and minimum of solar activity undoubtedly affects the composition of the upper atmosphere but the details are not at all well understood.

4. Effects of Disturbances

Abnormal solar radiation of short duration which is capable of producing changes in the composition of the upper atmosphere may be broadly classified as electromagnetic (X-rays and ultraviolet radiation) and particle (solar cosmic rays). The increased rate of dissociation of O_2 arising from the enhanced radiation is certainly not greater than $\sim 10^3$ cm^{-3} sec^{-1} as opposed to a normal rate of dissociation of O_2 at $\sim$ 90 km of 10^8 cm^{-3} sec^{-1}; the enchancement is therefore negligible. On the other hand the formation of nitrogen atoms proceeds via the processes

$$N_2^+ + e \rightarrow N + N \qquad (11)$$

$$NO^+ + e \rightarrow N + O \qquad (10)$$

rather than by direct dissociation of N_2. It is demonstrated in the section on ion-atom interchange that charge transfer to O_2 by N_2^+ is so rapid a process that N_2^+ is a negligible ionic component of the lower

ionosphere, although it is produced at a faster rate than any other ion. Undoubtedly some NO^+ is formed by the ion-atom interchange process

$$N_2^+ + O \rightarrow NO^+ + N$$

which is rather slow (D. R. Bates, private communication) as compared to other processes of similar type. Assuming that $[NO^+]$ is as large as $0.1\ [O_2^+]$, we obtain a production rate of N atoms of $\sim 10\ cm^{-3}\ sec^{-1}$ and an enhancement in the N concentration of $\leq 10^4\ cm^{-3}$ which is less than the normal concentration thought to arise via diffusion from higher altitudes. Even if the change in [N] were significant, the effect on ionospheric relaxation would still be negligible.

In the case of a high altitude nuclear burst, the molecular species are almost completely dissociated within the fireball. Just outside the fireball region ultraviolet radiation in the range 1300-1700 A is sufficiently intense to produce virtually complete dissociation. However, at altitudes below 90 km the attenuation of this radiation by absorption is so large that it has a range of < 1 km, assuming an absorption cross section of $10^{-18}\ cm^2$ (Watanabe, 1958). At an altitude of 100 km, dissociation of O_2 is already so great that nearly complete dissociation of the residual O_2 will not greatly affect the concentration of atomic oxygen although the concentration of O_2 may be decreased by as much as an order of magnitude until such time that recombination and diffusion can restore the system to equilibrium.

If we assume that the mean electron density at an altitude of 100 km is of the order of $10^8\ cm^{-3}$ over a period of at least one hour, the concentration of atomic nitrogen may be raised to a value as large as $10^{10}\ cm^{-3}$ which may in turn increase the concentration of NO by perhaps an order of magnitude; the increase in [N] may be detectable by airglow intensity measurements (NO γ bands). These changes in composition are not sufficiently great, however, to significantly affect the electron loss mechanism.

REFERENCES

Anderson, J. M. and L. Goldstein, Momentum transfer cross section and fractional energy loss in the collision of slow electrons with nitrogen molecules, Phys. Rev. 102, 388 (1956)

Anderson, K. A. and D. C. Enemark, Balloon observations of X-rays in the auroral zone II. J. Geophys. Res. 65, 3521 (1960)

Bailey, D. K., Abnormal ionization in the lower ionosphere associated with cosmic-ray flux enhancements, Proc. IRE 47, 255 (1959)

Bailey, D. K. and L. M. Branscomb, Rate coefficient for O_2 collisional detachment, Bull. Am. Phys. Soc., 5, 123 (1960)

Barrington, R. E. and E. Thrane, The determination of D-region electron densities from observations of cross modulation, J. Atmos. Terr. Phys. 24, 31 (1962)

Barth, C. A., Nitrogen and oxygen atomic reactions in the chemosphere, in Chemical Reactions in the Lower and Upper Atmosphere, Interscience Publishers, New York, 1961

Bates, D. R., Dissociative recombination, Phys. Rev. 78, 492 (1950)

Bates, D. R., The Airglow, in Physics of the Upper Atmosphere, J. A. Ratcliffe, Ed., Academic Press, New York, 1960

Bates, D. R. and H. S. W. Massey, The basic reactions in the upper atmosphere, Proc. Roy. Soc. A 137, 261-296 (1946)

Bates, D. R. and M. Nicolet, Ion-atom interchange, J. Atmos. Terr. Phys., 18, 65 (1960)

Bates, D. R. and A. Dalgarno, in Atomic and Molecular Processes, Ed. by D. R. Bates, Academic Press, New York, 1962

Bialecki, E. P. and A. A. Dougal, Pressure and temperature variation of the electron-ion recombination coefficient in nitrogen, J. Geophys. Res. 63, 539 (1958)

Bigg, E. K., The detection of atmospheric dust and temperature inversion by twilight scattering, J. Meteorol. 13, 262 (1956)

Biondi, M. A., and S. C. Brown, Measurement of electron-ion recombination, Phys. Rev. 76, 1697 (1949)

Bortner, M. H., The chemical kinetics of the normal atmosphere, Tech. Information Series No. R 61 SD 122, Space Sciences Laboratory, General Electric Co., June 1961a (Unclassified)

Bortner, M. H. and C. W. Baulknight, Deionization kinetics, Scientific Report, Contract AF 19(604)-8820, Space Sciences Laboratory, General Electric Co., July 1961b (Unclassified)

Bortner, M. H. and C. W. Baulknight, Investigation of the chemical kinetics of atmospheric deionization, Quarterly Progress Report, Contract AF 19(604)-8820, Space Sciences Laboratory, General Electric Co., King of Prussia, Pa., March 29, 1962

Bourdeau, R. E., E. C. Whipple, and J. F. Clark, Analytic and experimental electrical conductivity between the stratosphere and ionosphere, J. Geophys. Res. 64, 1363 (1959)

Bourdeau, R. E., Ionospheric results with sounding rockets and the Explorer VIII satellite, NASA TN D-1079, 1961

Bowhill, S. A., The effective recombination coefficient of an ionoshere containing a mixture of ions, J. Atmos. Terr. Phys. 20, 19 (1961)

Branscomb, L. M., D. S. Burch, S. J. Smith, and S. Geltman, Photodetachment cross section and electron affinity of atomic oxygen, Phys. Rev. iii, 504 (1958)

Brown, R. R. and W. H. Campbell, An auroral-zone electron precipitation event and its relationship to a magnetic bay, J. Geophys. Res. 67, 1357 (1962)

Burch, D. S., S. J. Smith, and L. M. Branscomb, Photodetachment from O_2^-, Phys. Rev. 112, 171 (1958)

Chamberlain, Joseph W., Physics of the Aurora and Airglow. Academic Press, New York and London, 1961

Chanin, L. M., A. V. Phelps, and M. A. Biondi, Measurement of the attachment of slow electrons in oxygen, Phys. Rev. Letters, 2, 344 (1959); Measurement of the attachment of low-energy electrons to oxygen molecules, Phys. Rev. 128, 219 (1962)

Chapman, Sydney and C. Gordon Little, The nondeviative absorption of high frequency radio waves in auroral latitudes, J. Atmos. Terr. Phys. 10, 20 (1957)

Chapman, S., Disturbance in the lower auroral ionosphere. J. Atmos. Terr. Phys. 15, 29 (1959)

Chubb, T. A., H. Friedman, and R. W. Kreplin, Measurements made of high-energy X-rays accompanying three class 2^+ solar flares, J. Geophys. Res. 65, 1831 (1960a)

Chubb, T. A., and others, IGY Bull. No. 42, Trans. AGU 41, 717 (1960b)

Crain, C. M., Ionization loss rates below 90 km, J. Geophys. Res. 66, 1117 (1961)

Curran, R. K., Negative ion formation in ozone, J. Chem. Phys. 35, 1849 (1961)

Curran, R. K., Formation of NO_2^- by charge transfer at very low energies, Phys. Rev. 125, 910 (1962)

Dalgarno, A., Collision processes in the high atmosphere, National Bureau of Standards Tech. Note 124 (Papers on the Symposium on Collision Phenomena in Astrophysics, Geophysics and Masers), December 1961

Dalgarno, A., Charged particles in the upper atmosphere, Ann. Geophys. 17, 16 (1961)

Davis, L. R., O. E. Berg, and L. H. Meredith, Direct measurement of particle fluxes in and near auroras, Space research, North-Holland Publishing Co., Amsterdam, 1960, p. 721

Dickinson, P. H. G. and J. Sayers, Ion charge exchange reactions in oxygen afterglows, Proc. Phys. Soc., 76, 137 (1960)

Doering, J. P. and B. H. Mahan, Photoionization of nitric oxide, J. Chem. Phys. 36, 669 (1962)

Efremov, A. I., A. L. Padmoshenskii, O. N. Efimov, and A. A. Lebedov, A study of the short wavelength radiation of the sun, Earth Satellites, Vol. 9 and 10, p. 139, July 1962

Eyring, H., J. O. Hirschfelder and H. S. Taylor, Theoretical treatment of chemical reactions produced by ionization processes, Part I, J. Chem. Phys. 1, 479 (1936)

Faire, A. C., O. T. Fundingsland, A. L. Aden, and K. S. W. Champion, Electron recombination coefficient measurement in nitrogen at low pressure, J. Appl. Phys. 29, 928 (1958)

Faire, A. C. and K. S. W. Champion, Measurements of dissociative recombination and diffusion in nitrogen at low pressures, Phys. Rev. 113, 1 (1959)

Field, F. H. and J. L. Franklin, Electron Impact Phenomena, Academic Press, New York, 1957

Fite, W. L., J. A. Rutherford, W. R. Snow, and V. A. J. Van Lint, Ion-neutral collisions in afterglow; Report No. GA-2824, General Atomic, San Diego, Calif., Jan. 23, 1962

Formato, D. and A. Gilardini, Microwave determinations of afterglow temperatures and electron collision frequencies in nitrogen, Proceedings of the Fourth International Conference on Ionization Phenomena in Gases, Uppsala, 1959; North-Holland Publishing Co., Amsterdam 1960

Friedman, H., T. A. Chubb, J. E. Kupperian, Jr., and J. C. Lindsay, X-ray emission of solar flares, IGY Rocket Rept., Ser 1, 183, July 30 (1958)

Galejs, Janis, A further note on terrestrial extremely low-frequency propagation in the presence of an isotropic ionosphere with an exponential conductivity-height profile, J. Geophys. Res. 67, 2715 (1962)

Geltman, S., Theory of threshold energy dependence of photodetachment of diatomic molecular negative ions, Phys. Rev. 112, 176 (1958)

Gunton, R. C., and E. C. Y. Inn, Rates of electron removal by recombination, attachment, and ambipolar diffusion in nitric oxide plasmas, J. Chem. Phys. 35, 1896 (L) (1961)

Handbook of Geophysics, Geophysics Research Directorate, Air Force Research Division, ARDC, MacMillan, New York, 1960

Hertzberg, M., Ion-neutral reactions, J. Atmos. Terr. Phys. 20, 177 (1961)

Holt, E. H., Electron loss processes in the oxygen afterglow, Bull. Amer. Phys. Soc. 4, 112 (1959)

Inn, Edward C. Y., Origin of the D-region, Planet. Space Sci. 5, 70 (1961a)

Inn, E. C. Y., Further comments on the origin of the D-region, Planet. Space Sci. 8, 200 (1961b)

Istomin, V. G. and A. A. Pokhunkov, Fifth COSPAR meeting, Washington, D.C., May 1962

Johnson, C. Y., J. P. Heppner, J. C. Holmes, and E. B. Meadows, Results obtained with rocket-borne ion spectrometers, IGY Rocket Report Series No. 1, National Research Council, Washington, 30 July 1958

Johnson, C. Y., E. B. Meadows, and J. C. Holmes, Ion composition of the arctic ionosphere, J. Geophys. Res. 63, 443 (1958)

Jortner, J. and U. Sokolov, Spectrophotometric determination of the electron affinities of some diatomic molecules, Nature 190, 1003 (1961)

Kallmann-Bijl, H. K., Daytime and nighttime atmospheric properties derived from rocket and satellite observations, J. Geophys. Res. 66, 787 (1961)

Kane, J. A., Arctic measurements of electron collision frequencies in the D-region of the ionosphere, J. Geophys. Res. 64, 133 (1960)

Kanellakos, D. P. and O. G. Villard, Ionospheric disturbances associated with the solar flare of September 28, 1961, J. Geophys. Res. 67, 2265 (1962)

Kasner, W. H., W. A. Rogers, and M. A. Biondi, Electron-ion recombination coefficients in nitrogen and in oxygen, Phys. Rev. Lett. 7, 321 (1961)

Klein, M. M. and K. A. Brueckner, Interaction of slow electrons with atomic oxygen and atomic nitrogen, Phys. Rev. 111, 1115 (1958)

Kovar, F. R., E. C. Beaty, and R. N. Varney, Drift velocities in nitrogen at various temperatures, Phys. Rev. 107, 1490 (1957)

Kreplin, R. W., Solar X-rays. Ann. Geophys. 17, 151 (1961)

Kreplin, R. W., U.S. Naval Research Laboratory, Private communication, 1962

Kreplin, R. W., T. A. Chubb, and H. Friedman, X-ray and Lyman-alpha emission from the sun as measured from the NRL SR-1 satellite, J. Geophys. Res., 67, 2231 (1962)

Kuiper, G. P., editor, The Sun, University of Chicago Press, Chicago, 1953

Kunkel, W. and A. Gardner, Ionization accompanying long-lived nitrogen afterglow, Phys. Rev. 98, 558A (1955)

Kunkel, W., Free electrons in active nitrogen, Bull. Amer. Phys. Soc. (2) 2, 87 (1956)

Langstroth, G. F. O. and J. B. Hasted, General discussion, Discussions, Faraday Society 33, 298 (1962)

Lin, S. C., AVCO Research Note No. 210 (1960)

Lindsay, John C., National Aeronautics and Space Administration, Private Communication, 1962

Ludlam, F. H., Noctilucent clouds, Tellus 9, 341 (1957)

Mandel'shtam, S. L., I. P. Tindo, Yu. K. Voron'ko, A. I. Shurygin, and B. N. Vassil'ev, Investigation of solar roentgen radiation. I. Measurements using geophysical rockets. Earth Satellites, Vol. 9 and 10, p. 148, July 1962

Massey, H. S. W., Recombination of gaseous ions, Adv. in Physics 1, 395 (1952)

McElhinny, M. W., Some further analyses of E-layer measurements in South Africa during the solar eclipse of 25 December 1954, J. Atmos. Terr. Phys. 14, 273 (1959)

Meadows, E. B. and J. W. Townsend, IGY rocket measurements of arctic atmosphere composition above 100 km, Space Research; H. Kallmann-Bijl, Ed., North-Holland Publishing Co., Amsterdam, 1960

Minzner, R. A., K. S. W. Champion, and H. L. Pond, The ARDC Model Atmosphere, 1959; Geophysics Research Directorate Report No. 115, Air Force Cambridge Research Center, Bedford, Mass. (August 1959)

Mitra, A. P., Ionospheric effects of solar flares II--Ionization models, Pennsylvania State University Ionosphere Research Laboratory Scientific Rept. No. 142, December 1, 1960

Mitra, A. P., Nighttime ionization in the lower ionosphere--I. Recombination processes, J. Atmos. Terr. Phys. 10, 140 (1957)

Mitra, A. P., Time and height variations in the daytime processes in the ionosphere; Part I. A noontime model of the ionosphere loss coefficient from 60 to 600 km over middle latitudes, J. Geophys. Res. 64, 733 (1959)

Mitra, S. K., The Upper Atmosphere, 2nd ed., The Asiatic Society, Calcutta, 1952

Molmud, P., Langevin equation and the ac conductivity of non-Maxwellian plasmas, Phys. Rev. 114, 29 (1959)

Müller, E. A. W., Die Schwächung extraterrestrischen Röntgenstrahlen in der Atmosphäre, Z. Astrophys. 10, 52 (1935)

Nawrocki, P. J., Reaction rates, Scientific Report, Geophysics Corporation of America, January 1961a, ASTIA No. AD 252534

Nawrocki, P. J., and R. Papa, Atmospheric Processes, Prentice-Hall, Inc. Englewood Cliffs, N.J., 1963

Neupert, W. M., W. E. Behring, W. A. White, J. C. Lindsay, A proposal to continue the studies of the Solar Spectrum from 1-400 A using the orbiting solar observatory. NASA Goddard Space Flight Center (1962)

Newell, H., The upper atmosphere studied by rockets and satellites, Physics of the Upper Atmosphere, J. A. Ratcliffe, Ed., Academic Press, New York, 1960. This article presents the results of numerous measurements of ionospheric electron concentrations, from which typical values were taken for use in this report.

Nicolet, M., Collision frequency of electrons in the terrestrial atmosphere, Physics of Fluids 2, 95 (1959)

Nicolet, M., Constitution of the atmosphere at ionospheric levels, J. Geophys. Res. 64, 2092 (1959)

Nicolet, M. and A. C. Aikin, The formation of the D-region of the ionosphere. J. Geophys. Res. 65, 1461 (1960)

Nicolet, M., The Properties and Constitution of the Upper Atmosphere, in Physics of the Upper Atmosphere, Ed. by J. A. Ratcliffe, Academic Press, New York 1960

Norton, R. B., T. E. Van Zandt, and J. S. Denison, A model of the atmosphere and the ionosphere in the E and F regions, in the The Proceedings of the Conference on the Ionosphere, London (July 1962)

Pedersen, Arne, D-layers in the subauroral zone, J. Geophys. Res. 67, 2685 (1962)

Phelps, A. V. and J. L. Pack, Electron collision frequencies in nitrogen and in the lower ionosphere, Phys. Rev. Lett. 3, 340 (1959)

Phelps, A. V. and J. L. Pack, Collisional detachment in molecular oxygen, Phys. Rev. Lett., 6, 111 (1961)

Poppoff, I. G., et al., Geophysical Experiments Pertinent to Nuclear Blackout Studies, Final Report prepared for Defense Atomic Support Agency, Stanford Research Institute, 31 December 1961

Poppoff, I. G. and R. C. Whitten, D-region ionization by solar X-rays, J. Geophys. Res. 67, 2986 (1962)

Pounds, K. A. and P. W. Sanford, Rocket measurements of the sun's X-ray 'tail' with a simple photographic detector. Paper read at International Conference on the Ionosphere, London, 2-6 July 1962

Pounds, K. A. and A. P. Willmore, Some early results from the X-ray spectrometer in satellite UK-1. Paper read at International Conference on the Ionosphere. London, 2-6 July 1962

Pounds, K. A., University of Leicester, Private communication (1962)

Pritchard, H. O., Determination of electron affinities. Chem. Rev. 52, 529 (1953)

Ratcliffe, J. A., editor, Physics of the Upper Atmosphere, p. 410, Academic Press, New York and London, 1960

Rawer, Karl, The Ionosphere, p. 96, Frederick Ungar Publishing Company, New York, 1952

Reid, G. C., A study of the enhanced ionization produced by solar protons during a polar cap absorption event, J. Geophys. Res. 66, 4071 (1961)

Saporaschenko, M., Ions in nitrogen, Phys. Rev. 111, 1550 (1958)

Sayers, J., Recent laboratory studies of recombination cross sections, Solar Eclipses and the Ionosphere, W. J. G. Beynon and G. M. Brown, Eds., Pergamon Press, London, New York, 1956

Sayers, J., Ionic recombination, in Atomic and Molecular Processes, Ed. by D. R. Bates, Academic Press, New York, 1962

Schulz, G. J., Cross section and electron affinity for O^- ions from O_2, CO, CO_2 by electron impact, Phys. Rev. 128, 178 (1962)

Smith, F. T. and C. R. Gatz, Ionization in afterburning rocket exhausts, Stanford Research Institute Tech. Report BSD-TR-61-76, November 8, 1961

Smith, S. J., D. S. Burch, and L. M. Branscomb, Experimental photodetachment cross section and the ionosphere detachment rate for O_2^-, Ann. Géophys. 14, 225 (1958)

Smith, S. J. and D. S. Burch, Relative measurements of the photodetachment cross section for H^-, Phys. Rev. 116, 1125 (1959)

Smith, S. J. and L. M. Branscomb, Optical methods for negative ion studies, Rev. Sci. Instr. 31, 733 (1960)

Spencer, L. V., Energy dissipation by fast electrons, National Bureau of Standards Monograph 1. September 10, 1959

Spencer, N. W., L. H. Brace, and G. R. Carignan, Electron temperature evidence for nonthermal equilibrium in the ionosphere, J. Geophys. Res. 67, 157 (1962)

Talrose, V. L., M. I. Markin, and I. K. Larin, The reaction $O^+ + N_2 \rightarrow NO^+ + N$, Discussions, Faraday Society 33, 257 (1962)

Taylor, H. A. and H. C. Brinton, Atmospheric ion composition measured above Wallops Island, Virginia, J. Geophys. Res. 66, 2587 (1961)

Van Allen, J. A., Interpretation of soft radiation observed at high altitudes in northern latitudes, Phys. Rev. 99, 608 (1955)

Watanabe, K. and H. E. Hinteregger, Photoionization rates in the E and F regions, J. Geophys. Res. 67, 999 (1962)

Watanabe, K., Ultraviolet absorption processes in the upper atmosphere, Advances in Geophysics 5, 153 (1958); Academic Press, New York

Webber, W. The production of free electrons in the ionospheric D-layer by solar and galactic cosmic rays, J. Geophys. Res. 67, 5091 (1962)

Whitten, R. C. and I. G. Poppoff, A model of solar-flare-induced ionization in the D-region, J. Geophys. Res. 66, 2779 (1961); J. Geophys. Res. 67, 2986 (1962) (corrigendum)

Whitten, R. C. and I. G. Poppoff, Associative detachment in the D-region, J. Geophys. Res. 67, 1183 (1962)

Willmore, A. P., University College London, Private communication, 1962

Winckler, J. R., P. D. Bhavsar, and K. A. Anderson, A study of the precipitation of energetic electrons from the geomagnetic field during magnetic storms, J. Geophys. Res. 67, 3717 (1962)

Yeung, T. H. Y., Recombination coefficients for positive and negative ions, Proc. Phys. Soc. 71, 341 (1958)

DISTRIBUTION LIST

Advanced Research Project Agency
The Pentagon
Washington 25, D.C. (6 copies)

Office of Aerospace Research
Washington 25, D.C. (1 copy)
Attn: RROP

Office of Aerospace Research
Washington 25, D.C. (1 copy)
Attn: RROS

AFSC
Andrews AFB
Washington 25, D.C. (1 copy)
Attn: SCRS

Air Force Cambridge Research Laboratories
L. G. Hanscom Field
Bedford, Mass. (1 copy)

Air Force Cambridge Research Laboratories
L. G. Hanscom Field
Bedford, Mass. (2 copies)
Attn: Dr. G. J. Gassmann, CRZI

Air Force Cambridge Research Laboratories
L. G. Hanscom Field
Bedford, Mass. (1 copy)
Attn: CRZI Official File

Director
U.S. Army Ballistic Research Laboratories
Aberdeen Proving Ground
Maryland
Attn: Mr. W. W. Berning
Dr. Frederick Kaufman
Mr. E. O. Baicy

Chief
U.S. Army Research Office
Box CM, Duke Station
Durham, North Carolina
Attn: Dr. R. Mace

Chief of Naval Research
Navy Department
Washington 25, D.C.
Attn: Dr. F. Byrne

Air Force Special Weapons Center
Kirtland AFB
New Mexico
Attn: Lt. R. Reynolds

Air Force Cambridge Research Laboratories
L. G. Hanscom Field
Bedford, Mass.
Attn: Dr. W. Pfister
Dr. K. S. W. Champion
Dr. Rita Sagalyn

Chief
Defense Atomic Support Agency
Washington 25, D.C.
Attn: Major J. E. Mock
Dr. C. A. Blank

Chief
Defense Atomic Support Agency
Washington 25, D.C.
Attn: DASA Library

Director
Armour Research Foundation
10 West 35th Street
Chicago 16, Illinois
Attn: Mr. C. M. Haaland

Director
National Bureau of Standards
Central Radio Propagation
Laboratory
Boulder, Colorado
Attn: Dr. T. E. Van Zandt
Mr. D. K. Bailey
Dr. W. H. Campbell

Director
The RAND Corporation
1700 Main Street
Santa Monica, California
Attn: Dr. Robert E. Lelevier
Dr. Cullen Crain
Dr. Forrest Gilmore

General Electric Company
Defense Electronics Division
Technical Military Planning
Operation
735 State Street
Santa Barbara, California
Attn: Dr. W. F. Dudziak

General Electric Company
Defense Electronics Division
Technical Military Planning
Operation
735 State Street, Santa Barbara
California
Attn: DASA Data Center

General Electric Company
Missile and Space Vehicle Dept.
3198 Chestnut Street
Philadelphia, Pennsylvania
Attn: Dr. M. H. Bortner

General Atomic
Division of General Dynamics Corp.
P.O. Box S, Old San Diego Station
San Diego 12, California
Attn: Dr. W. L. Fite
Dr. V. A. Van Lint

Lockheed Missiles and Space Division
Technical Information Center
3251 Hanover Street
Palo Alto, California
Attn: Dr. Roland E. Meyerott

Dr. F. H. Shelton
Kaman Aircraft Corporation
Nuclear Division
Garden of the Gods Road
Colorado Springs, Colorado

Los Alamos Scientific Laboratory
P.O. Box 1663
Los Alamos, New Mexico
Attn: Dr. Herman Hoerlin

Pennsylvania State University
University Park
Pennsylvania
Attn: Professor A. H. Waynick

University of Pittsburgh
Cathedral of Learning
400 Bellefield Avenue
Pittsburgh, Pennsylvania
Attn: Professor M. A. Biondi

University of Washington
Applied Physics Laboratory
1013 E. 40th Street
Seattle 5, Washington
Attn: Professor R. Geballe

New York University
College of Engineering
Main Campus, University Heights
New York 53, New York
Attn: Professor S. Borowitz

Director
National Bureau of Standards
Washington 25, D.C.
Attn: Dr. Lewis Branscomb

Goddard Space Flight Center
NASA
Greenbelt, Maryland
Attn: Dr. A. C. Aikin

Southwest Center for Advanced
Study
Dallas, Texas
Attn: Dr. S. A. Bowhill

U.S. Air Force Special Weapons
Center
Kirtland Air Force Base
Albuquerque, New Mexico
Attn: Capt. Wallace Henderson
Physics Division

Ionospheric Research Laboratory
Pennsylvania State University
University Park, Pennsylvania
Attn: Dr. A. P. Mitra

Goodard Space Flight Center
National Aeronautics and Space
Administration
Greenbelt, Maryland
Attn: Dr. R. E. Bourdeau

U.S. Naval Research Laboratory
Washington 25, D.C.
Attn: Mr. R. W. Kreplin

Stanford Research Institute
Menlo Park, California
Attn: Dr. A. M. Peterson
Dr. Edward T. Pierce
Dr. George Johnson

Physics Department
University of California
Berkeley 4, California
Attn: Dr. Kinsey Anderson
Dr. R. R. Brown

Westinghouse Research Laboratories
Pittsburgh 35, Pennsylvania
Attn: Dr. A. V. Phelps

STANFORD
RESEARCH
INSTITUTE

MENLO PARK
CALIFORNIA

Regional Offices and Laboratories

Southern California Laboratories
820 Mission Street
South Pasadena, California

Washington Office
808 17th Street, N.W.
Washington 6, D.C.

New York Office
270 Park Avenue, Room 1770
New York 17, New York

Detroit Office
1025 East Maple Road
Birmingham, Michigan

European Office
Pelikanstrasse 37
Zurich 1, Switzerland

Japan Office
911 Iino Building
22, 2-chome, Uchisaiwai-cho, Chiyoda-ku
Tokyo, Japan

Representatives

Honolulu, Hawaii
1125 Ala Moana Blvd.
Honolulu, Hawaii

London, England
19, Upper Brook Street
London, W. 1, England

Milan, Italy
Via Macedonio Melloni, 49
Milano, Italy

Toronto, Ontario, Canada
Room 710, 67 Yonge St.
Toronto, Ontario, Canada

UNCLASSIFIED